Numerical and Experimental Study of Thermal Stratification in Large Warehouses

Weigang Li

A Thesis

In the Department of

Building, Civil and Environmental Engineering

Presented in Partial Fulfillment of the Requirements

for the Degree of

Master of Applied Science (Building Engineering) at

Concordia University

Montreal, Quebec, Canada

April 2016

CONCORDIA UNIVERSITY

School of Graduate Studies

This is to certify that the thesis prepared

By: Weigang Li

Entitled: **Numerical and Experimental Study of Thermal Stratification in Large Warehouses**

and submitted in partial fulfillment of the requirements for the degree of

Master of Applied Science (Building Engineering)

complies with the regulations of the University and meets the accepted standards with respect to originality and quality.

Signed by the final Examining Committee:

Dr. Samuel Li	Chair
Dr. Liangzhu Wang	Supervisor
Dr. Chevy Chen	Examiner External (to program)
Dr. Hua Ge	Examiner
Dr. Samuel Li	Examiner

Approved by _____

Dr. F. Haghighat, GPD
Department of Building, Civil and Environmental Engineering

_____

Dr. Amir Asif, Dean
Faculty of Engineering and Computer Science

Date _____

Abstract

Numerical and Experimental Study of Thermal Stratification in Large Warehouses

Weigang Li

Thermal stratification in large warehouses is a common phenomenon in winter, especially in regions with cold climates. Natural buoyancy causes warmer air to move upwards towards the ceiling. The relatively high temperature beneath the roof leads to a large amount of heating energy loss. Nowadays, mixing the air is one of the effective methods for reducing thermal stratification which have started to be used in industrial warehouses. This thesis aims to determine thermal stratification conditions in five warehouses via field measurement. Furthermore, this thesis also aims to investigate the effects of mechanical mixing of indoor air with fans using CFD-based numerical simulations. For these objectives, field measurement of thermal stratification in five warehouses was conducted and used to validate CFD models. Meanwhile, two warehouses were simulated in CFD. ANSYS FLUENT, a commercial CFD package, was used to the indoor air flow in this thesis. The numerical temperature results were validated by comparison with the on-site measurement data. The vertical temperature profiles and rate of heat flow from different cases were compared. The effectiveness of different fan configurations in reducing thermal stratification was evaluated.

Acknowledgements

Firstly, I would like to take this opportunity to express my gratitude to Dr. Liangzhu Wang for his guidance and support during the whole process of this study. Secondly, I would like to thank the owners of the five warehouses in which the field measurements of this study were conducted. They kindly allowed the measurements to be taken on their property even though we are strangers to each other who were only in contact by email.

I would also like to thank Dr. Hua Ge, Dr. Samuel Li and Dr. Chevy Chen for being my thesis defense committee. Their comments on the thesis and insightful questions during the thesis defense helped me very much in the final process of finishing this thesis.

Fellow students in the same research group also supported me in many ways. Shawn Si Tu helped me set up the equipment for the field measurements. Dahai Qi, Jeremy Zhao, Cheng-Chun Lin and Pu Yang all gave insightful suggestions during the process of this study. Mr. Luc Demers provided patient assistance during the tricky process of thermocouple welding and kindly provided equipment for the field measurements. When I was first using the ANSYS software package, many people in the EV 9.169 office whose names are unknown to me provided very helpful tips and guidance regarding 3D modeling.

Meanwhile and very importantly, the support from my family let me never feel alone during master's program.

Table of Contents

LIST OF FIGURES

LIST OF TABLES

LIST OF VARIABLES

g	Gravity
k	Turbulent kinetic energy
p	Pressure
t	Time
T	Temperature
R	Thermal resistance
ν	velocity
β	Thermal expansion coefficient
ε	Turbulent dissipation coefficient
μ	Dynamic viscosity
ρ	Density
R	Thermal resistance
ACH	Air change rate

CHAPTER 1. INTRODUCTION

1.1 Thermal stratification

1.1.1 Thermal stratification phenomenon in large warehouse spaces

Warmer air tends to rise and cooler air to descend due to their variance in buoyancy. In an indoor environment without active air flow circulation, different layers of air stratify vertically (Ramki, 2012). Hot air with lower density stays above cold air with higher density. The stratification of temperature and density usually remains stable in the building if there are no other mechanisms to disturb and reverse it. To some extent, thermal stratification in buildings is similar to the phenomenon of temperature inversion in meteorology (NOAA, 2016).

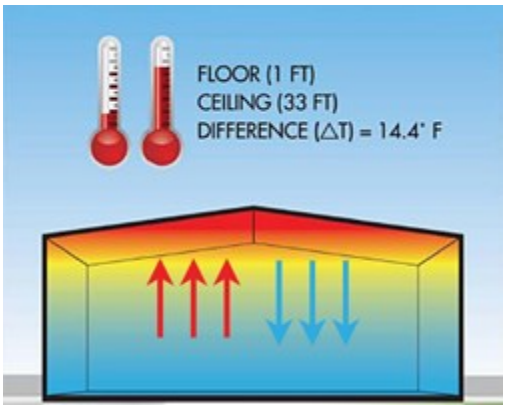

Figure 1-1. The movement of air with different temperature (Ramki, 2012)

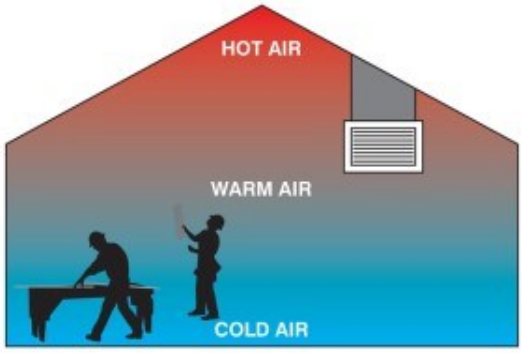

Figure 1-2. Thermal Stratification (Puravent, 2016).

Large buildings such as warehouses, shopping malls, distribution centers and high-ceilinged livestock barns are subject to a higher temperature difference between the higher and lower regions

of their space. The higher the ceiling, the more severe the temperature difference will be. The air temperature beneath the ceiling of a warehouse more than 5 m in height will be higher than that of a building with normal ceiling height (around 3 m) assuming both buildings have the same vertical temperature gradient and the same temperature at thermostat height (near the ground.) For example, if the temperature gradient is taken as 1 ˚C/m, the air temperature beneath the warehouse ceiling is more than 2 ˚C higher than that of the normal building.

1.1.2 Heating energy loss caused by thermal stratification

As stated above, warm air will accumulate in the upper region of indoor space if the building's heating device is set to maintain an acceptable temperature at thermostat level. One of the critical factors in determining heat transfer through the building envelope is the difference in temperature between indoor and outdoor air. The large temperature difference caused by thermal stratification leads to high heat flux through the walls and roof. Furthermore, the flat geometry of large warehouses means the roof area makes up a higher percentage of the envelope area compared to residential buildings. This implies a relatively larger portion of heating energy is lost through the roof in warehouse buildings than in residential buildings. In conclusion, the high temperature beneath the ceiling and the large area percentage of the roof of warehouse buildings leads to severe heating energy waste.

1.1.3 Heating energy consumption in Canada

Canada experiences cold winters, heavy snowfall and severe wind chill due to its geographic location of high latitude. Most of its population and industry are located near its southern border.

Canada's harsh climate means intense heating is necessary to maintain human activity and industrial production. For example, in 2009, space heating made up 63% of residential energy use and 50% of commercial and industrial energy use in Canada (Behidj, et al., 2011). However, this also indicates that a large amount of energy could potentially be saved by improving energy efficiency. The energy-saving potential for the residential and industrial sectors is 470.6 PJ and 881.5 PJ respectively (Behidj, et al., 2011). The optimization of heating energy plays an important role in improving energy efficiency. Furthermore, thermal stratification is currently believed to be the largest cause of building energy wastage (Anodisers, 2015).

1.1.4 Other problems caused by thermal stratification

Thermal stratification also causes problems with regard to the comfort of the building's occupants. The uneven temperature distribution at different layers can be too cold for an occupant at a lower level and too warm for an occupant who stays at a higher position in the building. Furthermore, thermal stratification leads to a slower response in the thermostat's temperature control as hot air from the heaters tends to rise and accumulate in higher levels.

Thermal stratification is also a concern in factories and storage buildings. The products stored in some warehouses are temperature sensitive. For example, in large wine storage cellars, wine must be stored within a precise temperature range. Broiler and poultry buildings also have specific temperature control requirements. The need for temperature control in industrial warehouses is not limited to these examples.

Thermal stratification is also a concern in refrigerated buildings. The cold air must be distributed evenly throughout the building, as uneven temperature distribution will cause some areas of a refrigerated building to become overly cool.

Condensation is another problem that may be caused by thermal stratification as the lower region of the air is cooler and thus has a lower saturation point. Indoor swimming pools are one type of building which suffers from condensation.

1.2 Removal of thermal stratification

The key to removing thermal stratification is to circulate and mix the air from different strata. In residential buildings, a well-designed HVAC system can prevent the generation of thermal stratification. However, in most existing warehouse buildings, there are no specific design guides or standards in place to prevent the formation of thermal stratification. In addition, the installation of new HAVC systems to solve thermal stratification is not economically feasible.

Currently, the most straightforward and feasible method for eliminating thermal stratification is the installation of mechanical fans in the building to mix the air. Several types of fans which are specifically designed to eliminate temperature stratification are available on the market.

Traditionally, fans are used to increase indoor air speed during warmer seasons to encourage evaporation on human skin and cool the body. In summer, an installed mixing fan still can work as a cooling device. A local air speed of 3 m/s generated by a circulation fan is equivalent to a cooling effect of 7˚C. For office environments, where air speed should be limited to less than 1 m/s, the cooling effect is equivalent to 3 ˚C, saving about 20% in cooling energy (Aynsley R. , 2005).

1.2.1 Removal of thermal stratification by mixing fan

Ceiling fans are most commonly used to remove thermal stratification. The downwash propelled by the rotating foil drives the warm air downwards to mix with the cold air on ground level, countering the effects of buoyancy. As ceiling fans have long been used during summer to improve air movement, they are relatively cheap products which are widely available on the market. However, the efficiency of ceiling fans in removing thermal stratification remains unclear. Further research comparisons were required to investigate the effectiveness of ceiling fans.

Figure 1-3. A bucket fan mounted beneath the ceiling of the QT warehouse.

Axial turbine fans are another type of fan installed beneath the ceiling (ZooFans, 2015). They have a more compact size compared to traditional ceiling fans. The air flow from axial turbine fans has higher speed and is more concentrated. These characteristics mean the air flow from axial fans has further penetration length.

Bucket fans and ceiling fans have been commercialized on the marketplace. A new type of fan (HVLS) has emerged on the market which is also used to remove thermal stratification (MarcoAir, 2015) (Aynsley R. , 2005).

Wall-mounted fans are a relatively new type of fan designed to mix the air in large buildings. They are typically installed on the wall of the building which makes them easier to install and maintain compared to ceiling fans. Unlike ceiling fans, wall-mounted fans push cold air from a low level at an angle aimed at the center of the ceiling.

1.2.2 Problems of mixing fan

For industrial buildings which are sensitive to dust, air flow derived from fans is not preferable. Also, the draft flow from fans at occupant level can cause comfort issues. The generation of dust from different types of mixing fans remains a problem requiring further investigation.

It has been reported that destratification fans have been required to run at reduced speed as the draft disturbs fabric material in warehouses (Armstong, Chihata, & MacDonald, 2009). In office environments, air moving at a speeds equal to or higher than 1 m/s will disturb paper (Aynsley R. , 2007).

In addition to drafts, noise is also a concern. Some mixing devices are specifically designed to reduce the noise from the fan foil. For example, it has been proven that the noise level of the bucket fan (a small axial fan) can be reduced if the fan's foil is designed to have the characteristic features of owl wing feathers (Chen, et al., 2012).

1.3 Study objective and thesis outline

Considering the severe waste of heating energy and other problems caused by thermal stratification in large buildings, the importance of mixing fans in solving these problems has been increasingly recognized by the industry. Reports discussing this issue have been released by fan manufacturing companies. Previous research on warehouses has been focused on analysis of temperature measurements (Porras-Amores, Mazarrón, & Cañas, 2014) (Said, MacDonald, & Durrant., 1996). However, research has not yet been conducted which focuses on comparing the working performance of different types of mixing fans in eliminate thermal stratification. Furthermore, research with the aim of determining optimal installation rules for different types of building spaces and fans has not yet been done. Based on these considerations, the objectives of this thesis research are listed as follows:

- Take field measurements to determine the conditions of thermal stratification in warehouses in the Montreal region.
- Develop a method to simulate large warehouses with the processes of both heating and fan mixing in CFD.

- Explore the effectiveness of different mixing fan settings in reducing thermal stratification in large warehouses.

The study methods, field measurements, and CFD simulations proposed in this research project are necessary in the investigation of this problem. It is expensive and labor intensive to test different types of fans in different types of large buildings under different working conditions. The experimental process is very expensive and time-consuming. In contrast, these tests can be resolved by simulating different fan setting scenarios in CFD.

This chapter focuses on giving a brief introduction to thermal stratification as well as general information about mixing fans and the warehouses under investigation in this study. Chapter 2 is a literature review of the previous research and documented reports about thermal stratification and destratification. Chapter 3 presents the methodology of this study, which includes field measurement and CFD simulation. Chapter 4 presents the results and discusses them. Chapter 5 focuses on the application and analysis of different mixing fan settings. Chapter 6 draws a conclusion and provides suggestions for further research. Appendix about the other detail information is attached at the end of this thesis.

CHAPTER 2. LITERATURE REVIEW

2.1 Thermal stratification during heating season

Thermal stratification has been investigated in several previous studies. Boon and Battams (1988) reported that a temperature difference of up to 10 ˚C between the floor and the ceiling had been measured in a broiler building with a height of 3.4 meters. In a 5.2 m tall poultry building with a heater and low-speed ceiling fan examined by Bottcher et al. (1988), a temperature difference of 18 ˚C was observed between the ceiling and the floor.

The climatic structure in which warm air stays above and cold air stays below is a common phenomenon in nature too. Temperature inversion is encountered in the study of meteorology. As reported by Wei et al. (2013), when there are heating effects at higher air volume and a cooling process occurring on the ground due to the effects of radiation, temperature inversion can persist for a long period of time.

One of the important characteristic parameters in evaluating thermal stratification is the vertical temperature gradient. Boon and Battams (1988) reported that the greater the temperature gradient, the more severe the thermal stratification. Aynsley (2007) reported a temperature gradient of 1.4 ˚C per m from a building which was heated at floor level. Forrest and Owen (2010) mentioned a vertical temperature gradient of 1 ˚C per m in a warehouse case study.

The temperature gradient is not vertically uniform in large buildings. As Said et al. (1996) reported in a measurement of several aircraft hangars, there are two layers with different temperature gradients. The lower layer, which spans from floor level to 2 m in height, has a steeper temperature gradient of 0.8 to 2.6 ˚C per m. The upper layer, which spans from the 2 m mark to the ceiling, tends to have a more uniform temperature of around 0.5 ˚C per m. This characteristic of two-layer distribution has been observed in various type of hangars with varying roof geometry, types of doors and ceiling height. Furthermore, Said et al conclude that the vertical temperature profile is not significantly affected by factors such as roof geometry, door type or ceiling height. Another study by Aynsley (2005) came to a similar conclusion about the two-layer feature of temperature distribution. According to the on-site measurement of a shipping and receiving warehouse, there

is a uniform temperature layer below the ceiling spanning up to 2 m. The difference between these two studies is that the latter does not show a steep temperature gradient in the lower layer. In Aynsley's (2005) study, the largest temperature gradient occurred at the transient boundary between the two layers.

Under the same temperature gradient, the height of the ceiling is also a factor in affecting thermal stratification. All of the industrial warehouses in this study have ceilings with heights greater than 5.8 m.

Thermal stratification can also be beneficial during the cooling season. The warmer upper layer in the building acts as a buffer zone which prevents the heat from transferring from the higher layer to lower and cooler layers. Hence, as reported by Said et al. (1996), a lower cooling load is required to maintain a suitable temperature in the building's occupant zone due to thermal stratification.

2.2 Removal of thermal stratification

Armstrong et al. (2009) reported a 4 ˚C decrease in ceiling temperature and 1.5 ˚C increase in floor temperature when utilizing five ceiling fans to mix the air in a case study. The final temperature difference between the ceiling and floor was reduced to 0.5 ˚C.

Canvas boots have also been used to eliminate thermal stratification. Said et al. (1996) reported that canvas boots mounted on a heater outlet were used to deliver hot air to the ground level of an aircraft hangar.

2.3 Heating Energy consumption

A 26.4% reduction in gas usage was achieved by destratification in a distribution warehouse as reported by Aynsley (2005) in a case study. Armstrong et al. (2009) presents a 19.3% reduction in the use of heating energy in a warehouse with five destratification fans operating inside. Said et al. (1996) predicted that, in cases with no destratification, an extra 38% of heating energy is required for an 8 ˚C temperature difference in hangar buildings.

The flat cuboid geometry of warehouses gives them a higher surface area to volume ratio compared with residential buildings. Based on results from the website CLEAR (2016), a building with higher surface area to volume ratio is subject to heating energy loss. To some extent, this is similar

to the distribution of animal body size in nature. According to Allan's law, minimization of the exposure surface in cold climates can minimize heat loss from body (Allen, 1877). As mentioned in Bergmann's rule (Blackburn, M., J. Gaston, & Natasha, 1999), animals in higher latitude and colder regions tend to have larger body sizes so that the surface to body ratio is smaller and more efficiently keeps the heat from escaping.

2.4 Temperature measurement of thermal stratification

In an on-site measurement of thermal stratification conducted by Said et al. (1996), thermocouple trees were used to measure temperature from points along vertical lines. They reported that the thermocouple trees were composed of type T copper-constantan thermocouples which are tied to nylon rope. The thermocouples were about a 5 cm distance from the nylon rope. The uncertainty of the type T thermocouples used in this study was reported to be ± 0.1 ˚C. Thermocouple trees were also used in the measurement of temperature distribution in a ceiling-mounted cassette-type indoor unit (Lian, Qi, Liu, & Song, 2010).

2.5 Numerical simulation

Momoi et al. (2004) conducted an experimental and numerical study on the airflow of ceiling fans. In the study, the velocity components from designated spots were measured and compared with the numerical simulation. The study tested the velocity distribution when the ceiling fan was running both downward and upward. In order to minimize the influence of the walls on the air flow, the experiment site was conducted in a 15 m × 15 m space.

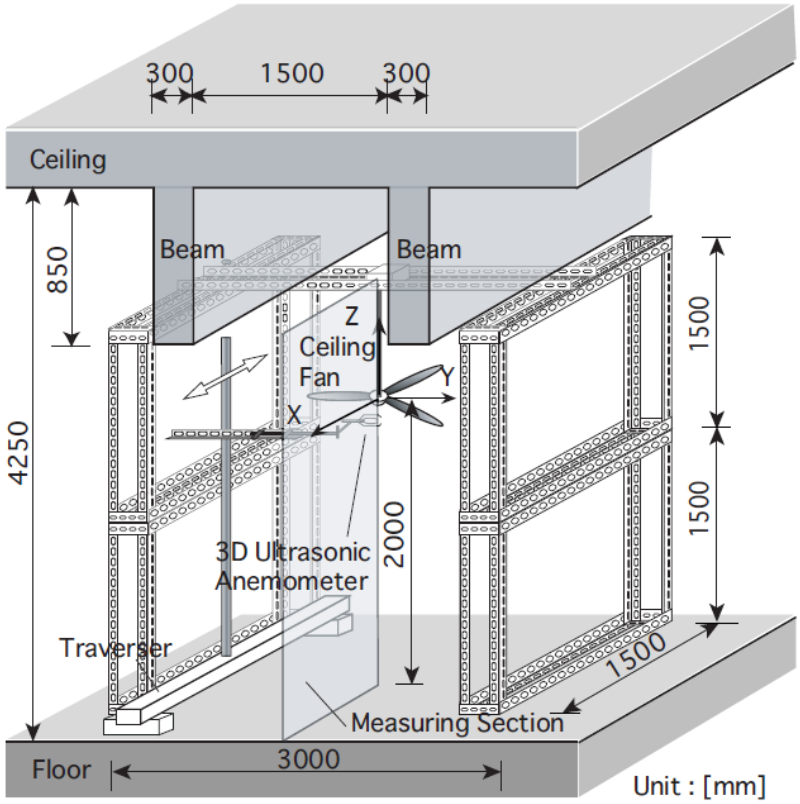

Figure 2-1. Experiment setting for Momoi's (2004) study on velocity of ceiling fan.

Zhu et al. (2014) presented a numerical method for simulating the rotation of a ceiling fan in a room. In the study by Zhu et al. (2014), the rotating reference frame method was used to simulate the rotation of a ceiling fan with a specific designated speed. In the CFD mesh, the center axis of the ceiling fan was located at the symmetrical axis of a cylindrical domain (Figure 2-2). A rotational speed relative to the domain outside of the cylinder was defined by the user (ANSYS, 2009).

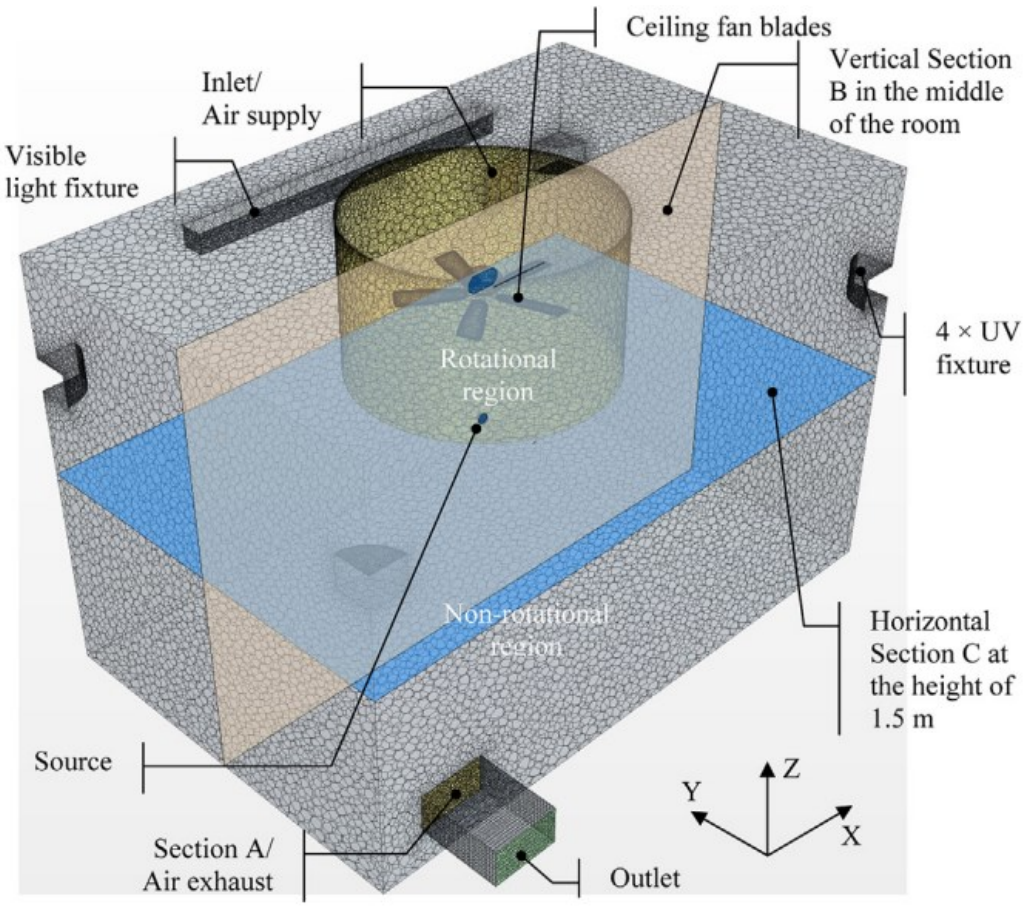

Figure 2-2. The ceiling fan inside a cylindrical mesh for single rotating reference method (Zhu, Srebric, Rudnick, Vincent, & Nardell, 2014).

The heaters in the warehouses are the source of heating energy. A previous study by Forrest and Owen (2010) developed a method to simulate forced air heaters. In their model, the forced air heater is composed of a heat source and a pressure jump surface. The heat source can be set to generate a constant value of heat. Meanwhile, the pressure jump surface pushes the air through the heater.

Li et al. (2009) conducted a study on a train station by CFD. In the study, various design schemes for the HVAC system were compared. The different schemes included various distributions of artificial air diffuser pillars. Meanwhile, different turbulence models were tested in simulating the air flow inside the train station. Li et al. (2009) discovered that the k-ε turbulence model with buoyancy source term turned on performed well in the simulation of indoor air flow.

2.6 Summary

In summary, thermal stratification is a common phenomenon in large warehouse buildings. It is one of the factors that causes heating energy waste in warehouse buildings. Earlier investigators have conducted a series of studies on thermal stratification in warehouse buildings. These previous studies were based on the measurement of existing buildings.

In the industry, there are emerging methods of reducing thermal stratification by installing various mixing fans in the buildings. An investigation is required to compare and evaluate the effectiveness of different fan types and installation methods in achieving thermal destratification. Experimental testing and measurement of different fan installations in real warehouses is expensive and time-consuming to carry out. CFD provides a method of simulating temperature conditions in warehouses with various mixing fan installations.

CHAPTER 3. METHODOLOGY

In this study, on-site measurements were conducted to acquire temperature information from buildings which suffered from thermal stratification. Once data was taken from field measurements and building information was collected, a series of numerical simulations were done with the aim of reconstructing the buildings' thermal stratification conditions. The on-site measurement data validated the numerical modelling of the buildings. Based on the CFD model, which can represent the thermal stratification of the measured buildings, other cases which featured a mixing fan running in the building were simulated to investigate the effectiveness of the various types of fan settings for achieving destratification.

3.1 Field measurement

Field measurement is necessary to learn the temperature conditions of large buildings for analysis. In order to investigate the temperature conditions in large warehouses during the heating season in Canada, field measurements were taken for this study during winter of 2014 and 2015.

In total, five buildings were chosen at which to take field measurements. They are referred to as the QT, MG, DT, XL and KS buildings in the following text of this study.

Table 1. General information on the five measured buildings.

Name	QT warehouse	MG stadium	DT logistics warehouse	XL distribution center	KS warehouse
Dimension (m)	12.01×9.3×6.62	88×53	74×31.8×5.8	124.85×72.38×9.20	41.12×17.5×6.85
Outdoor Temperature:	-21.5 ˚C	-13.1 ˚C	-7.0 ˚C	-10.7 ˚C	-6.7 ˚C
Heating Device	Electronic force air heater + fan	HVAC system	Electronic infrared heaters	Infrared heater and forced air heater + fan	HVAC system + baseboard heater + fan

QT warehouse

The QT building is a storage warehouse for a company which manufactures HAVC components. It is composed of two separate warehouses which are both 10.7 m by 12.2 m in area and 6.62 m in height.

About half of the area of both warehouses is divided horizontally into two sections (an upper section and a ground section) to maximize the amount of storage space. In the room where the measurements were taken, space is heated by an electronic heater hanging beneath the ceiling which pushes air downward. There is a small internal fan at the inlet of the heater to push air through the electronic coil and carry the heat into the room. There is also a bucket fan installed by the warehouse owner running beneath the ceiling to mix the air in the warehouse.

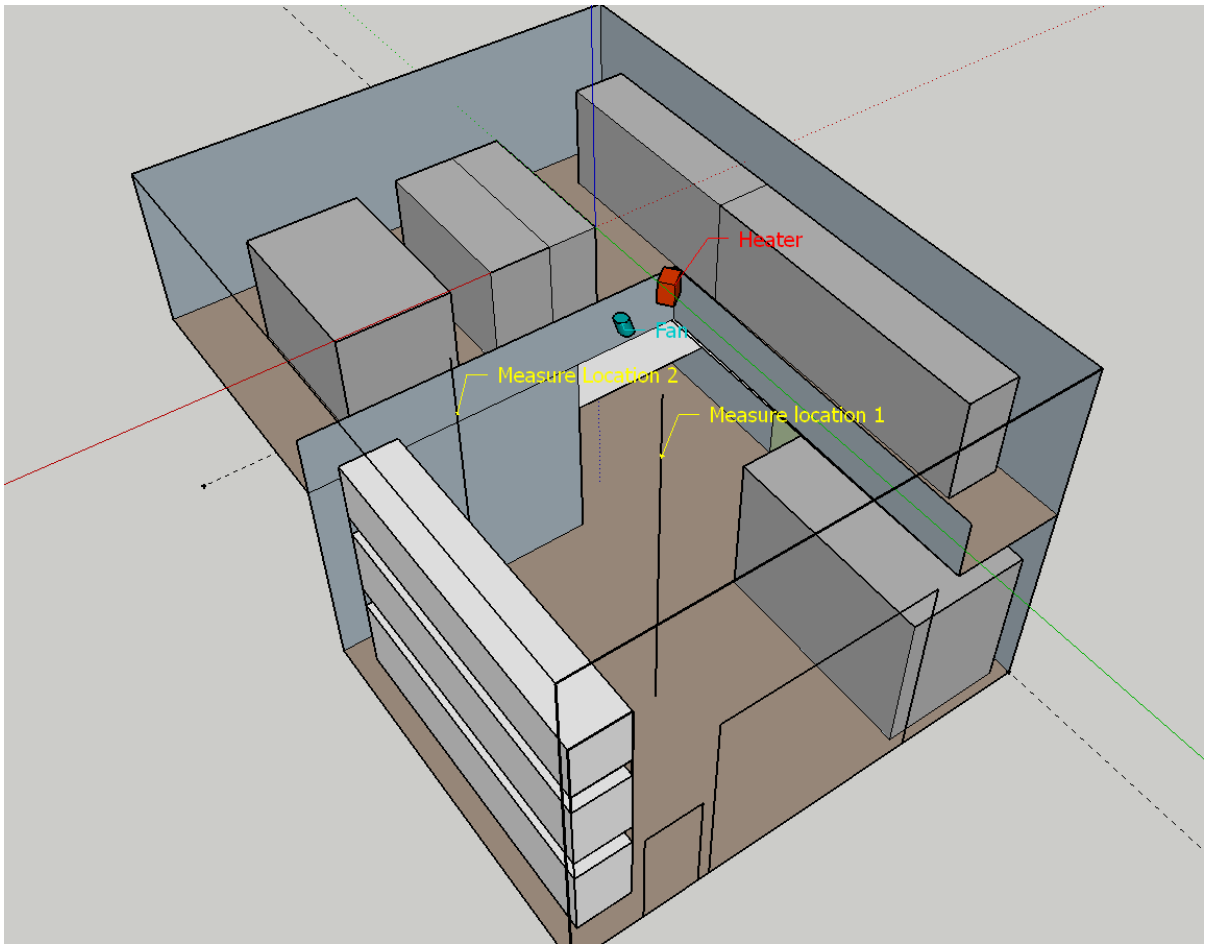

(a)

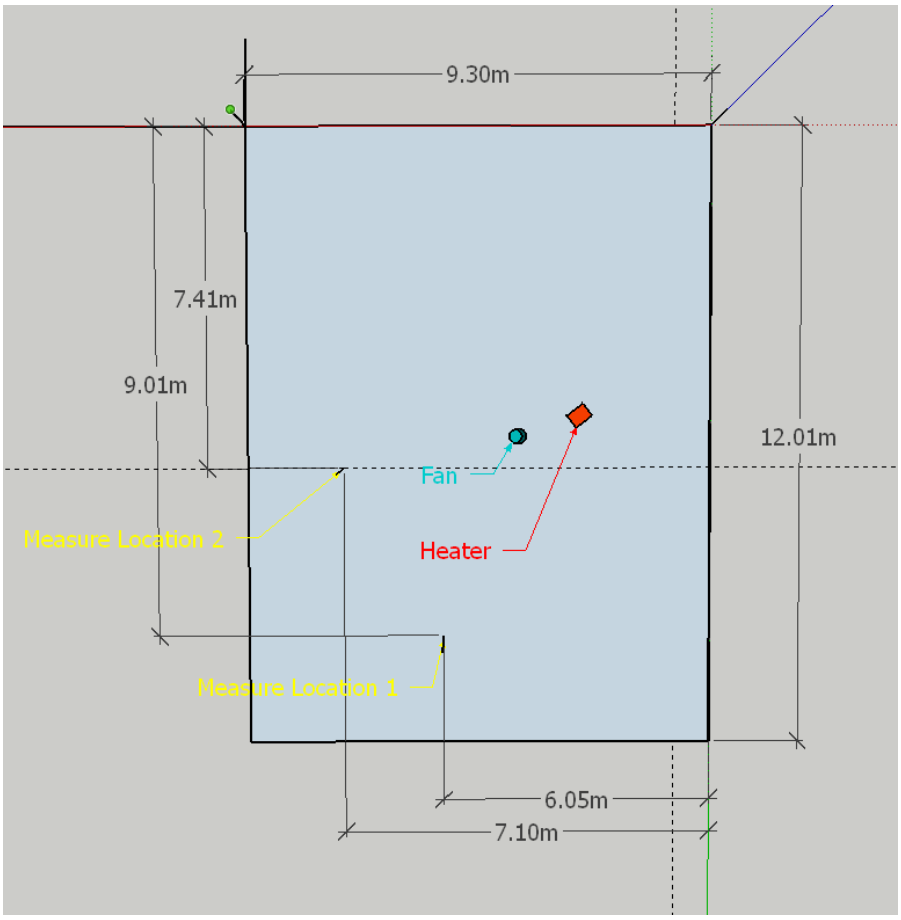

(b)

Figure 3-1. Schematic diagram of the QT warehouse layout.

MG stadium

The second building, MG, is the stadium of a university in downtown Montreal. Its length and width are 88 m and 53 m respectively. For security reasons and due to the stadium's regulations, height was not taken during the measurement. The stadium uses an HVAC system to maintain air quality. On the side walls, there are two rows of air diffusers injecting air into the stadium, and 12 further fabric diffusers are distributed beneath the ceiling. The fabric diffusers blow the conditioned air downward.

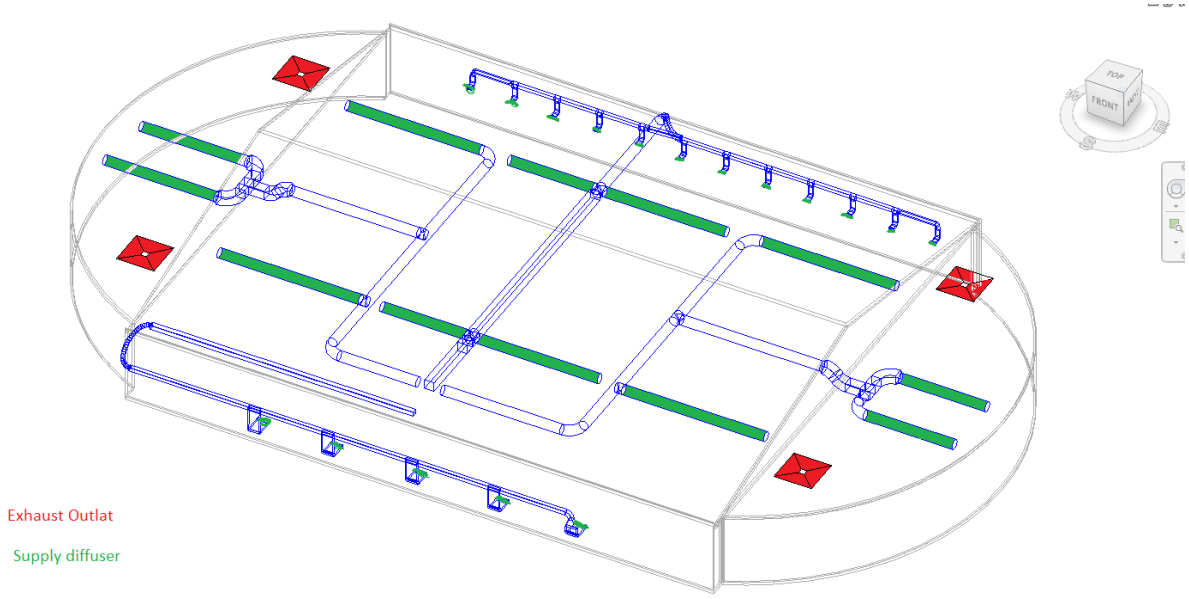

(a)

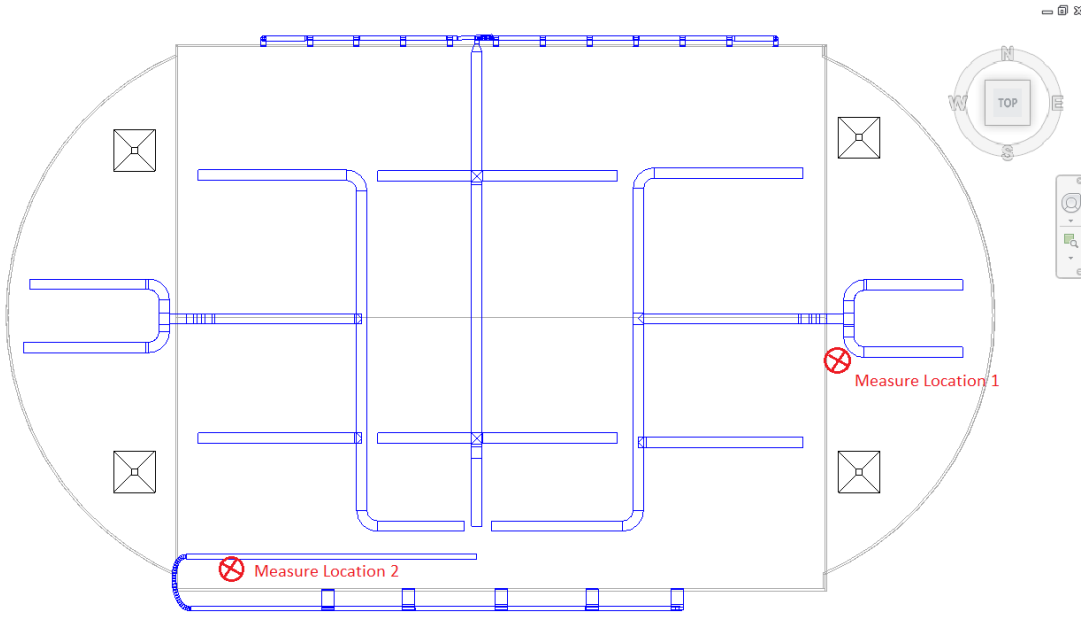

(b)

Figure 3-2. (a): Schematic diagram of the MG stadium. The fresh air duct system has been marked in green. (b): Top view of the MG Stadium. The two measurement locations have been marked in red.

DT warehouse

The third building, the DT Logistics warehouse, is located to the north of the city of Montreal. Its length, width, and height are 74 m, 31.8 m, and 5.8 m respectively. The warehouse is heated by

infrared heaters hanging beneath the ceiling. Six further heaters are distributed along the exterior parameter of the warehouse. In this building, it is the surface of the racking and wall are heated first and the heat is then transferred to the indoor air.

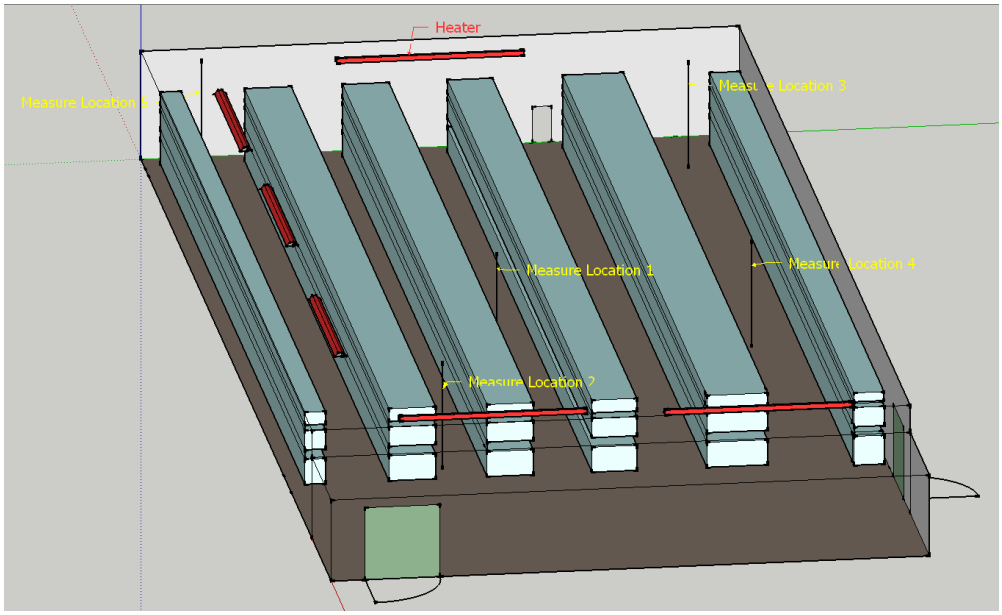

(a)

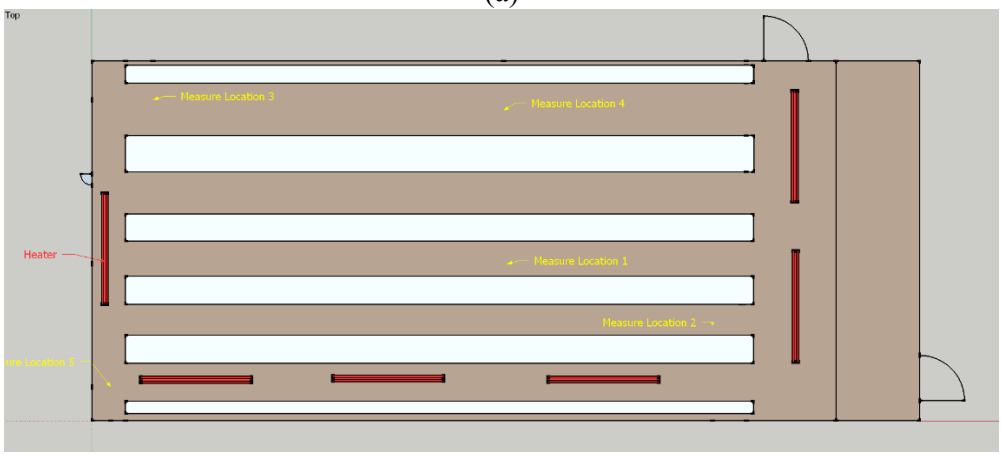

(b)

Figure 3-3. (a): Schematic diagram of the DT warehouse. (b): Top view of the layout of the DT warehouse.

XL warehouse

The fourth building, the XL warehouse, is a storage and distribution center for raw paper. The length, width, and height of the warehouse are 124.85 m, 72.38 m and 9.2 m respectively. There

are two types of heaters (infrared heaters and forced air heaters) installed in the building. There are also 18 standard ceiling fans installed in the building to mix the air.

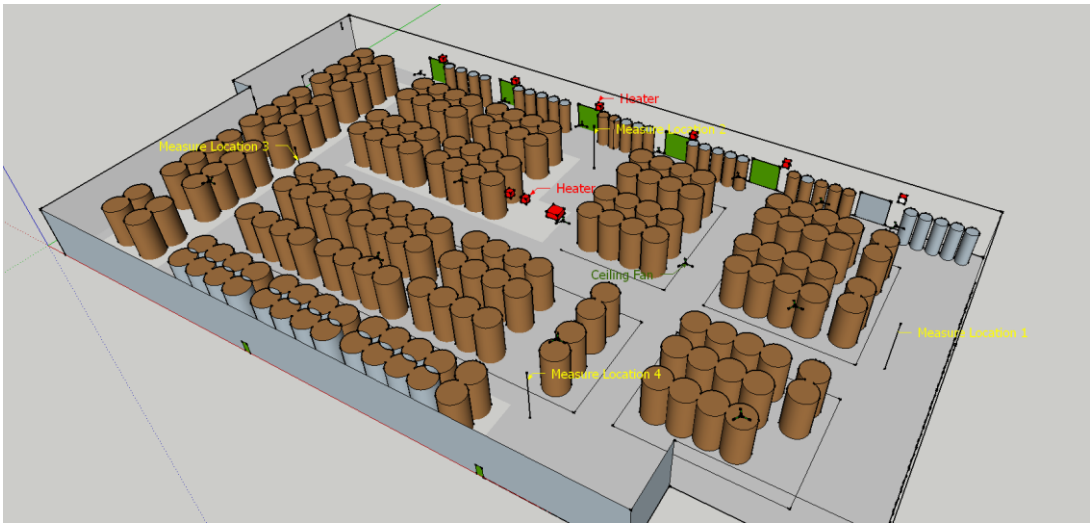

(a)

(b)

Figure 3-4. (a): Schematic diagram of the XL warehouse. (b): Top view of the layout of the XL warehouse.

KS warehouse

The fifth building, the KS warehouse, is located in the Laval region of greater Montreal. The length, width, and height of the building are 41.12 m, 17.5 m and 6.85 m respectively. The KS building is heated by warm air which is pumped from the mechanical room as well as six baseboard

heaters beneath the windows on the exterior wall near the ground level. Fresh air from the fabric diffusers has a constant temperature of 40 ˚C and a supply volume flow rate of 100 cfm per outlet. There are 15 outlets in total, meaning 1.4158 m^3/s of total volume flow rate. The temperature of the HVAC system was set to 23 to 24 ˚C. The air is mixed by eight fans: six bucket fans and two ceiling fans. The two ceiling fans work at low enough speeds as to be negligible. The warm fresh air is projected horizontally into the room at a high level. The six baseboard heaters generate warm air below the windows.

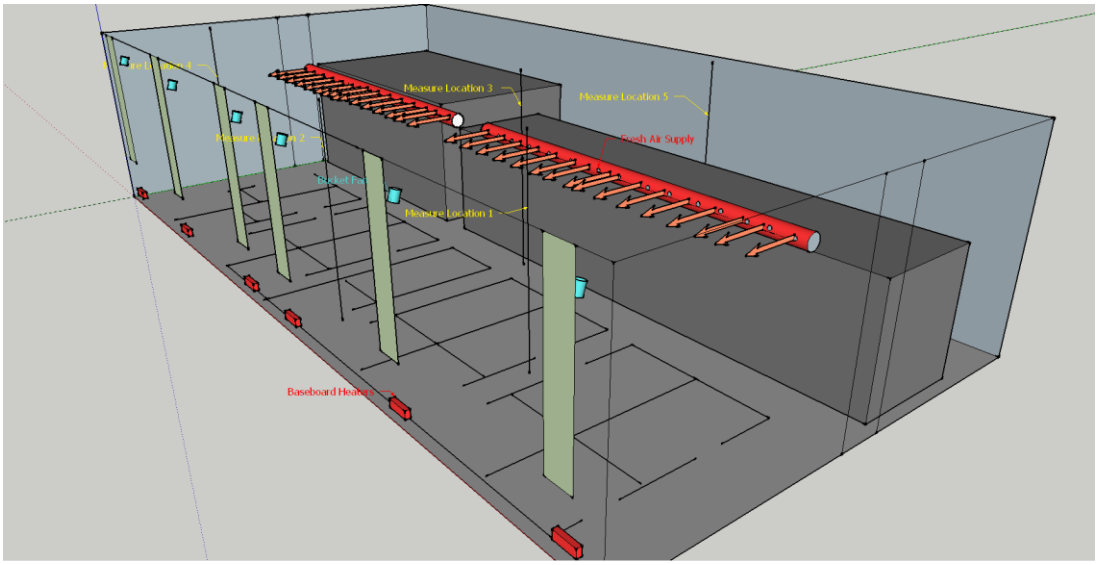

(a)

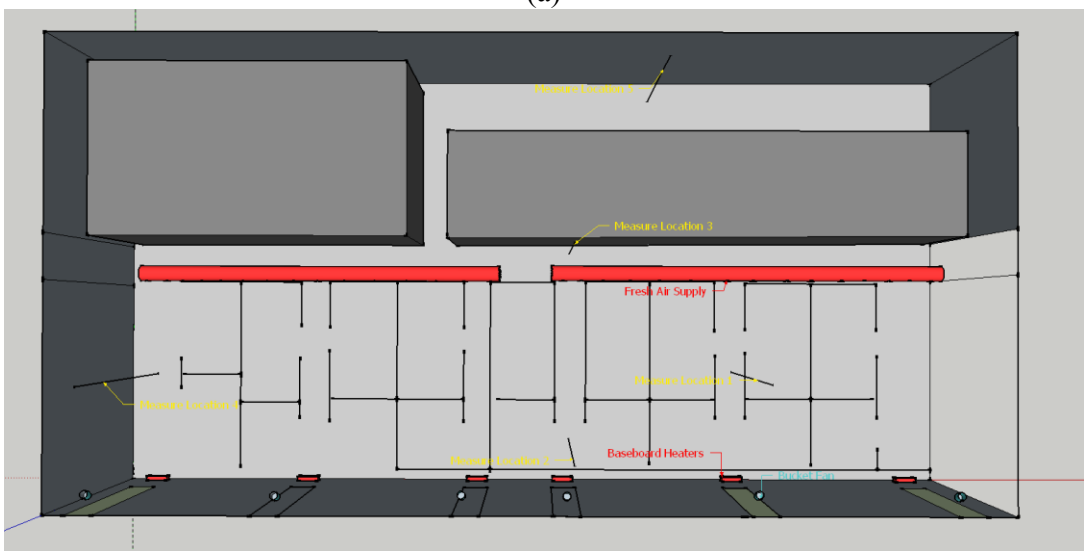

(b)

Figure 3-5. (a): Schematic diagram of the KS warehouse. (b): Top view of the KS warehouse layout and the measurement locations.

3.2 On-site measurement setup

3.2.1 Vertical temperature profile measurement

The thermocouple trees used in this study were constructed out of thermocouple wire and cotton rope. Since the heights of the buildings to be measured were not equal, the interval distance between each thermocouple was not fixed. There are knots on the rope, allowing rubber bands to be used to adjust the rope length and the position of the thermocouple to the rope. In this way, the vertical distance among thermocouples was adjusted according to the ceiling height of the measured building. At least eight points along the vertical line were measured (Table 2. Height of thermocouples during the field measurement.). Type T copper-constantan thermocouples were chosen for this study due to their accuracy (their margin of error is ± 0.5 ˚C.) (ASHRAE, 2013).

Thermocouple trees should not be placed too close to heating sources, lighting devices, doors or windows because the temperature in these areas is strongly influenced by the warm or cold air flow. These arrangements make the measurements more representative of the overall indoor temperature distribution in the building. A data acquisition system was used in this study to collect data from the thermocouple. Temperature readings were taken every 2 seconds. The full process of measurement lasted for more than two hours.

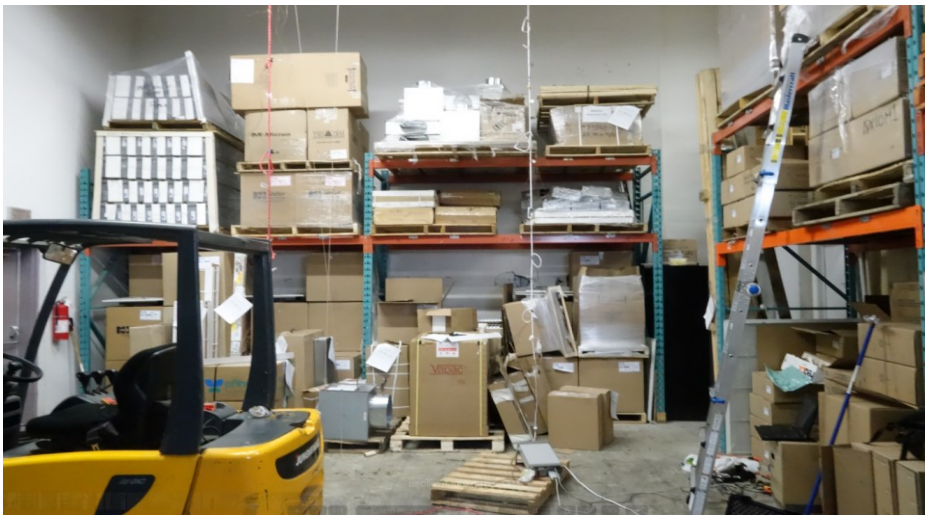

Figure 3-6. Two vertical ropes (red and white in color) with thermocouples attached to them during the measurement process.

As shown in Figure 3-6, 12 thermocouple joints were distributed on a cotton rope with a specific length. The thermocouples' height was not fixed on the cotton line. They were tied to the line by rubber bands so that the length interval could be adjusted according to the building being measured.

Table 2. Height of thermocouples during the field measurement.

Warehouse		Height of thermocouples (Unit: m)											
QT	Location 1	5.93	5.33	4.73	4.13	3.53	2.93	2.33	1.73	1.13	0.7	0.14	0.07
	Location 2	5.90	5.30	4.70	4.10	3.50	2.90	2.30	1.70	1.10	0.70	0.22	0.03
MG	Location 1A	6.95	5.78	4.78	3.86	3.18	1.96	1.16	0.16				
	Location 2B	7.64	6.84	5.74	4.78	3.56	2.86	1.90	0.80				
DT	Location 1-5	5.80	5.20	4.60	4.00	3.40	2.80	2.20	1.60	1.00	0.63	0.09	0.00
KS	Location 1	6.25	5.65	5.05	4.45	3.85	3.25	2.65	2.05	1.45	0.85	0.27	0.00
	Location 2	6.35	5.75	5.15	4.55	3.95	3.35	2.75	2.15	1.55	0.95	0.42	0.00
	Location 3	6.65	6.05	5.45	4.85	4.25	3.65	3.05	2.45	1.85	1.25	0.75	0.30
	Location 4	6.39	5.79	5.19	4.59	3.99	3.39	2.79	2.19	1.59	0.99	0.48	0.10
	Location 5	6.30	5.70	5.10	4.50	3.90	3.30	2.70	2.10	1.50	0.90	0.35	0.02
XT	Location 1	8.68	7.88	6.78	5.83	4.70	3.88	2.91	1.93	0.93	0.50	0.00	
	Location 2	8.58	7.78	6.68	5.73	4.60	3.78	2.81	1.83	0.83	0.40	0.00	
	Location 3	8.68	7.88	6.78	5.83	4.70	3.88	2.91	1.93	0.93	0.50	0.00	
	Location 4	8.78	7.98	6.88	5.93	4.80	3.98	3.01	2.03	1.03	0.60	0.00	

Table 3. Measurement duration at each location.

Warehouse		Measurement duration (Unit: s)
QT	Location 1	1101
	Location 2	
MG	Location 1A	612
	Location 2B	570
DT	Location 1	472
	Location 2	574
	Location 3	348
	Location 4	604
	Location 5	182
KS	Location 1	1052
	Location 2	694
	Location 3	690
	Location 4	844
	Location 5	1604
XT	Location 1	1422
	Location 2	3558
	Location 3	834
	Location 4	1096

3.2.2 Building information collection

General building information was recorded, including the height, length and width of the warehouses, the size of the doors and windows, and connections to neighboring rooms or buildings. Through communication with the warehouse owners, some critical information can be collected. For example, the date of construction can be learned from the building owner. The racking in a warehouse occupies a large amount of the total area, so the racking layout should also be recorded during field measurements. Furthermore, the position of the heating devices should also be recorded. Measurements for the same surface should be taken at different heights. The indoor surface temperature measurements include the ground, wall, window and ceiling temperature taken by FLIR thermal cameras. The building envelope information can be collected from the owner or engineer.

3.3 Numerical approach

This section provides an overview of the methodology of computational fluid dynamics used by this thesis. The methodology of computational fluid dynamics is a set of numerical methods which uses digital computers to approximate and solve the partial differential equations of fluid dynamics. In traditional experiments, a real model has to be made and a series of measurements have to be taken in the model. Computational fluid dynamics can also be seen as an experiment, but one which is conducted in a digital computer which simulates the movement of the fluid and its interaction with the environment. All the CFD simulations in this study were done using ANSYS Fluent which is a commercial software package.

3.3.1 Physics

To simulate airflow, the CFD solves the conservation equations. They are the laws of conservation of mass, conservation of momentum and conservation of energy. The law of conservation of mass regulates mass continuity in the fluid. Within a control volume, the net change of the mass inside should be equal to the sum of flow in and out of the boundary of that control volume. The law of conservation of momentum states that the change of momentum of the fluid in a control volume should be equal to the sum of the net momentum change of the fluid through the boundary and the net momentum enforced on the control volume by the external force. The law of conservation of energy states that the total energy in a system should remain constant even when the energy transforms from one form into another. In this study, the air flow speed is low and also the density variation is negligible so the air flow was considered as an incompressible flow.

3.3.2 Governing equation

The physical variables in the CFD model are governed by the conservation equations. The conservation equations for incompressible flow are listed as follows (Stoakes, 2009):

$$\nabla \cdot \vec{v} = 0 \qquad (1)$$

$$\frac{\partial \vec{v}}{\partial t} + \vec{v}\nabla \cdot \vec{v} = -\frac{1}{\rho_0}\nabla p + \frac{\mu}{\rho_0}\nabla^2 \vec{v} + S \tag{2}$$

$$\frac{\partial T}{\partial t} + \vec{v} \cdot \nabla T = \alpha \nabla^2 T \tag{3}$$

In the conservation equations above, ν, T, ρ represent velocity, temperature and density respectively. The S, α, p, and t stand for the source term, thermal diffusion coefficient, pressure and time respectively.

Simulations in this thesis used the Boussinesq approximation to simulate buoyancy-driven flow. Buoyancy-driven flow is the major cause of natural convection. Natural convection leads to thermal stratification. The Boussinesq approximation assumes that the variation of density in a fluid depends only on the temperature of the fluid, so that the density is in linear relation to the temperature. The Boussinesq approximation method is easy to use in simulation compared with other density models. The thermal expansion coefficient β (Stoakes, 2009) is defined as

$$\beta = -\frac{1}{\rho}(\frac{\partial \rho}{\partial T})_p \tag{4}$$

In this equation, ρ and T are density and temperature respectively. The thermal expansion coefficient was required as an input for the simulation when using the Boussinesq approximation. The Boussinesq approximation assumes that the density is in linear relation to the temperature. Under this approximation, the Boussinesq approximation (Stoakes, 2009) can be expressed by:

$$\rho_0 - \rho = -\rho_0 \beta (T - T_0) \tag{5}$$

In the above equation, ρ_0 and T_0 are the reference values of density and temperature respectively.

After taking the sum of the force of gravity and the Boussinesq approximation as the source term, the momentum conservation equation is given by (Stoakes, 2009):

$$\frac{\partial \vec{v}}{\partial t} + \vec{v}\nabla \cdot \vec{v} = -\frac{1}{\rho_0}\nabla p + \frac{\mu}{\rho_0}\nabla^2 \vec{v} + \vec{g} - \beta(T - T_0)\vec{g} \quad (6)$$

Where μ is the dynamic viscosity.

3.3.3 Discretization

The governing equations of fluid dynamics use the continuum assumption. This assumption states that in a fluid, physical properties such as velocity, temperature and pressure all have specific values at any given point which are continuous with adjacent points. In computational fluid dynamics, this continuum assumption is replaced by discretization. Discretization assumes that within a small finite space, physical properties will have the same value. Under this assumption, the partial differential form of the governing equations of the fluid dynamics can be transformed into a set of algebraic equations. The algebraic equations are solved by numerical methods. And hence, numerical solutions for the governing equations can be accomplished.

There are three common types of discretization. They are the finite difference method, the finite element method and the boundary element method.

3.3.4 Turbulence Model

Indoor air movement is turbulence flow. With the turbulence model established in CFD, the flow characteristics generated by the turbulence can be simulated.

The model for turbulence used in this thesis is the standard k-ε turbulence model. The k-ε turbulence model performs more accurately in predicting the stratification caused by buoyancy (Nielsen, 1998). In Momoi's (2004) study of ceiling fans, the standard k-ε two-equation turbulence model was used to predict the velocity field around the ceiling and the results fit the experiment's measurements well. In this turbulence model, specific transport equations were designated to calculate k (the turbulent kinetic energy), and ε (the turbulent dissipation rate). The turbulent kinetic energy and the turbulent dissipation rate are used to calculate the turbulence viscosity for the momentum conservation equation.

For numerical simulations of indoor air flow, research by Mathews, E. H. suggests that the k-ε turbulence model is the most practical (Mathews, 1989). This turbulence model is also used in the study of numerical simulations of ceiling fans in Momoi's (2004) research.

3.3.5 Grid

The entire computational domain is deconstructed into small elements. Each element has its own set of physical variables during the numerical simulation. There are two types of grid: structured grids and unstructured grids. Structured grids use a systematic method for dividing the domain. For example, a grid which is composed of uniformly sized cubic mesh is a structured grid. On the other hand, the grid cells do not have a uniform pattern.

The grid resolution should be fine enough to catch small-scale flow features. For areas where the velocity gradient or temperature gradient are estimated to be large, a finer mesh resolution should be deployed so that the grid is sufficient to catch the flow features in these complex parts of the domain. In this thesis, the fan body, the heater, the inlet and the outlet of the model all have much finer mesh compared to the empty volume of space in the room which contains only air.

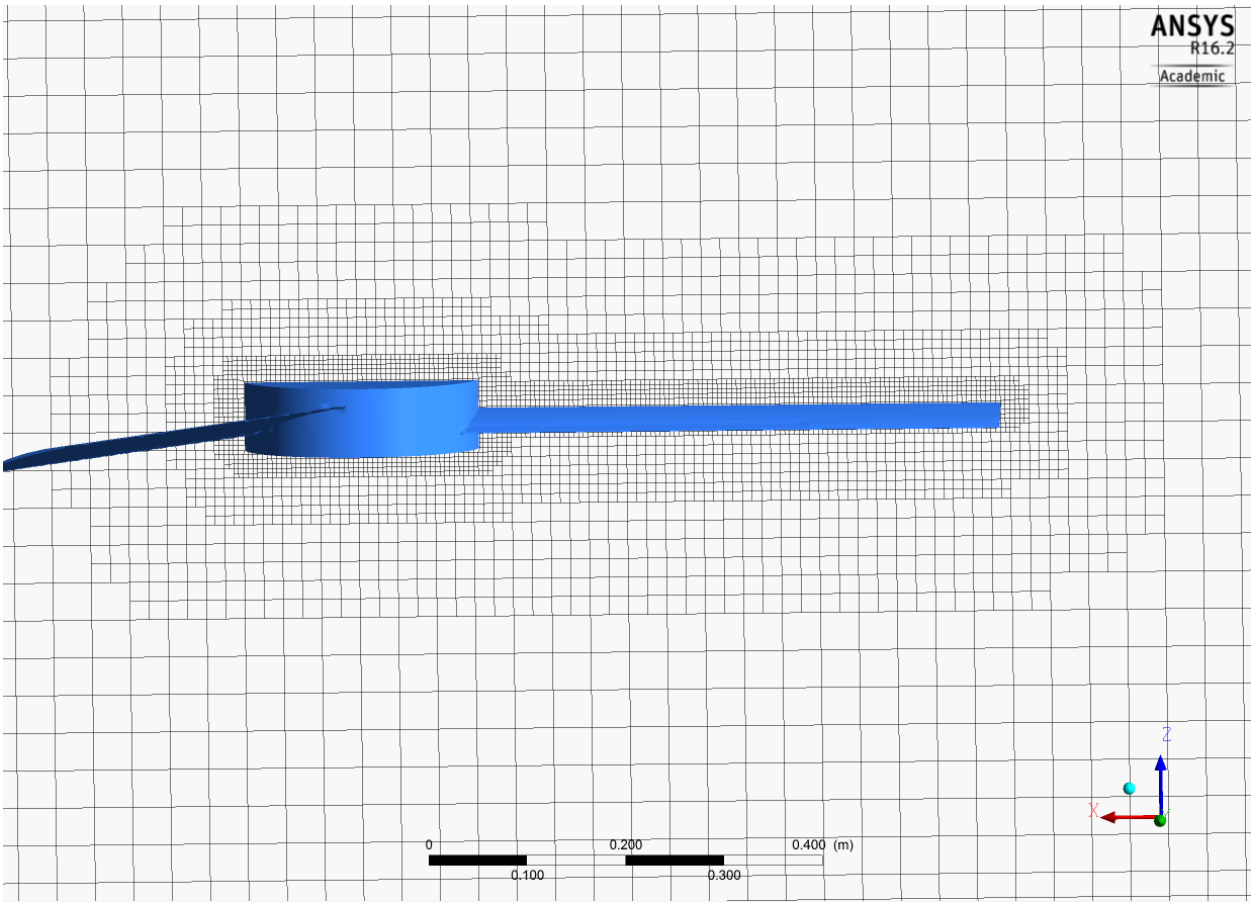

Figure 3-7. Mesh around the fan blade.

However, the grid resolution cannot be refined indefinitely. The greater the fineness of the mesh, the more time required to do the numerical simulations using the limited computational resources available.

3.4 Model setup and simplification

3.4.1 3D modeling

Two of the five investigated warehouses were chosen for CFD simulations. They are the QT and KS warehouses. The temperature measurement data of the QT building revealed that it has the most severe thermal stratification of the five measured sites. Furthermore, its heating device, which is a forced air heater, is the most common heating method used by the warehouses. Of the five buildings investigated, the KS building offered the most complete information on the building

envelope, the capacity of the heating device, and the various layout charts available. Hence, these two sites are the most representative and suitable cases for the thermal stratification simulation.

The geometry of the buildings in this thesis was modeled entirely using the ANSYS Geometry component. In the process of creating 3D models of these two warehouses, several simplifications were made to the building's geometry. The racking in the warehouse occupies a large part of the building's volume, so the stocked freight and the racking in the warehouse were simplified into empty square blocks. Inside of the blocks representing the racking, no mesh was generated. Walls with a certain thickness in reality were replaced by surfaces without thickness.

The buildings were modeled according to their real size with no scaling. The fabric diffuser in the KS building was simplified into two horizontal cylinders with 15 ducts opening on each surface.

The ceiling fan was modeled according to Matsushita Electric Industrial's FM131H-W model. It is the same ceiling fan used for measuring and modeling ceiling fan velocity in Momoi's (2004) study. The ceiling fan is simulated by single rotating reference frame method (ANSYS, 2009). For the bucket fan, the geometry was modeled according to the Zoo fan company's H30 model.

3.4.2 Boundary condition

In this study, boundary conditions on walls and roofs are set according to the building envelope's R value and the outdoor weather. For indoor space in CFD simulations, various kinds of boundary conditions are available. Li et al. (2009) applied constant temperature boundary conditions in a CFD study for a large train station building. Qi et al. (2013) also applied constant temperature boundary conditions in a simulation of full-size chamber. Wang et al. (2013) applied a constant heat transfer coefficient (U values) condition to simulate the heat exchange between the indoor and outdoor air.

One of the objectives of this study is to investigate the effects of fans on temperature distribution and then change the heat exchange between two sides of the wall. Therefore, constant heat transfer coefficient boundary conditions were chosen for the wall and the roof. The exterior boundary of the building is the main area for heat exchange between the indoor and outdoor air. The wall was simulated by a surface containing material with a specific thermal conductivity. Furthermore, a value was also set for the heat transfer coefficient of the outside air boundary in the model. The

interior wall had similar settings to the exterior wall; however, the R value of the wall and the temperature on the other side were different from those of the exterior wall. When R value is not available, the boundaries were set as a constant temperature surface. The temperature is based on result of FLIR thermal cameras.

Table 4. Boundary conditions in QT case.

Boundary	Boundary conditions (R 1 equal to 1 h·ft^2·°F/Btu = 0.176110 K·m^2/W)
Roof	R 13
Exterior wall	R 12
Interior wall	R 5
Exterior door	R 8
Ground surface	Constant temperature (13 ˚C)
Interior door surface	Constant temperature (20 ˚C)

The outdoor air temperature in the QT case is set as -21 ˚C as indicated by the weather report.

Table 5. Boundary conditions in KS case.

Boundary	Boundary conditions (R 1 equal to 1 h·ft^2·°F/Btu = 0.176110 K·m^2/W)
Roof	R 18.8
Ground	Constant temperature 21 ˚C
Exterior wall (upper area)	R 21.2
Exterior wall (lower area)	R 17.6
Interior side wall	Constant temperature 24.8 ˚C
Interior wall	Constant temperature 24 ˚C
Corridor	Constant temperature 23.5 ˚C
Divided plane	Constant temperature 24 ˚C
Window	R 2
Diffuser pipe surface	Constant temperature 29.9 ˚C
Diffuser surface	10.349196 m/s of 40 ˚C air

The outdoor air temperature in the KS case is set as -6.7 ˚C as indicated by the weather report.

For the ground and surface of the fabric diffuser, constant temperature conditions were applied. Meanwhile, for the inlets on the fabric diffusers, constant velocity and temperature with values corresponding to the HVAC monitoring device readings and on-site measurements were set for the air blowing into the room.

3.4.3 Heating component

There are several types of heating device in the warehouse. The most common heating device is the forced air heater which has an internal fan to blow hot air forward and downward into space. Based on the method stated in the report by Forrest and Owen (James & Ieuan, 2010), this component was simulated by a heat source with a specific heat generation rate which was calculated according to the heater's capacity and volume. Meanwhile, a surface with a constant pressure jump was set in the heater to blow the air and function as the internal fan. The heat generation rate was set according to the heating power marked on the heater. As some of the heaters had been used for decades, the power of their heated air supply may have been less than the marked value on their nameplates.

Due to the limitations of the field measurements, no smoke tests were conducted to measure the infiltration rate. The air exchange caused by infiltration and exfiltration is based on hand calculations. The air change rate by infiltration for QT warehouse is calculated to be 0.9 and for the KS warehouse it is estimated to be 0.5. The heat loss by the infiltration of the indoor space was simulated by setting a heat sink for the indoor domain.

3.4.4 Running the simulations

All the cases in this thesis are steady cases. The measurements were taken in short and specific time periods during the day. The temperature conditions were considered to be unchanged during these periods. Based on this assumption, the numerical cases are set up to simulate the air conditions at the precise times when the measurements were taken. The changing of the diurnal cycle or the seasonal cycle are beyond the range of this study. During the simulation, the under relaxation numbers were modified based on the previous residual result. It is a trial and error process of changing the under relaxation number to tune to the model to reach a low residual level.

Furthermore, during the simulation, temperature was monitored at certain points. The natural convection case, consider the convergence was achieved while the variables monitored had come to the stable stage.

The results from the simulation were compared with the measurement data to validate the models. The velocity component from the ceiling fan was compared to the experimental measurement to evaluate the performance of the CFD simulation. Furthermore, the temperature along the vertical lines was compared with the temperature data which was taken from the field measurements at the corresponding locations.

Table 6. Simulation cases.

Warehouse	Case	Description
QT	q1	Bucket fan #1 on
	q2	All fans off.
	q3	Ceiling fan on.
	q4	Bucket fan #3 on (upward).
	q5	Bucket fan #1 & #2 on.
	q6	Bucket fan #1, #2 & #3 on.
KS	k1	Fan 30% speed, fresh air throw horizontally.
	k2	Fan off, fresh air throw horizontally.
	k3	Fan 100% speed, fresh air throw horizontally.
	k4	Fan 30% speed, fresh air throw 45 degree downward.
	k5	Fan 30% speed, fresh air throw vertical downward.

3.5 Evaluation

3.5.1 Non-uniformity coefficient of temperature

Different temperature profiles for thermal stratification have been examined in a study measuring indoor thermal stratification (Aynsley R. , 2005). However, a number indicating the degree of temperature stratification is necessary to compare the results from different cases.

In this study, measured and simulated temperature data was processed into a dimensionless number, the non-uniformity coefficient of temperature, which is defined as the standard deviation of the temperature on the vertical line divided by the average temperature. It has been used as an evaluation of the uniformity of temperature distribution in indoor environments (Su, Zhang, &

Gao., 2009) (Lian & Qi, 2009). It reveals the severity of temperature stratification in the studied space. It is a quantified indication of the degree of thermal stratification.

$$\text{Non} - \text{uniformity coefficient of temperature} = \frac{Standard\ deviation\ of\ temperature}{Average\ temperature} \quad (7)$$

3.5.2 Temperature and rate of heat flow

The temperature in the occupant zone and beneath the ceiling zone are two places to pay attention to. In addition, the average temperature is a reference value for evaluating the energy performance of the building with different types of fan settings. With the same energy supply from the heaters or air diffusers in multiple cases, cases with a higher temperature at the occupant zone have a larger potential for reducing the heating energy supply to reach the temperature level.

The heat loss through the walls and roof is responsible for a large share of the heating energy budget. By tracking the heat flow through each boundary, the influence of different fan settings on the heat flow can be revealed.

CHAPTER 4. RESULTS AND DISCUSSION

This chapter first shows the measured temperature profile from all five buildings. What follows is the validation of the fan and building simulations. In the final part of this chapter, the rate of heat flow on boundaries and the non-uniformity coefficient from the simulated cases are presented.

4.1 Field Measurement

Temperature data from each thermocouple, which are time series data, were used to establish the average over the time series. Temperature data from each thermocouple tree was plotted into the temperature profile along the height. The error bar was calculated by taking the standard deviation of the measurement plus the 0.5 ˚C tolerance of the T-type thermocouple used in the measurement of this study.

4.1.1 QT warehouse

Two sets of measurements were taken from the field. One set was measured while the mixing fan was running. Another set was taken without the fan running. As observed in Figure 4-1, when the fan is running, there are 20.0 ˚C and 17.3 ˚C temperature differences between the ceiling zone and the ground level at location 1 and location 2 respectively. This warehouse was suffering from severe thermal stratification despite the bucket fan running to mix the air inside.

The QT warehouse was heated by a forced air heater with 15 kW of power. The temperature of the air blowing out from the heater was more than 60 ˚C. The temperature was beyond the range of the electric anemometer. The condition of high temperature air coming from a single source is a factor that contributes to the formation of severe thermal stratification in this warehouse. The hot air coming out of the heater has a much higher temperature and lower density than the air in the room, so there is a strong buoyant force causing the air to float upward before mixing thoroughly with the colder air below. If the source of heat was distributed among separate heaters spread around the warehouse, the air temperature and density difference would be reduced. For example, in contrast with the QT warehouse, the DT warehouse (Figure 3-3) had heaters distributed widely around the indoor space. While having around the same ceiling height (6 m), the DT warehouse only had 2 ˚C of temperature difference.

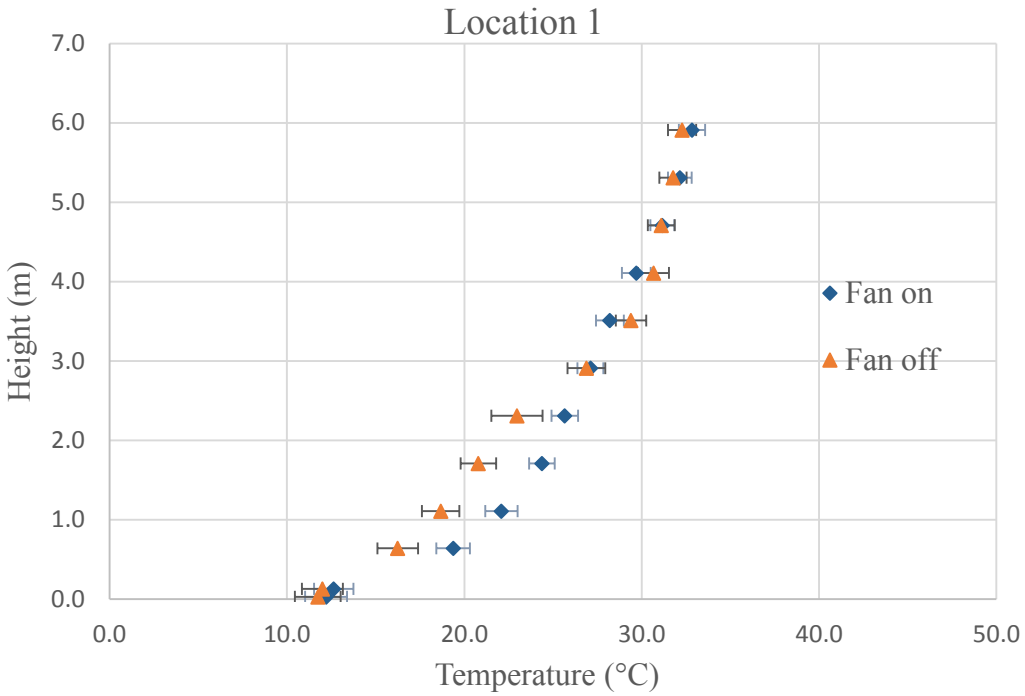

(a)

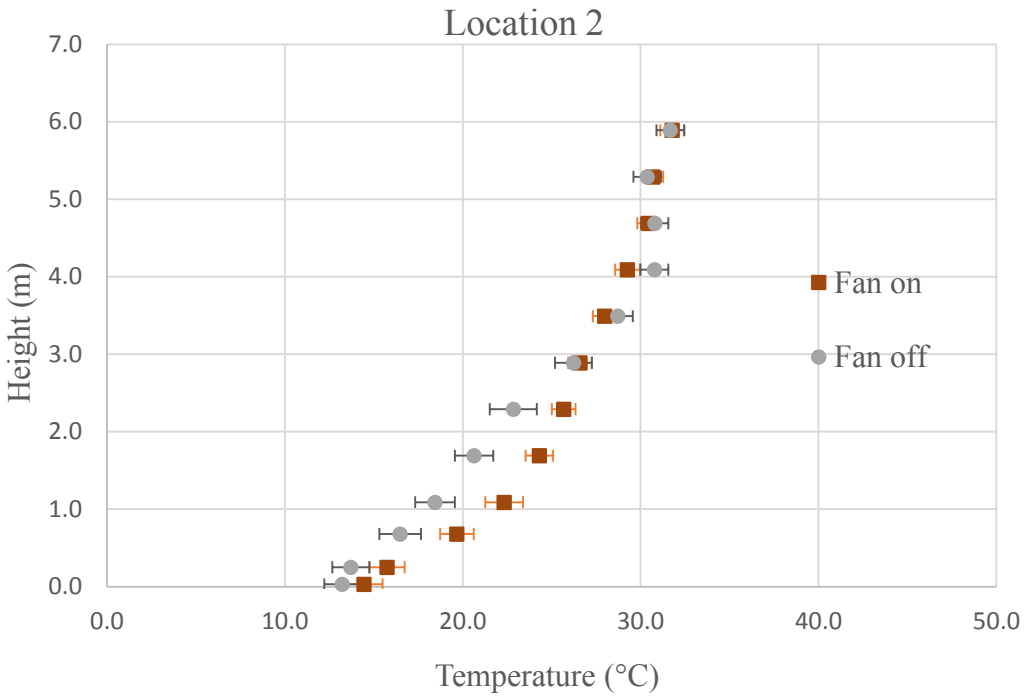

(b)

Figure 4-1. Measured temperature profile while the mixing fan is running and turned off from measurement location 1 (a) and measurement location 2 (b).

Compared to the conditions when the fan is running, larger error bars have been observed for conditions when the fan is off at lower height in Figure 4-1. The measurement of the fan-off condition was severely disturbed by the gate-opening and goods-loading processes of the warehouse. This is primarily caused by the influence of outdoor air. The deck door was opened for two long periods and the smaller gate was also opened several times. The outdoor air, which is below -20 ˚C, flowed into the warehouse and mixed with the indoor air at the lower layer of the warehouse. During these intervals, the temperature measurements at lower height dropped drastically as shown in Figure 7-6 of Appendix C. However, although the interval when the door was open was excluded when calculating average temperature, the inflow of cold air still affected the indoor air, as the indoor air temperature was in the process of increase as observed on Figure 7-6.

In addition, the measurements were taken immediately after the fan had been turned off. Since solid material has a large heat capacity, meaning its temperature does not change as fast as the air, the thermal conditions inside the warehouse are not at equilibrium stage if the fan was just turned off for a short period. The goods and racking inside were still releasing heat from their surfaces into the air.

The increase of temperature during the fan-off measurements can be attributed to these two factors. Since the error bar depends on the standard deviation of the temperature measurement, the temperature change increases the standard deviation of the temperature data as can be observed in a and b of Figure 4-1. Thus, the fan-off condition has larger error bars than the fan-running condition.

Furthermore, although the fan-off measurements were not taken under equilibrium conditions, the difference in the temperature profiles of the fan-on and fan-off measurement data nevertheless reveals the effectiveness of the mixing fan. As shown in Figure 4-1, after the fan was turned off, the temperature between 3.5 m and 5 m increased at both locations. The maximum increase was found at the height of around 4.1 m. At this height, the temperature in the case when the fan was off was 1.0 ˚C and 1.5 ˚C higher, at locations 1 and 2 respectively, than in the case when the fan was running. Meanwhile, for the area below 2.8 m, the temperature in the fan-off state was 0.2 - 3.6 ˚C and 0.4 - 3.9 ˚C lower than in the fan-running state at location 1 and location 2 respectively.

This temperature difference shows that the mixing fan has the effect of reducing the temperature in the higher area and increasing the temperature in the lower area.

4.1.2 MG stadium

In the MG building, the temperature difference was less than 1 ˚C all along the measurement line, as can been seen in Figure 4-2. This indicates that thermal stratification has been reduced to a minimum level in this building. For the two measured locations, which were more than 50 m away from each other (Figure 3-2), the temperature difference was less than 0.5 ˚C, which suggests there is temperature uniformity across the building.

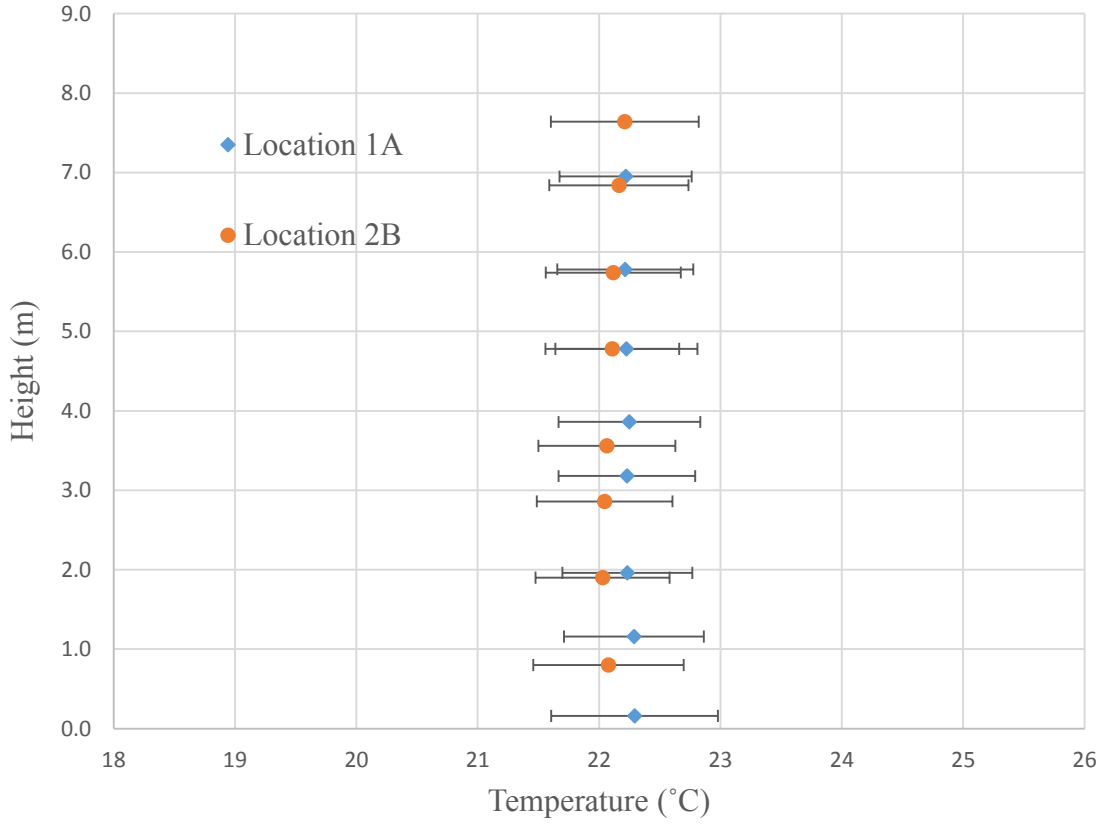

Figure 4-2. The measured temperature profile of measurement location A and measurement location B from the MG stadium.

The actual height at the center of this building is more than 7 m. Due to security concerns, these measurements only recorded the temperature from ground level to 7 m of height. This section of

air, which spans from the ground to the fabric air diffusers (Figure 7-4), is mixed by the air jets from the wall diffusers and fabric diffusers above.

4.1.3 XL distribution center warehouse

The XL warehouse had a temperature difference of 5 ˚C along its 9 m of height. The average temperature gradient is less than 0.5 ˚C/m. The XL warehouse had the highest ceiling in the five investigated buildings. However, the thermal stratification in this building was not severe. These temperature conditions were mainly due to the 18 ceiling fans distributed beneath the roof as shown in Figure 3-4. In addition, the installation of heaters above the deck doors and near the exterior wall also contributed to this low temperature difference.

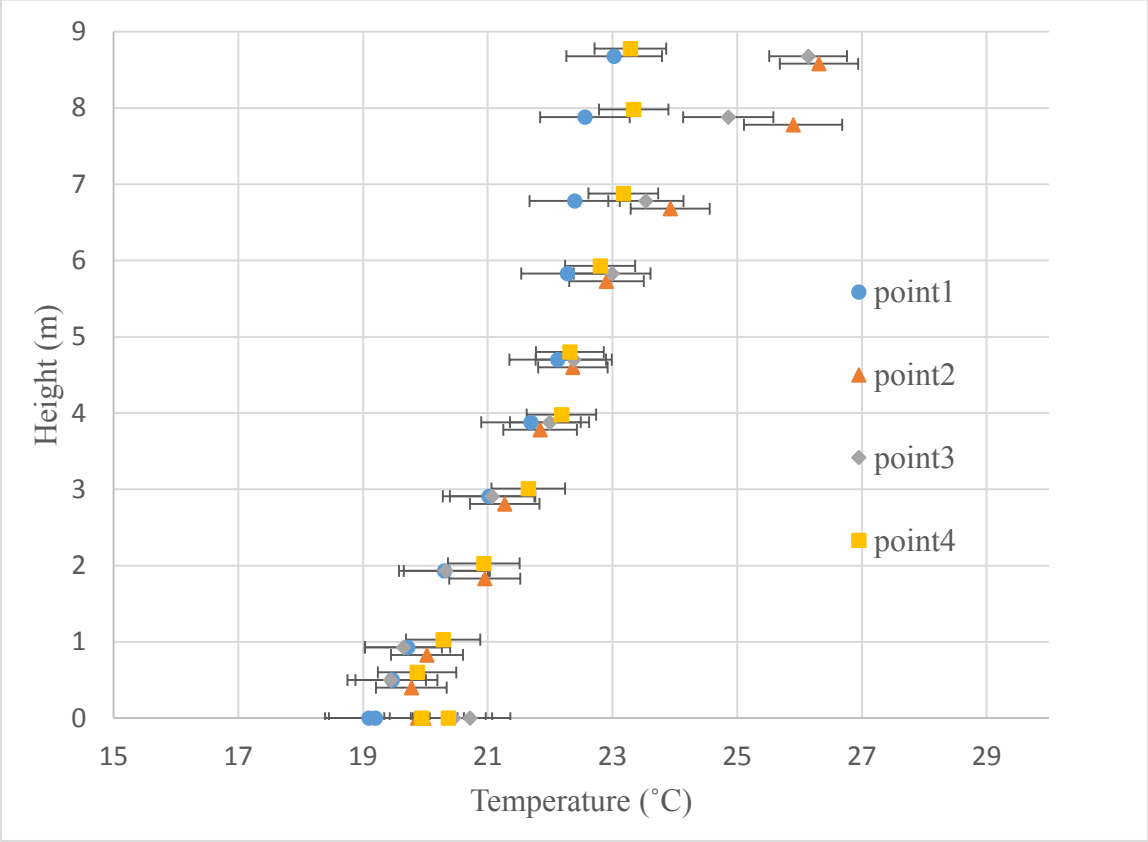

Figure 4-3. The measured temperature profiles of 4 different locations from the XL warehouse measurements.

4.1.4 DT warehouse

The DT warehouse had a temperature difference within the range of 2.5 ˚C to 5.5 ˚C along its 6 m of height. The majority of measured spots had temperatures within the range of 17 ˚C to 21 ˚C. Meanwhile, the temperature differences at the same height level (from 0.5 m to 4.5 m) but from different locations were less than 2 ˚C.

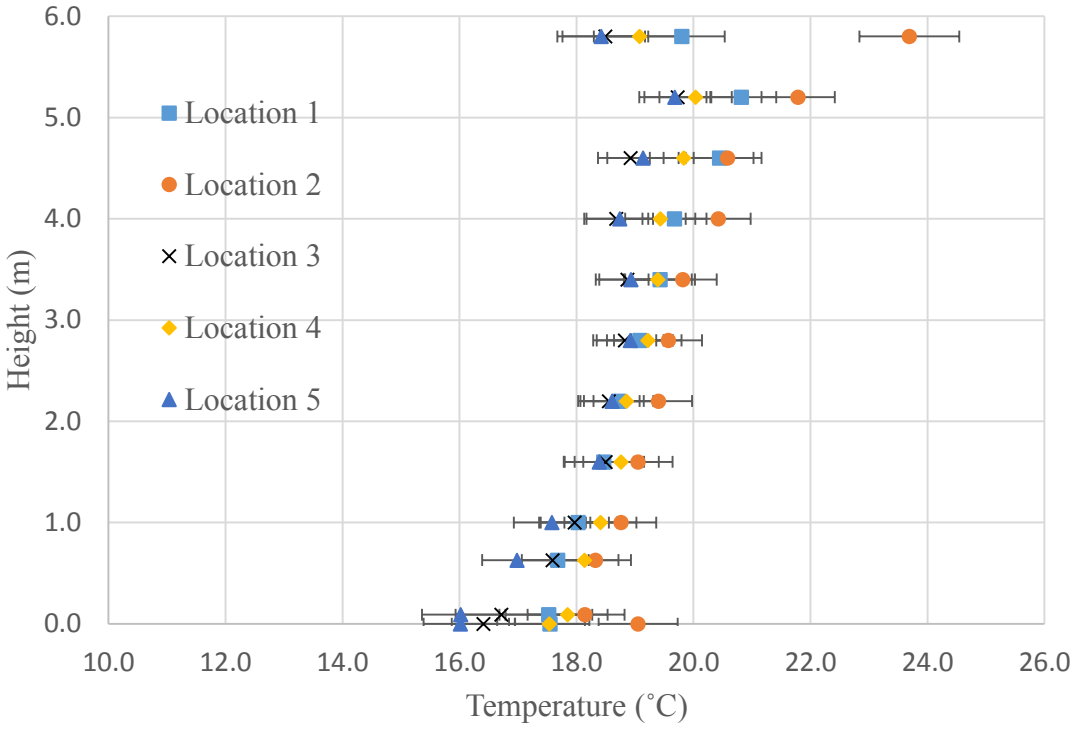

Figure 4-4. The measured temperature profiles of 4 different locations from the DT warehouse measurements.

The heating device contributed to achieving this condition of low thermal stratification. As shown in Figure 3-3, this warehouse had six long radiation heaters along the exterior walls rather than using a single force air heater as a heat source as in the QT building. The radiation heater emits infrared radiation. The surfaces of the material in the warehouse are warmed by the infrared radiation. Meanwhile, the surfaces warm up the air inside the building. In this way, the air is heated evenly by different objects in the warehouse, thus no severe temperature stratification was observed in this building.

4.1.5 KS warehouse

The KS building had a temperature difference ranging from 2.7 ˚C to 4.4 ˚C along its 6.5 m of height as shown in Figure 4-5. At the occupant level, the temperature was within the range of 21 ˚C to 23 ˚C. On the horizontal axis, for spots at the same height, the temperature difference from different locations was less than 1 ˚C.

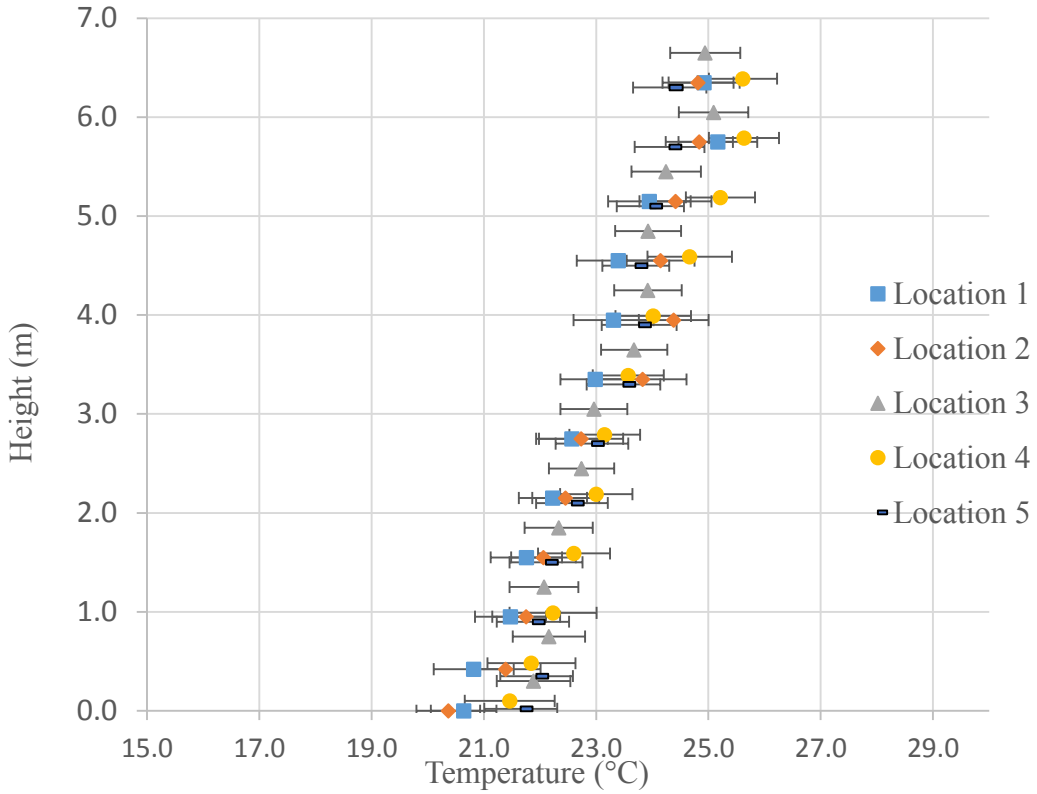

Figure 4-5. The measured temperature profiles of 5 different locations from the KS warehouse measurements.

This uniformity of temperature was due to the wide distribution of the diffusers and bucket fans as shown in Figure 3-5. The fresh warm air from the diffusers was evenly blown into the interior space. Meanwhile, the six mixing fans, which were distributed along the longer wall, blew the air further downward to achieve uniformity in the whole room.

4.1.6 Non-uniformity coefficient of temperature of measurement

Figure 4-6 shows the calculated result of the non-uniformity coefficient of temperature from the measurements. It shows that the MG building had the minimum non-uniformity coefficient which

are 0.001 and 0.002. Meanwhile, the QT building had the maximum non-uniformity coefficient (fan on: average 0.141, fan off: average 0.213). The non-uniformity coefficient of the measurement of the QT building (Figure 4-6) also indicates the building was still experiencing severe thermal stratification.

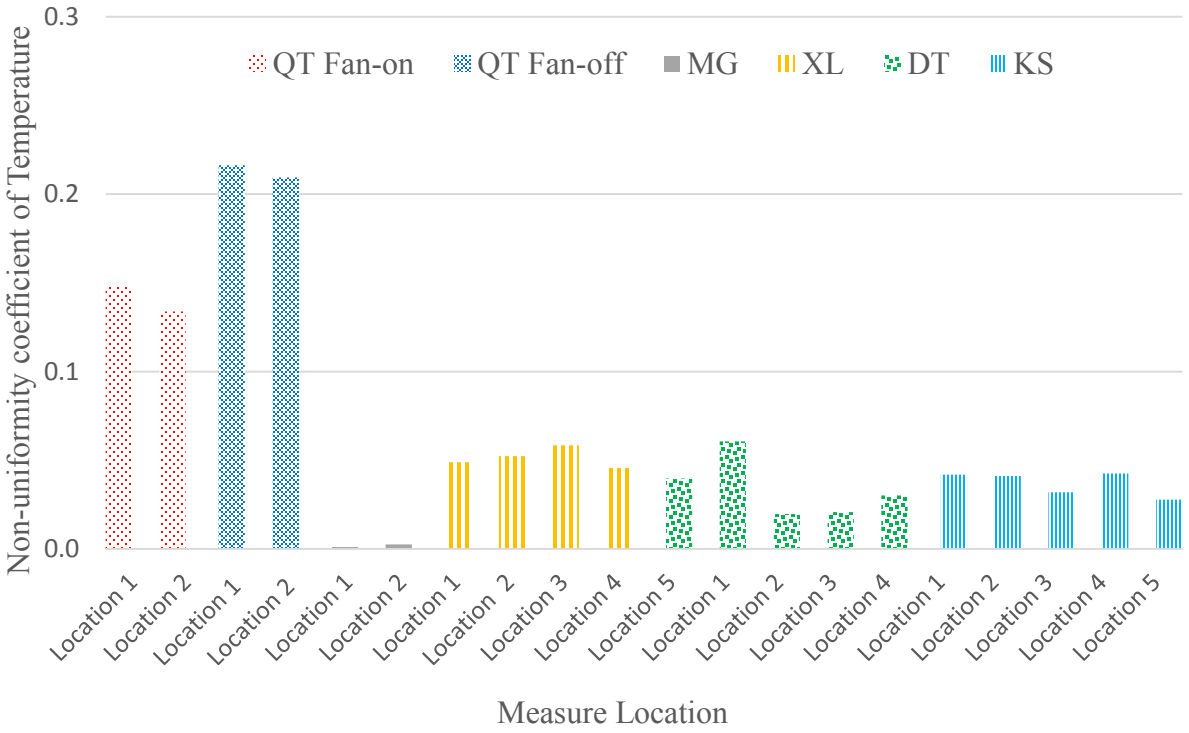

Figure 4-6. Comparison of non-uniformity coefficients of temperature from measurement data of 5 warehouses.

The MG's outstandingly low thermal stratification was due to the high volume flow rate of its fresh air supply and the wide distribution of its air diffusers. The temperature at the highest measured point was 22.2 C˚. The temperatures at the two lowest points are 22.07 C˚ and 22.29 C˚ respectively. Thus, the temperature difference along the vertical axis was less than 1 C˚ as shown by the measurements. This temperature difference in the stadium was due to the well-designed HVAC system in the building as depicted in Figure 3-2. On the side wall, there were two rows of air diffusers to inject air into the stadium. Temperature and velocity data were taken by anemometer from the diffusers on the wall (refer to Table 11 in Appendix B). The measured velocity from one row ranged from 4.2 m/s to 6m/s. The measured temperature ranged from 22.2

- 22.5 C˚. For another row, the velocity ranged from 2.5 m/s to 3.5 m/s. The temperature was 22.1 C˚. The detail of the velocity and temperature measurements is included in

Table 11 in the appendix B. In addition to the conditioned air injected into the stadium from two sidewalls, 12 fabric diffusers were distributed beneath the ceiling (Figure 7-4).

In conclusion, the three key points resulting in the low temperature stratification in the stadium were:

- The high air change rate.
- The wide distribution of air diffusers.
- The small temperature difference between the supplied air and the room air.

There was no hot air accumulated at the higher level. The high volume flow rate of fresh air caused the supplied air to have a relatively small temperature surplus compared to the room air. By comparison, a lower volume flow rate requires the supplied air to have a much higher temperature which will cause the hot air to easily ascend and accumulate at the highest part of the space as observed in the QT warehouse.

Although a temperature difference of less than 1 C˚ is desirable, it is not economically worthwhile for normal warehouses to install an expensive and energy-consuming HVAC system to achieve the temperature conditions observed in the MG building.

The size of the building also affects the temperature distribution. The XT and DX warehouses and the MG stadium have large indoor air volumes. The XT building has a length of 124 m. These buildings share the geometric characteristic of a higher ratio of roof surface area to volume. The cooling effect caused by heat loss through the roof counters the formation of thermal stratification. Furthermore, since larger buildings have a smaller area-to-volume ratio for the air body inside, the majority of the air volume is far away from the exterior wall and any infiltration from cracks.

The QT building had the most significant thermal stratification among the five sites. One of the major reasons for this is that this warehouse had only a single 15 kW forced air heater. Having one single heating source means the temperature of air coming from the heater is much higher than the surrounding air. The temperature measurements at the outlet of this heater had to be aborted since the temperature reading was beyond the range of the equipment. A much higher temperature leads

to much lower density due to thermal expansion. The upward buoyancy quickly neutralized the projected descending momentum of the hot air. The hot air floated up and accumulated at the ceiling level.

4.2 Validation of CFD model

The velocity of the ceiling fan and the temperature results from the CFD simulations must be validated. In this section, the CFD results are compared with the measurement data.

4.2.1 Validation of ceiling fan simulation

The velocity components of U, V and W have been extracted from the model. Their directions were illustrated in Figure 4-7. The positions where the velocity measurements were taken were 20 cm above and 20 cm beneath the ceiling fan. Figure 4-8 presents the comparison of velocities between Momoi's (2004) measurements and this study's CFD simulation results. Series a and b present the U, V and W components from 20 cm above and 20 cm beneath the fan respectively.

The shape of the velocity curve from the simulation follows the curve pattern of Momoi's (2004) measurement data dots. In particular, the w component, which is the vertical direction below the fan, has less than a 0.2 m/s difference from the measurements. This result indicates that the simulation method developed in this study can accurately generate the air flow of a ceiling fan in a CFD model. This method and the entire ceiling fan component are applied in the other cases.

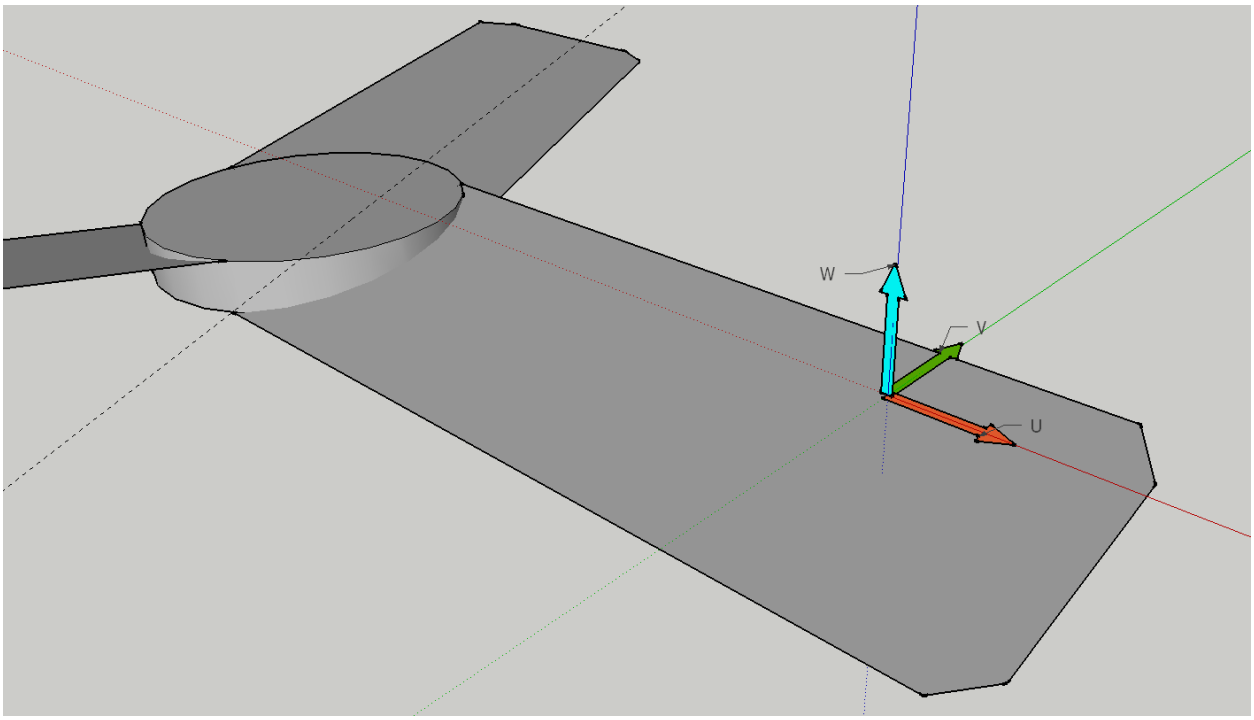

Figure 4-7. Illustration of the direction of the velocity components of U, V and W.

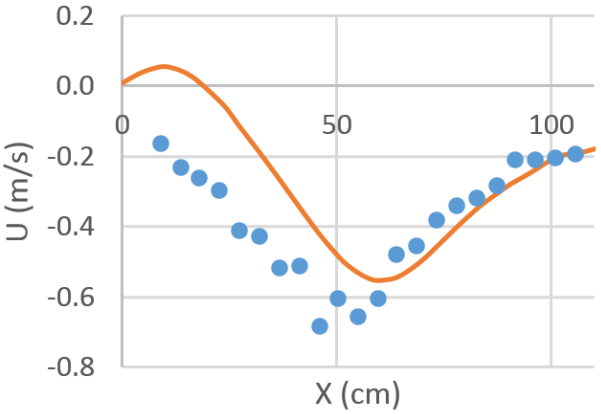

(a1)

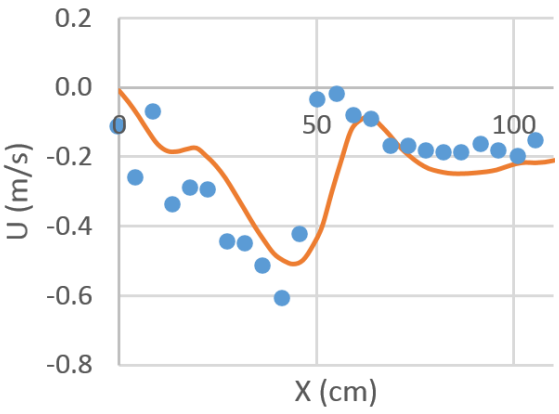

(b1)

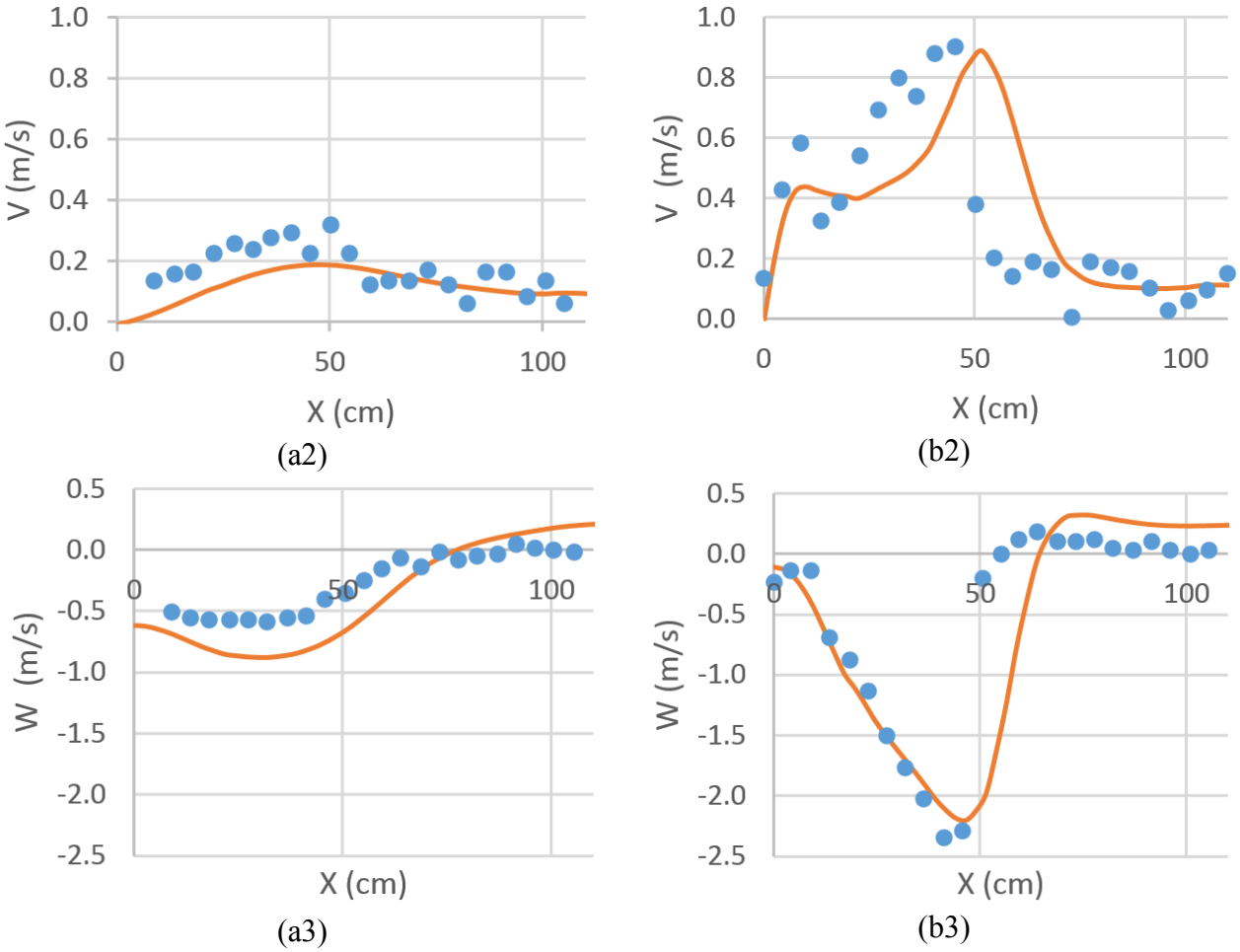

Figure 4-8. Velocity component comparison between the Fluent simulation and measurement results from Momoi's (2004) paper. a1, a2, a3 present the U, V, W components at 20 cm above the ceiling fan. b1, b2, b3 present the U, V, W components at 20 cm below the ceiling fan.

4.2.2 Validation by QT case

The temperature profile of the CFD results has the same curve pattern as the measurement data dots. The temperature difference between the simulation and the measurements ranged from 1 to 5 ˚C depending on the height. The result at the highest level is closer to the measurements. The temperature difference between the simulation and the measurements is less than 3 ˚C in the lowest section. The temperature difference in the middle section, where the difference is largest, is less than 5 ˚C. Overall, the simulated result underestimates the temperature in the building.

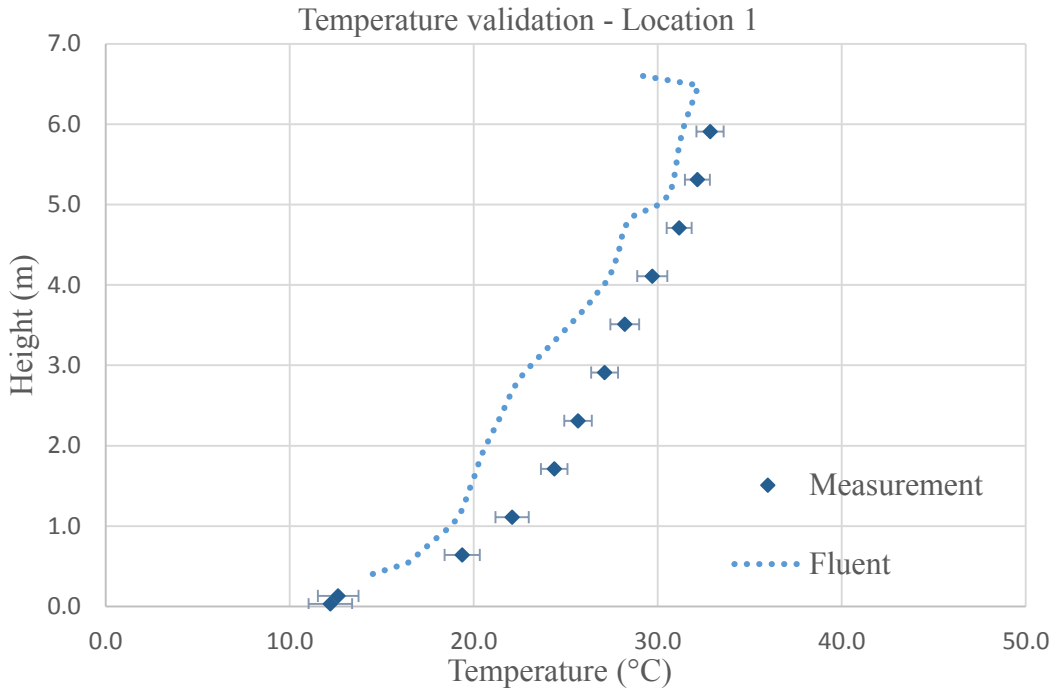

(a)

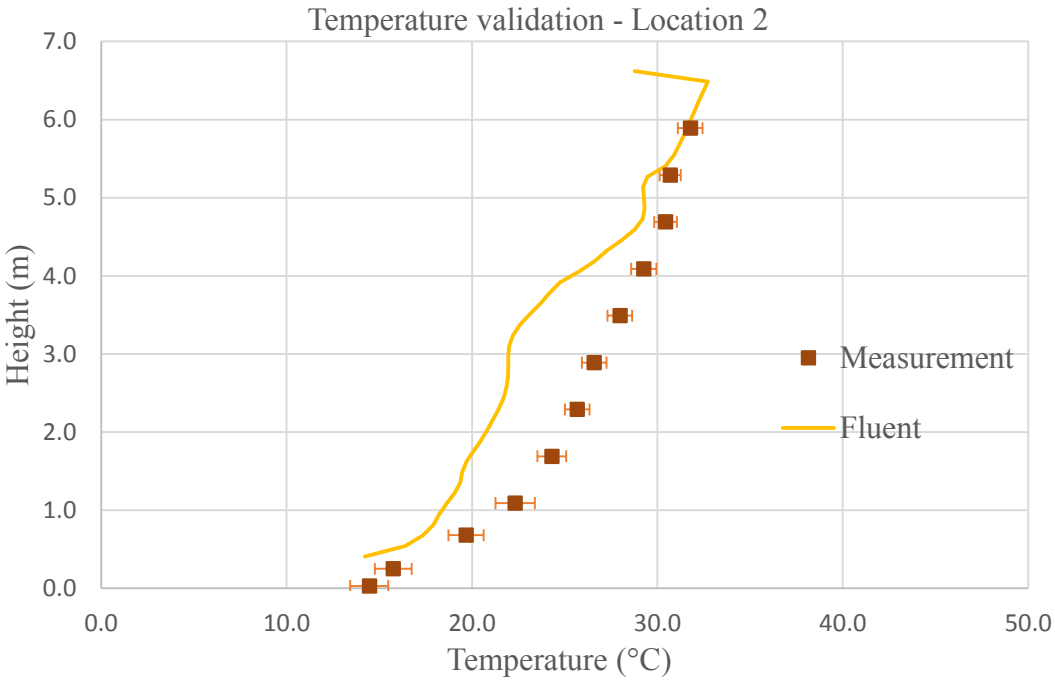

(b)

Figure 4-9. Comparison between the Fluent simulation results and the measurements taken while the fan was running. (a) is from measurement location 1, (b) is from measurement location 2.

4.2.3 Validation of KS case

Figure 4-10 presents the temperature result comparison between the simulation and the field measurements. For the area below 2.5 m, the temperature difference is less than 1.5 ˚C. For the part above 2.5 m, the temperature is higher than predicted. In most of the area, the temperature difference is less than 3 ˚C. The temperature discrepancies are different depending on the location.

The temperature profile of the case where the fan was running shows a clear two-layer shape, which is a typical phenomenon in temperature stratification. The cause of this phenomenon could be that the set value of volume flow rate for the bucket fan in the model is lower than the real volume flow rate of the bucket fan in reality. The 30% volume flow rate of the bucket fan is just an estimation provided by the warehouse's engineer. Thus, in the model, the effect of mixing air and pushing warm air downward is weaker than in reality. This leads to the two-layer air temperature distribution in the CFD results.

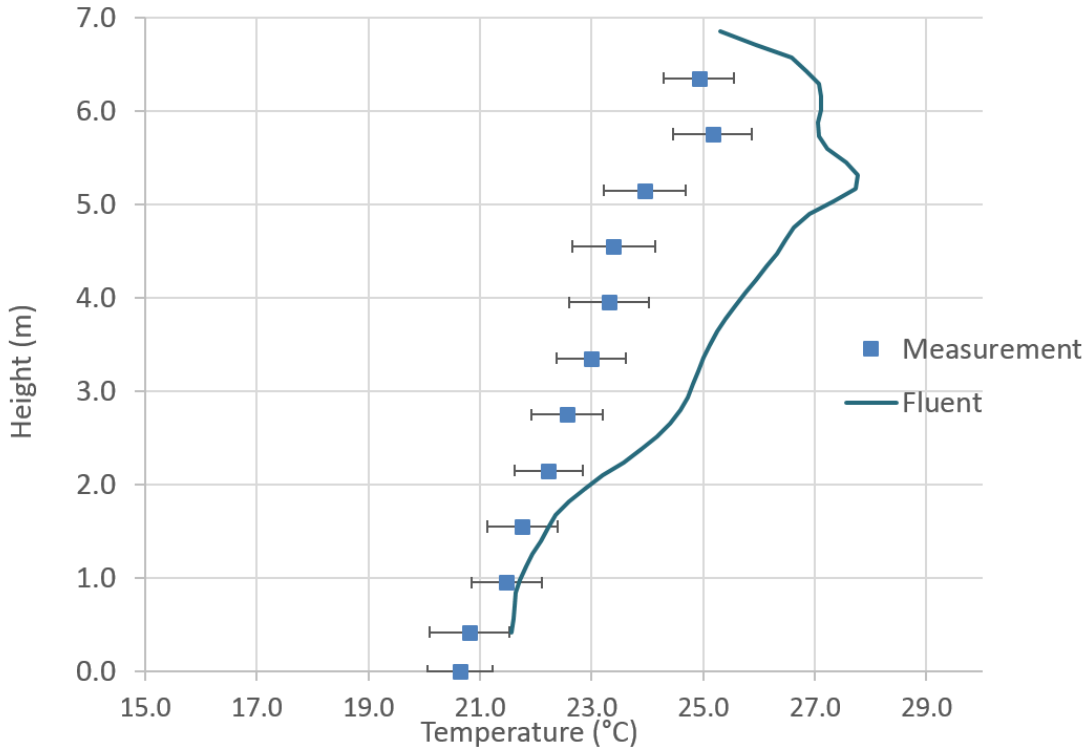

(a)

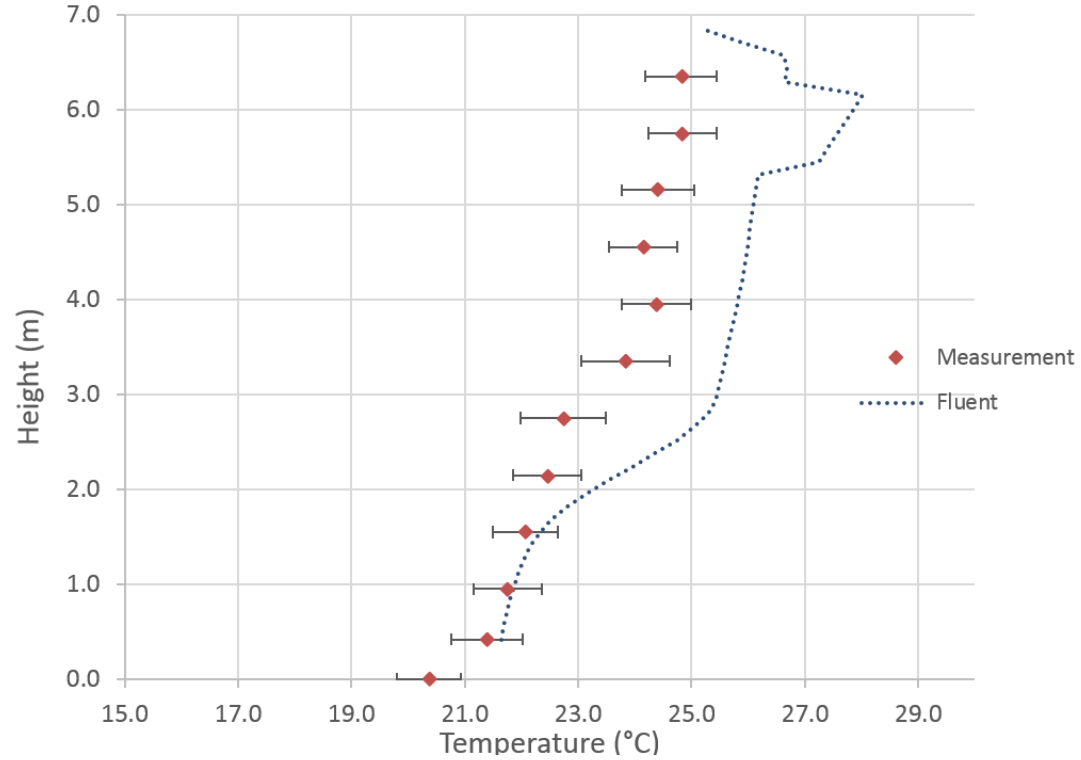
7.0
6.0
5.0
4.0
3.0
2.0
1.0
0.0
Height (m)
15.0
17.0
19.0
21.0
23.0
25.0
27.0
29.0
Temperature (°C)
Measurement
Fluent

(b)

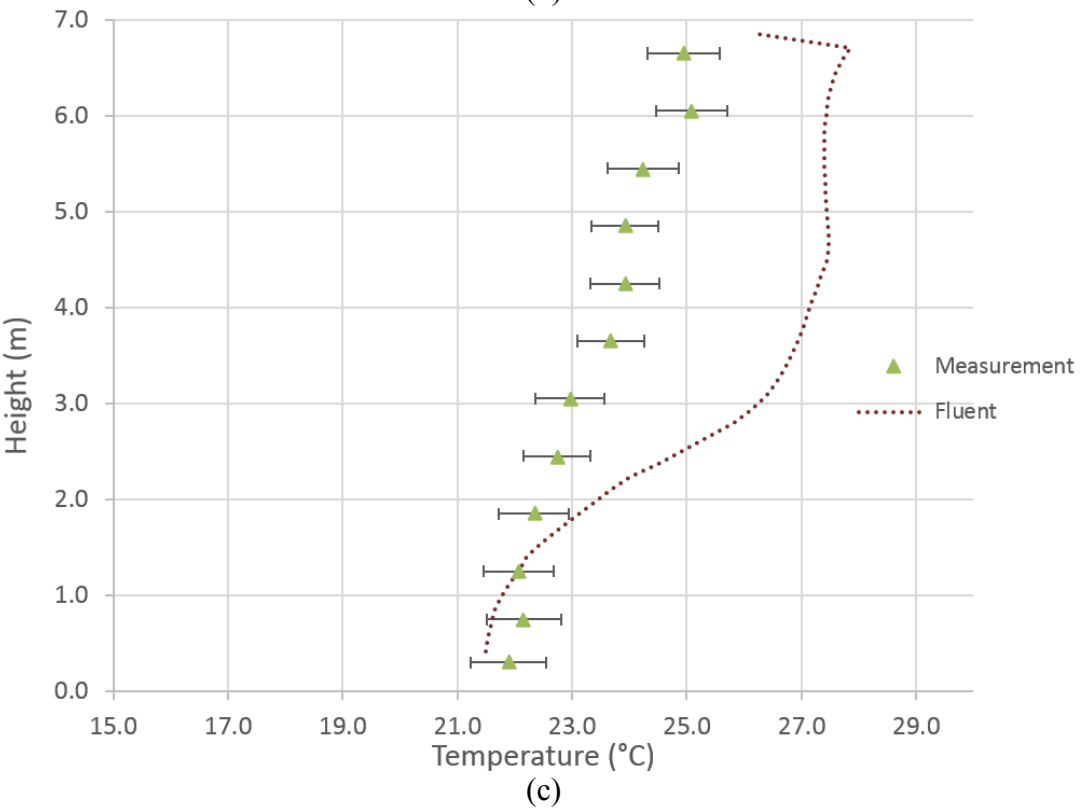
7.0
6.0
5.0
4.0
3.0
2.0
1.0
0.0
Height (m)
15.0
17.0
19.0
21.0
23.0
25.0
27.0
29.0
Temperature (°C)
Measurement
Fluent

(c)

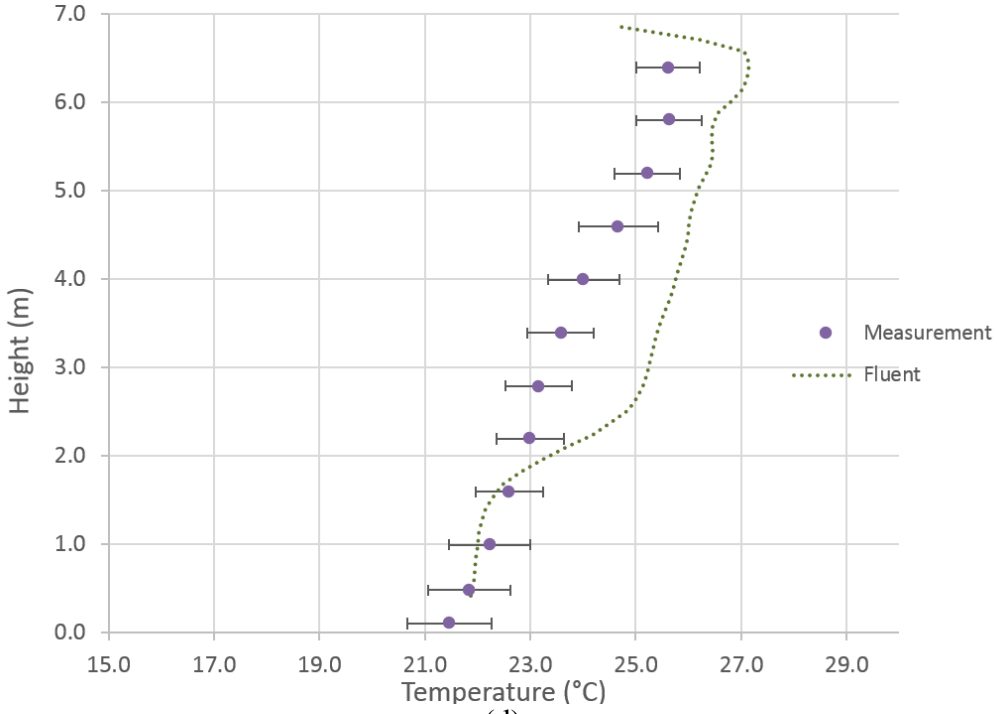

(d)

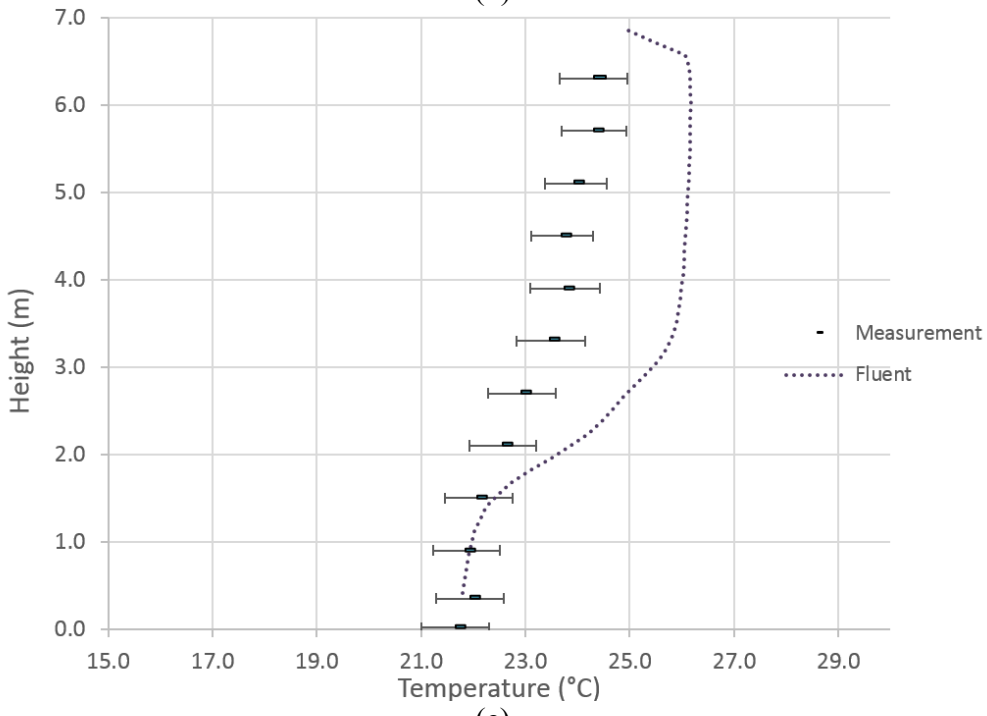

(e)

Figure 4-10. Temperature profile comparison between the measurements and the Fluent simulation results. a, b, c, d and e correspond to measurement locations 1, 2,3,4 and 5 respectively.

One of the reasons for the temperature overestimation is that the three corridors are set at an overly high temperature. In the model, the corridors have been set to be wall boundaries with a constant temperature of 23.5 ˚C. According to the engineer of this building, the intended indoor temperature range is 23 to 24 ˚C. So the wall boundaries that represent the corridors were set to have a constant temperature averaging between 23 and 24 ˚C. However, in reality, the three corridors do not have heating devices. In addition, the corridors connect to the main gate and the back side of the building where the temperature is lower. To sum, the temperature setting on the corridor boundaries is too high. This is one of the reasons leading to the overestimated temperature in the CFD model. A further modification of boundary conditions based on this conclusion is recommended for future work.

4.3 CFD result

4.3.1 Rate of heat flow through boundary

The rate of heat flow through boundaries provides a reference for tracking the distribution of heating energy loss in the building. The CFD cases in this study all have a constant heating energy supply from heaters or air diffusers. Meanwhile, a constant heat sink was set up for the entire indoor air volume to account for heat lost via infiltration. The rest of the heating energy is transferred through all the boundaries. Except for the ground surface, which is set as a surface of constant temperature, all the surfaces (the walls, doors, and roof) are set to have a constant R value and a constant outside temperature (refer to Appendix D. Boundary value in QT case and KS case.).

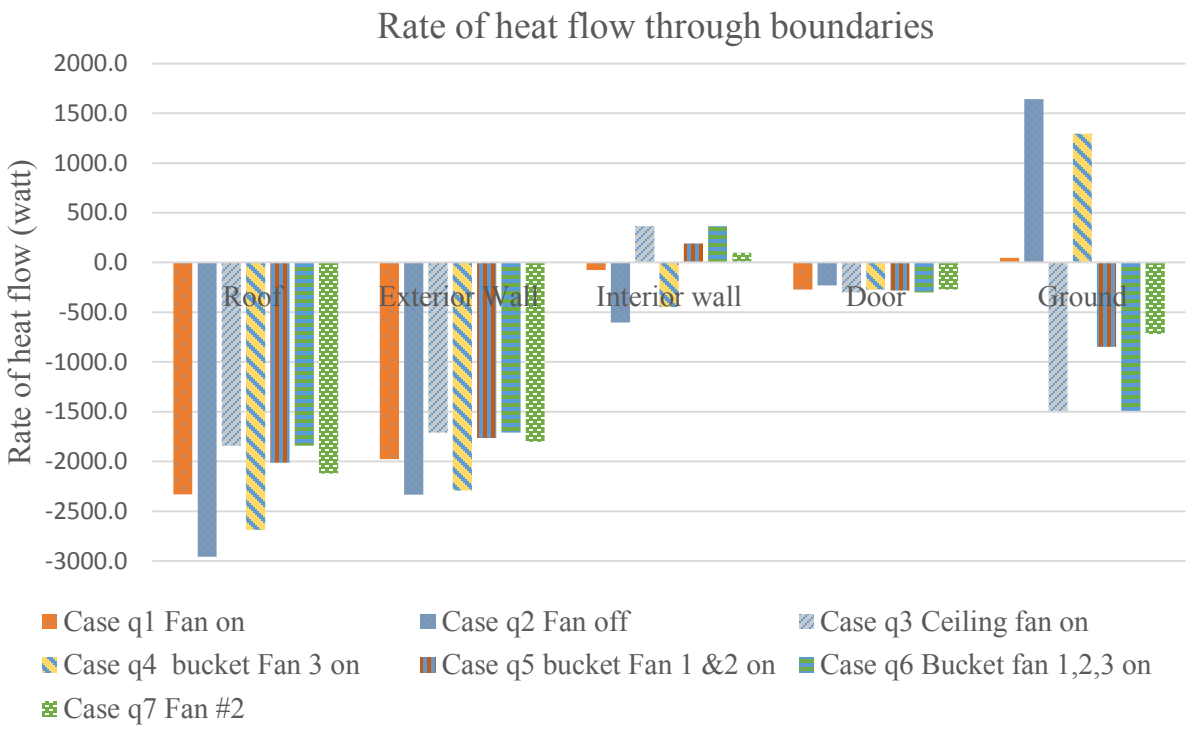

Figure 4-11. Rate of heat flow through boundaries from different cases in the QT model.

Table 7. Heat lost through boundaries. (Unit: watt)

Heat lost	Case q1 Fan	Case q2 No Fan	Case q3 Ceiling Fan	Case q4 bucket Fan 3	Case q5 bucket Fan 1 &2	Case q6 Bucket fan 1,2,3	Case q7 Fan #2
Roof	-2331.46	-2957.15	-1840.73	-2679.35	-2011.79	-1840.73	-2120.58
Exterior Wall	-1976.72	-2332.50	-1709.49	-2291.03	-1765.54	-1709.49	-1802.15
Interior wall	-76.98	-602.65	363.63	-445.45	189.88	363.63	97.94
Door	-272.25	-231.74	-300.72	-273.72	-280.22	-300.72	-270.78
Ground	47.00	1641.08	-1489.94	1364.21	-849.27	-1489.94	-718.77
Total	-4610.41	-4482.96	-4977.25	-4325.33	-4716.93	-4977.25	-4814.34

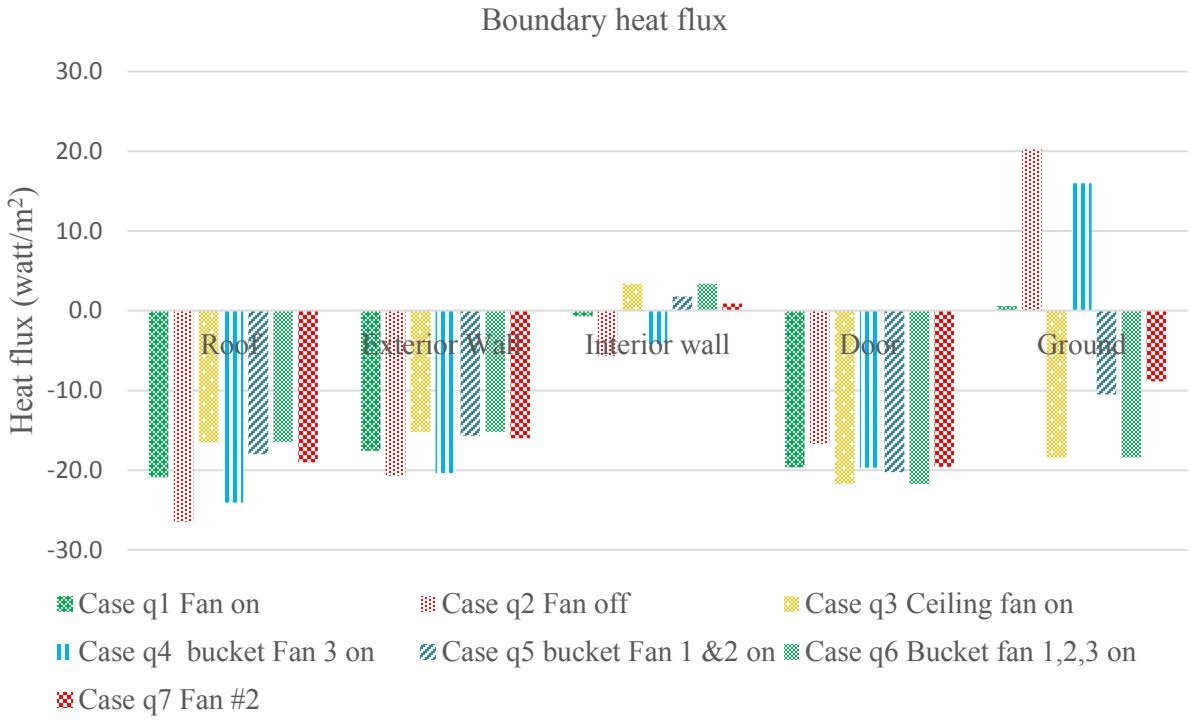

Figure 4-12. Heat flux density through the boundaries from different cases of the QT model.

As observed in Figure 4-11, in all five cases, rate of heat flow through the roof and exterior walls makes up the dominant portion of the total heat flow through all the boundaries. This indicates that the majority of the heat is lost through the roof and wall. This is reasonable as the roof (111.69 m^2) and the exterior wall (112.66 m^2) compose half (52%) of the total warehouse envelope area. Furthermore, the roof and the exterior wall make up the part of the warehouse that is directly exposed to the cold outside air. On the other hand, the interior wall is exposed to room temperature air. There are thus large portions of heat lost through the roof and exterior walls.

The boundary heat flux density is also highly dependent on the ΔT (temperature difference between the outdoor air and indoor air). Hence, the roof, exterior wall, and door have high heat flux densities greater than 15 watt/m^2 as observed in Figure 4-12.

The ground boundaries were set to have a constant temperature in all cases. In Figure 4-11and Figure 4-12, the rate of heat flow and the heat flux density are both high. In cases 1, 2 and 4, the rate of heat flow from the ground to the indoor air is positive, which is not reasonable. The positive value means that the heat is transferring from the ground to the air in the domain. This positive

rate of heat flow from the ground into the air of the room is caused by the air temperature above the ground being lower than the constant temperature of the ground surface as set in the boundary conditions. Unreasonable heat gains or losses through the ground should be considered when interpreting the temperature profiles in these cases. For cases 3, 5, 6 and 7, the rate of heat flow and the heat flux density show that a large portion of heat was lost through the walls.

4.3.2 Non-uniformity coefficient of temperature of CFD cases

The non-uniformity coefficient of temperature is defined as the standard deviation of the temperature on the vertical line divided by the average temperature. The higher the non-uniformity coefficient of temperature, the more severe the temperature stratification. A perfectly uniform temperature along the whole vertical line has a non-uniformity coefficient of zero.

Table 8. The non-uniformity coefficients of temperature of the QT model.

	Measurement		Simulation						
Location	Fan on	Fan off	Bucket Fan on	All Fan off	Ceiling Fan on at 100%	1 bucket fan (#3) blow upward	2 bucket fans blow downward	three bucket fans on	Bucket fan #2 on
1	0.148	0.216	0.194	0.489	0.057	0.360	0.149	0.078	0.152
2	0.134	0.210	0.194	0.487	0.072	0.362	0.126	0.054	0.092
3			0.194	0.487	0.077	0.356	0.163	0.116	0.166

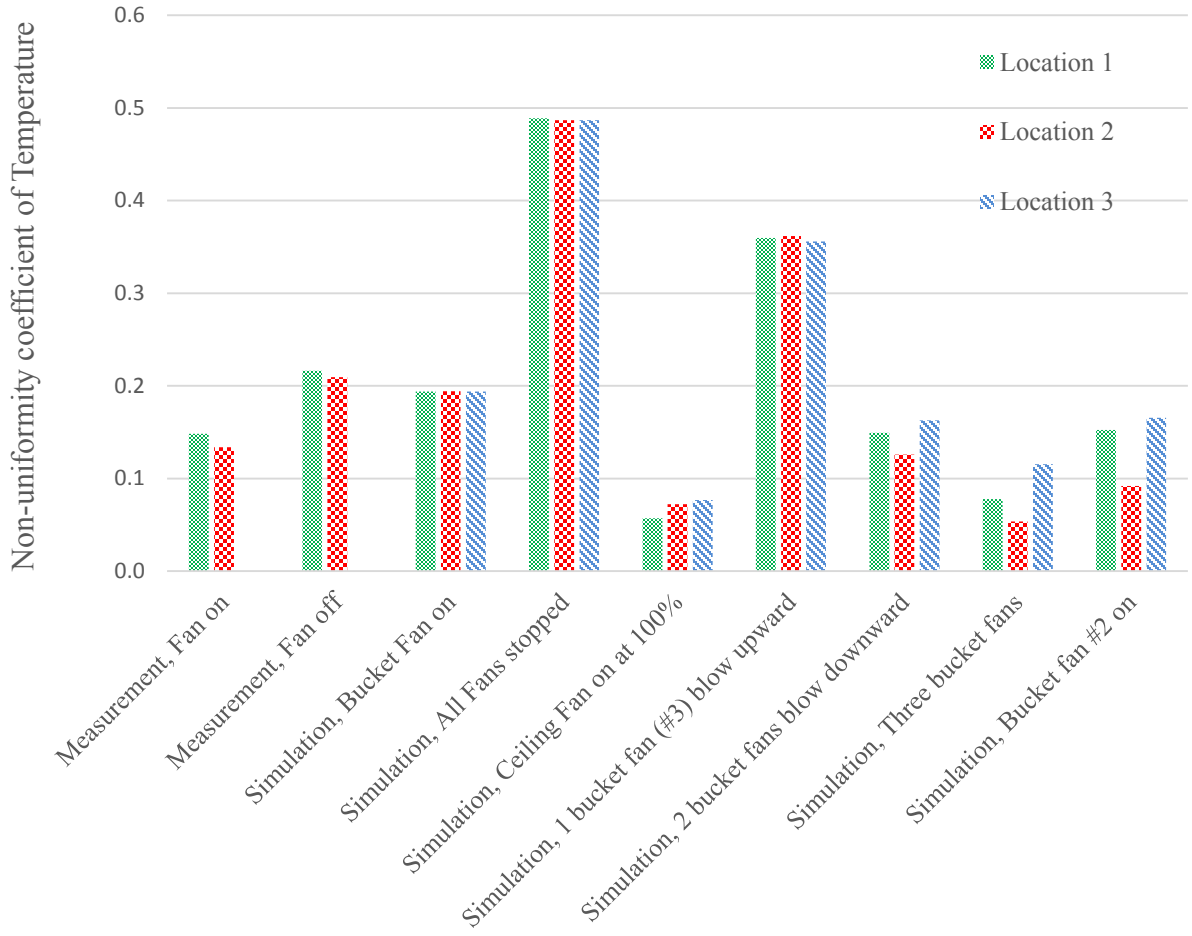

Figure 4-13. Comparison of simulation results with non-uniformity coefficients of temperature for the QT warehouse.

The non-uniformity coefficient of temperature of the QT warehouse is shown in Figure 4-13. For the case where one bucket fan was running, the simulated results (average value 0.194) are close to the measured results (average value 0.141). The highest value (0.487) is from the case where all fans were stopped. In contrast, the lowest value (average value 0.065) is from the case where one ceiling fan was running. This is attributable to the high volume flow rate driven by the large blades of the ceiling fan.

Table 9. The non-uniformity coefficient of temperature for the KS building measurements and simulation.

	Location 1	Location 2	Location 3	Location 4	Location 5
Measurement	0.042	0.041	0.032	0.042	0.028
Fan 30%, fresh air throw horizontally.	0.083	0.067	0.076	0.049	0.065
Fan stopped, fresh air throw horizontally.	0.096	0.078	0.089	0.069	0.067
Fan 100%, fresh air throw horizontally.	0.032	0.034	0.036	0.031	0.041
Fan 30%, fresh air throw 45 degree downward.	0.029	0.039	0.036	0.020	0.028
Fan 30%, fresh air throw vertical downward.	0.012	0.022	0.011	0.006	0.018

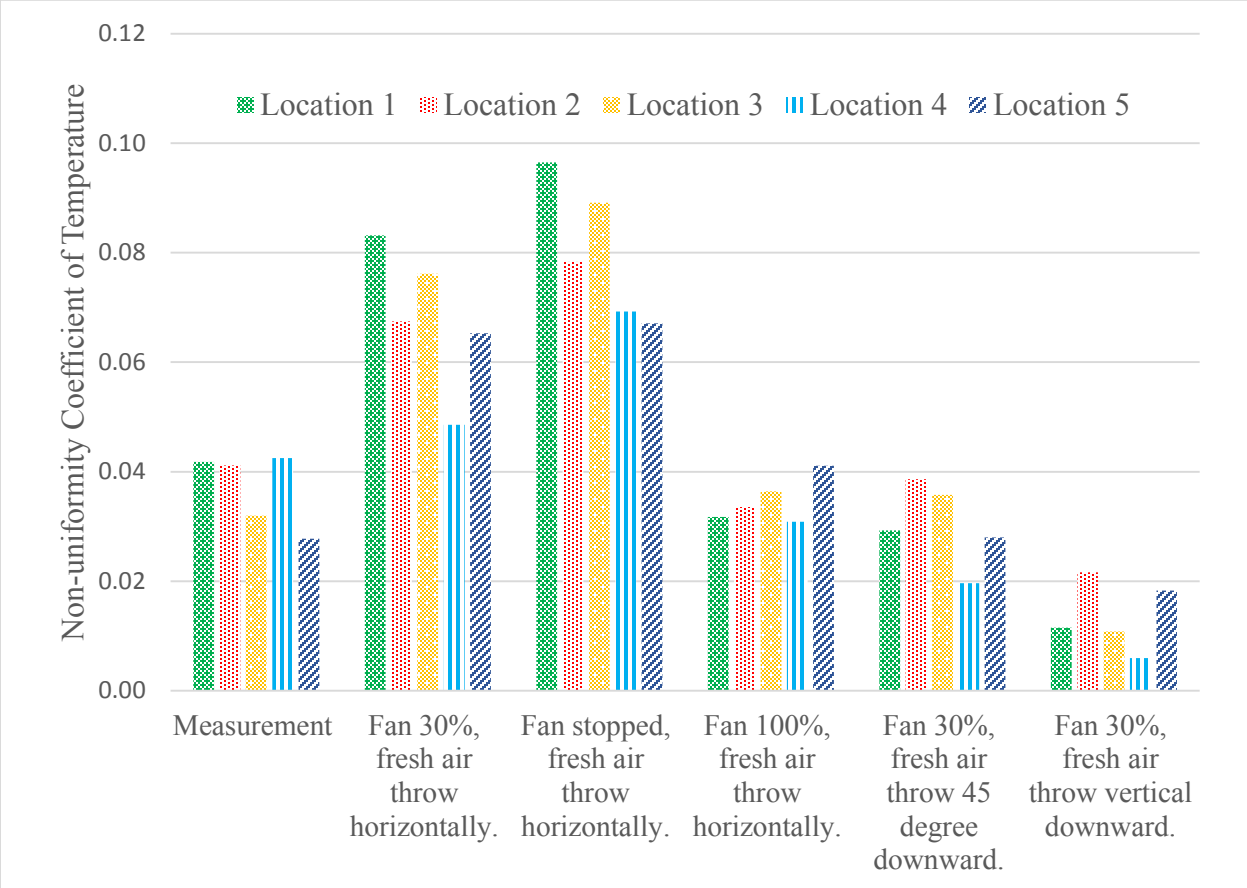

Figure 4-14. The non-uniformity coefficient of temperature of the KS building measurement and simulation results from different cases.

The non-uniformity coefficient of temperature of the KS warehouse is shown in Figure 4-14. The simulation of the 30% volume flow rate of the bucket fan and horizontal air projection cases

predicts the non-uniformity of the coefficient of temperature compared to the measurements. The case of downward projection of diffuser air shows the lowest non-uniformity coefficient of temperature out of the five cases (average 0.014).

CHAPTER 5. APPLICATION AND OPTIMIZATION

Different fan application methods will result in different distributions of air velocity, rates of heat flow through boundaries, distributions of temperature, drafts, etc. The performance of mixing fans in decreasing thermal stratification can be evaluated by the non-uniformity coefficient of temperature.

The energy saving effect caused by of mixing fans can be evaluated by determining the temperature increase at the occupant level. In this study, simulation cases for the same warehouse all use the same heating energy supply from the heater or diffuser. A higher temperature at the occupant zone indicates that less heating energy is required to sustain a comfortable temperature. In other cases where the temperature stratification is severe, the temperature at the occupant zone is low and hence requires extra heating energy to sustain a comfortable temperature.

5.1 QT warehouse

The QT warehouse model is composed of three bucket fans, one heater, and one ceiling fan. Location 1 and location 2 in the model are at the same position as in the field measurements. The ceiling fan does not exist in the warehouse itself. It was added to the model to investigate the air-mixing performance of ceiling fans. Fan #2 and Fan #3 also do not exist in the warehouse. Fan #3 was added to the model to investigate the effect of the upward air flow of bucket fans.

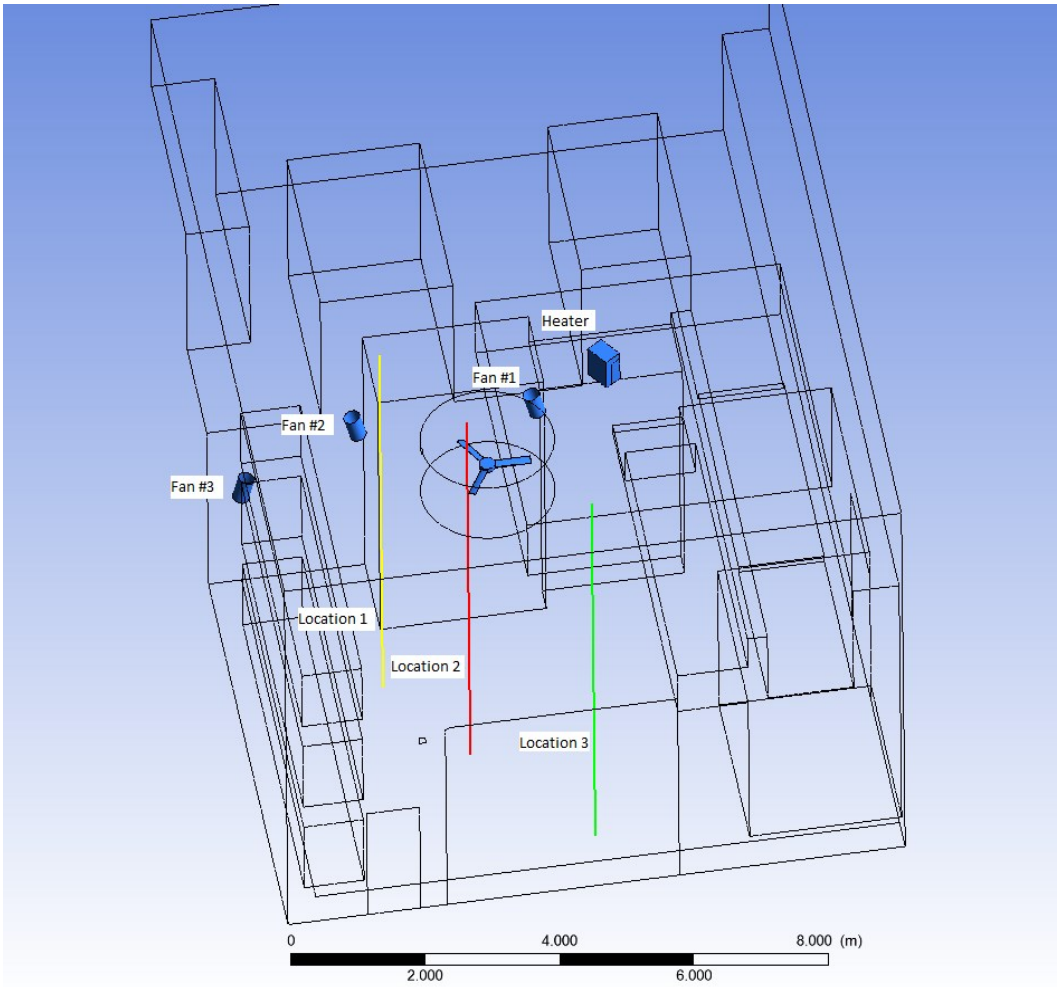

Figure 5-1. The geometry of the QT model. Fan #2, Fan #3 and the ceiling fan were added to the model and do not exist in the original warehouse.

5.1.1 Comparison of cases with the bucket fan running and the bucket fan turned off

In Figure 4-13, the mixing fan shows decisive effectiveness in reducing thermal stratification in this warehouse. The average non-uniformity coefficient of temperature is reduced from 0.49 to 0.19 while the fan is switched from off to on. When the mixing fan is not running, the result clearly shows two-layer thermal stratification as in Figure 5-2. The profile features in the case where the fan is stopped fit the description of two-layer distribution. The average temperature of the air volume in the upper half ranges from 35 to 45 ºC. The temperature of the lower part of the air volume ranges from 7 to 14 ºC. In the upper part, the warm air is pushed by the initial momentum from the heater. However, due to the buoyancy of the warm air, its downward momentum is neutralized by the upward floating force before it reaches ground level. Meanwhile, the cold air at

the bottom has higher density and is not disturbed by other forces which would cause it to move upward and mix with the warm air above. Hence, this temperature stratification can be very stable and last for the whole heating season unless countermeasures are taken to solve it.

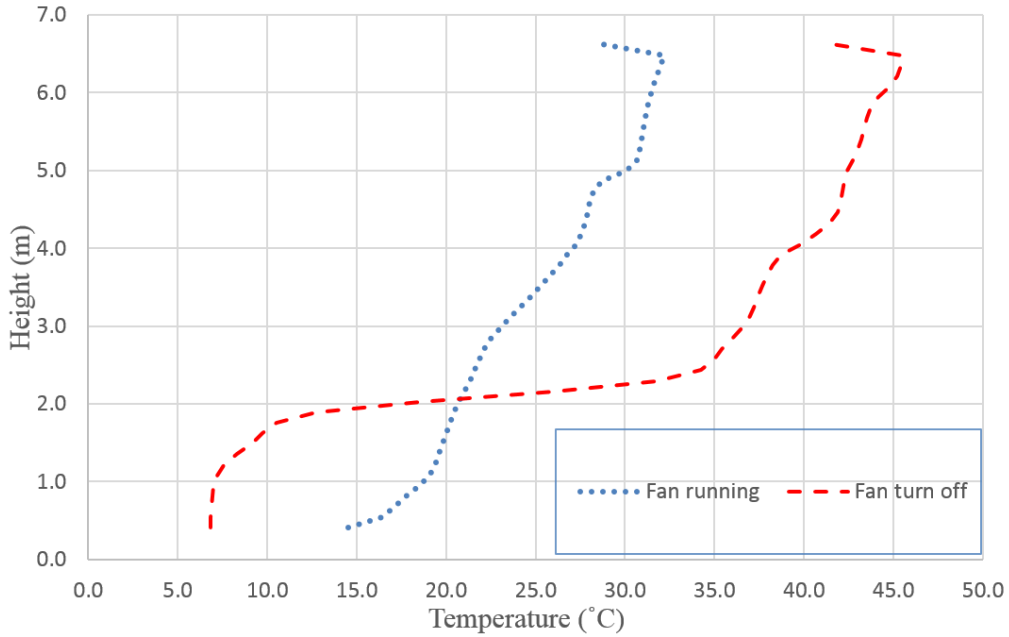

(a)

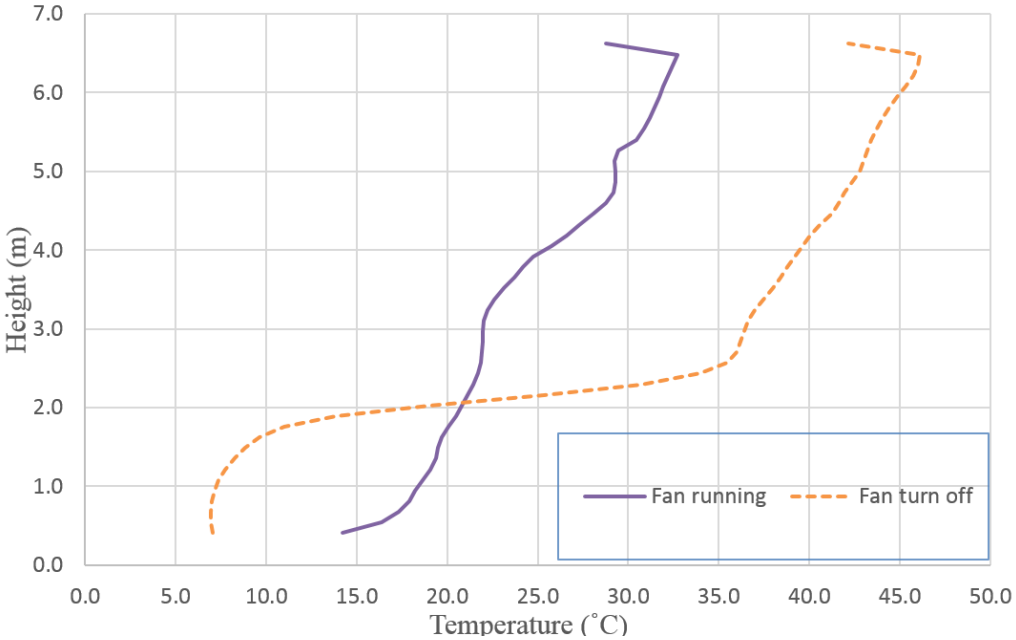

(b)

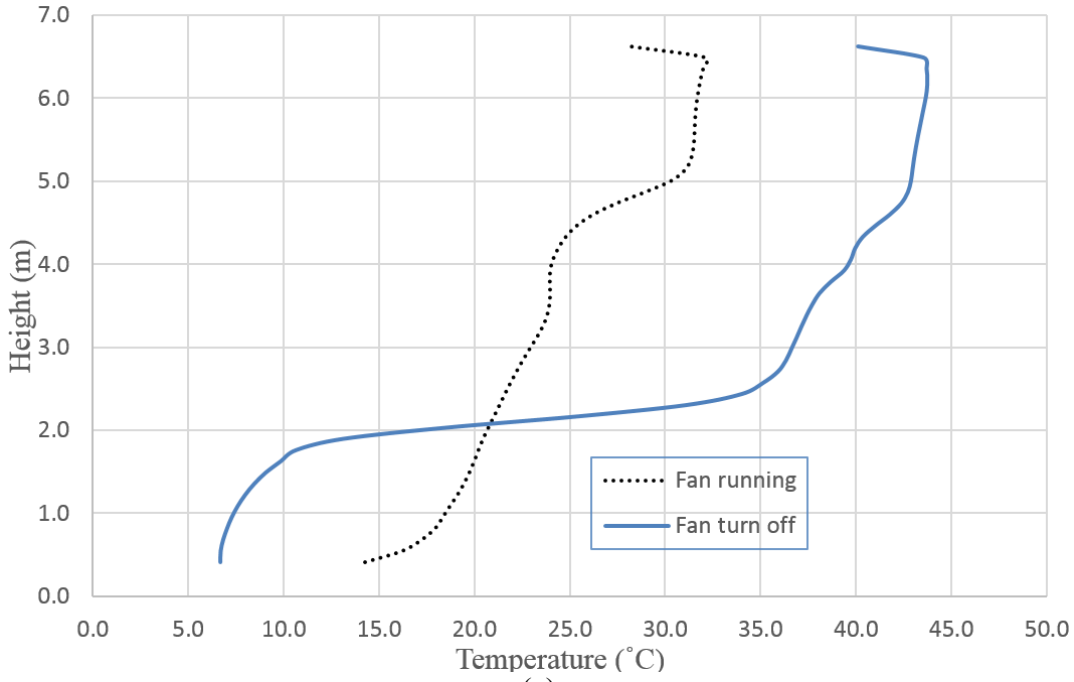

(c)

Figure 5-2. Temperature profile comparison between the case where the bucket fan is running and the case where it is turned off. A, b, and c present locations 1, 2 and 3 respectively.

In the case where the fan is running, the air temperature in the lower part (below 2 m) ranges from 15 ˚C to 22 ˚C. In contrast, the temperature when the fan is off is around 10 ˚C less. When the mixing fan is not running, the heat source in the warehouse needs to provide extra heating energy to reach the same temperature as in the case when the fan is running. This temperature difference represents the heating energy saved by utilizing a mixing fan. The rate of heat flow from the roof is 21.2% lower than in the case with no fan running.

In this comparison, a clear improvement in temperature mixing was observed when the mixing fan was running.

5.1.2 The effects of changing the direction of bucket fan

In this comparison, bucket fan #1 is blowing downward beneath the ceiling while in another case bucket fan #3 is blowing upward from a height of 2 m. Figure 5-3 shows that in the case where the fan is blowing upward, the air volume between 2.5 m and the ceiling (above the fan) is evenly mixed. The temperature difference within most parts of this height range is less than 5 ˚C. At locations 1 and 2, the temperature difference within most parts of this height range is even lower

than 2 ˚C. The air temperature difference within the corresponding sections in the case where the fan is blowing downward is around 10 ˚C at all three locations. The temperature profiles of this section (2.5 m above) from the two cases clearly show that the upward fan mixes the air in this section better than the fan blowing downward. However, the higher temperature in the case where the fan is blowing upward leads to a larger temperature difference between the air beneath the ceiling and the outdoor air above the roof. Furthermore, the upward-blowing fan creates faster air movement beneath the ceiling surface. This also contributes to the increase of the rate of heat flow through the roof. As can be observed from Figure 4-11, the rate of heat flow in case 4 wherein fan #3 is blowing upward is -2680 watts. Meanwhile, when the fan is blowing downward, the rate of heat flow loss through the roof is 348 watts lower.

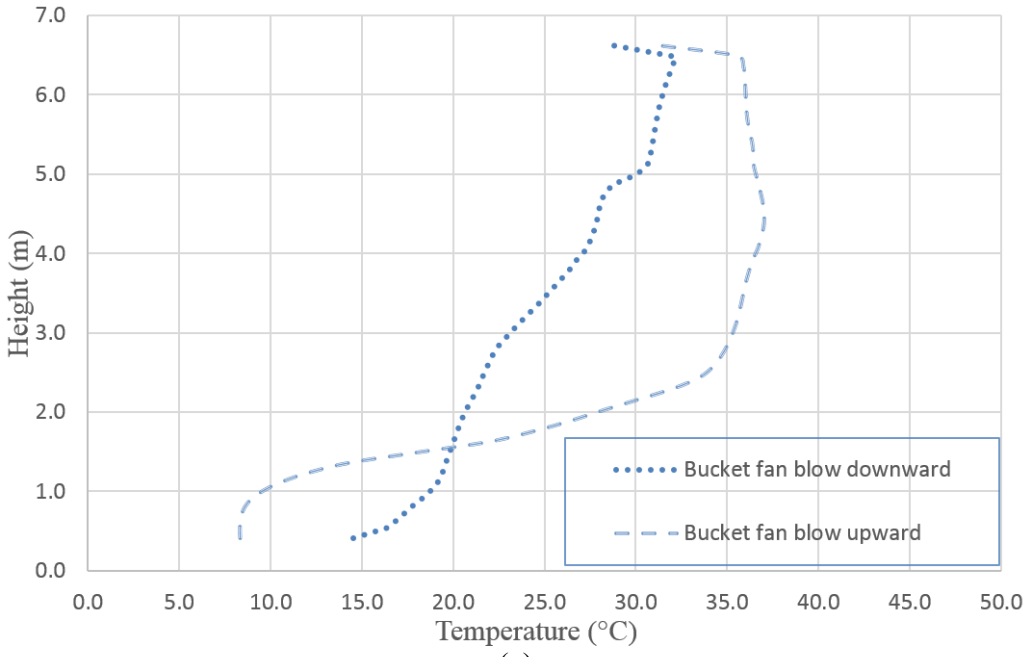

(a)

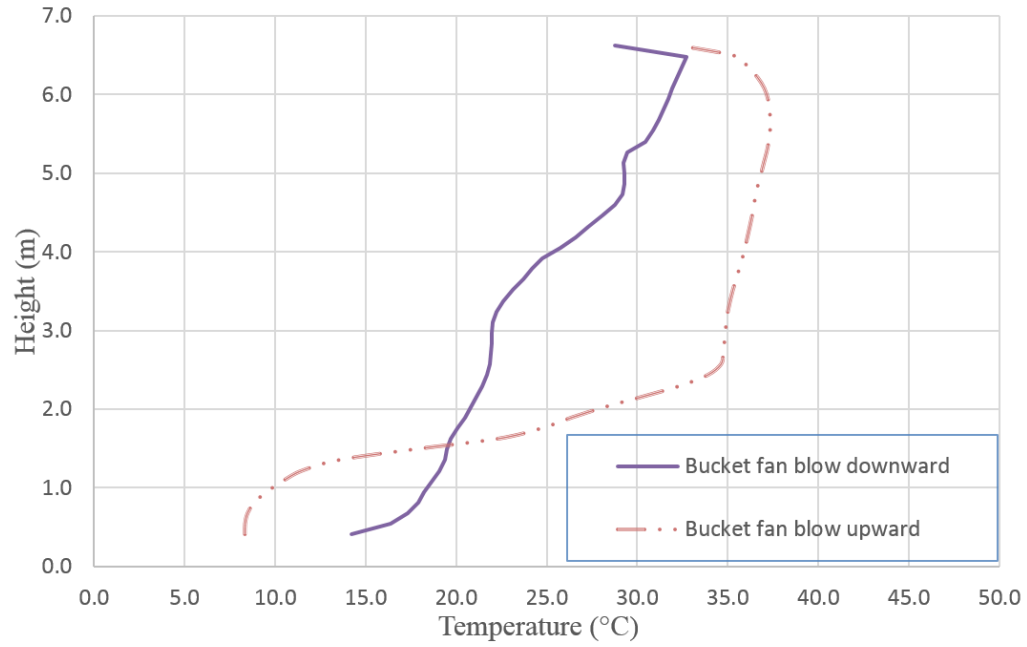

(b)

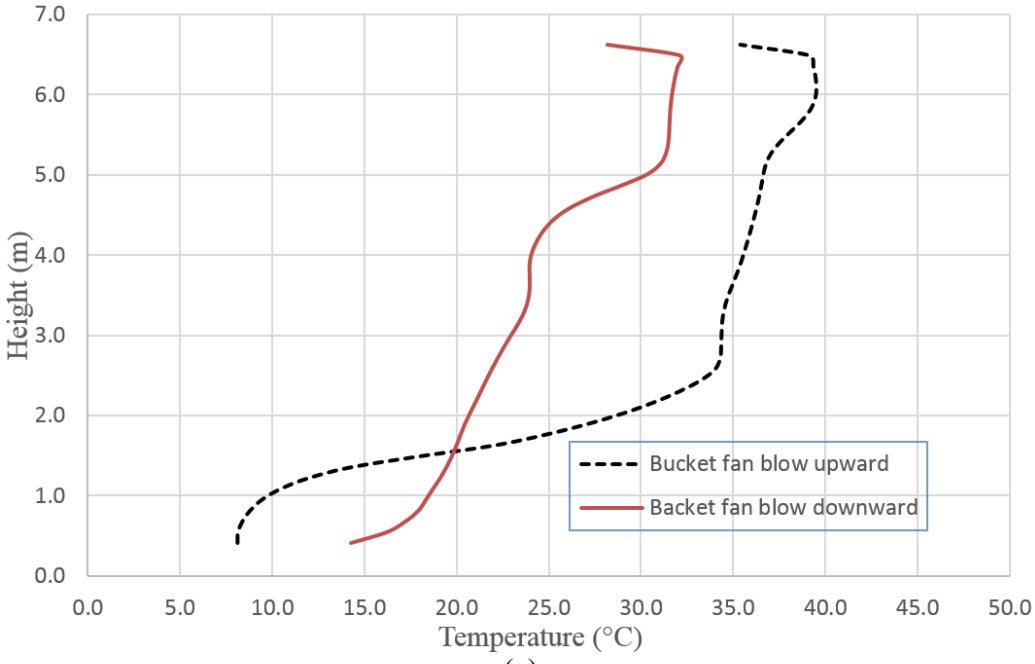

(c)

Figure 5-3. Comparison of temperature profiles between cases where the bucket fan is blowing downward and where it is blowing upward. (a), (b) and (c) present results from locations 1, 2 and 3 respectively.

For the air volume below 2.5 m, a drastic temperature gradient is observed in the upward-blowing fan case. The temperature difference and gradient in this section are larger than the whole line in

the downward-blowing fan case. The air temperature in most parts of this section is lower than in the case where the fan is blowing upward. The coldest temperature is 6-7 ˚C.

The case with the upward-blowing fan reaches a larger temperature difference at all three locations. The average non-uniformity coefficient of temperature in the upward-blowing fan case is 0.36. For the downward-blowing fan case, the value is 0.19.

Based on the results revealed in the above discussion, the downward-blowing mixing fan performs better in terms of thermal stratification reduction, energy-saving potential and occupant comfort.

5.1.3 The effects of changing the position of the bucket fan

The temperature profile is affected by the position of the mixing fan. Bucket fan #1 is located near the compartment that divides the first floor and the second floor of the warehouse and blows air toward the edge between the wall and ground. Bucket fan #2 is located near the measurement location 1 and blowing air toward the center of the empty space of the warehouse (Figure 3-1).

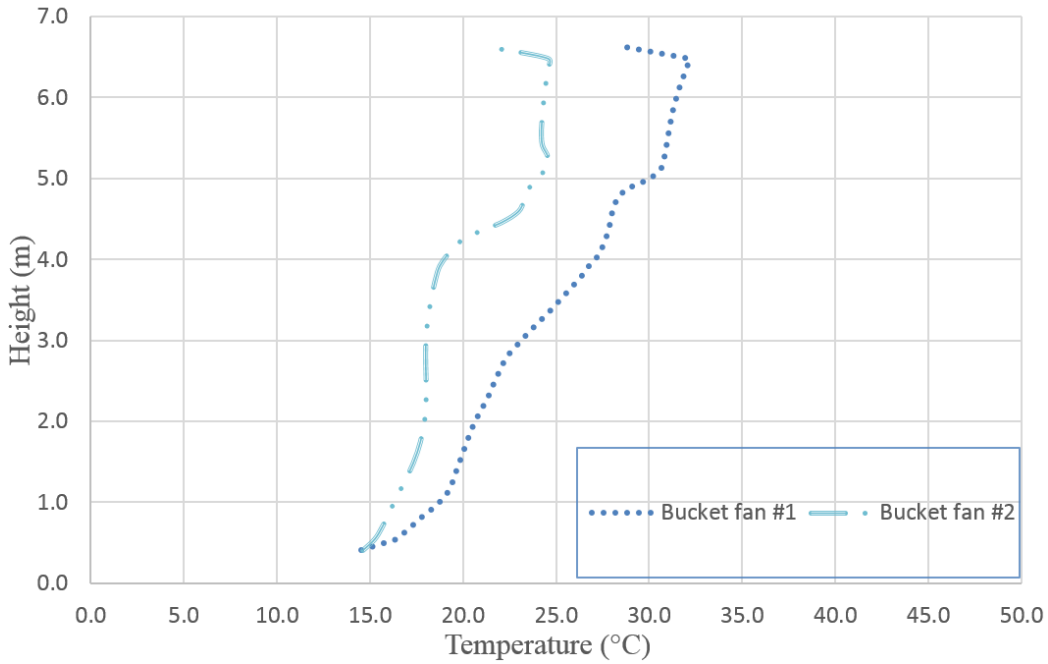

(a)

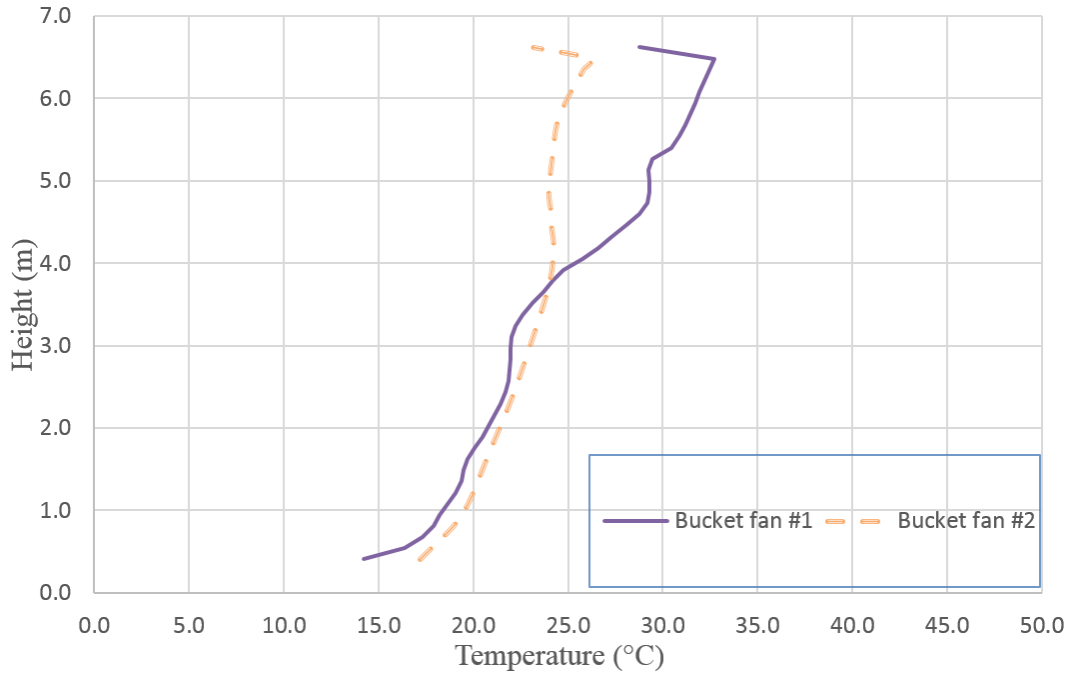

(b)

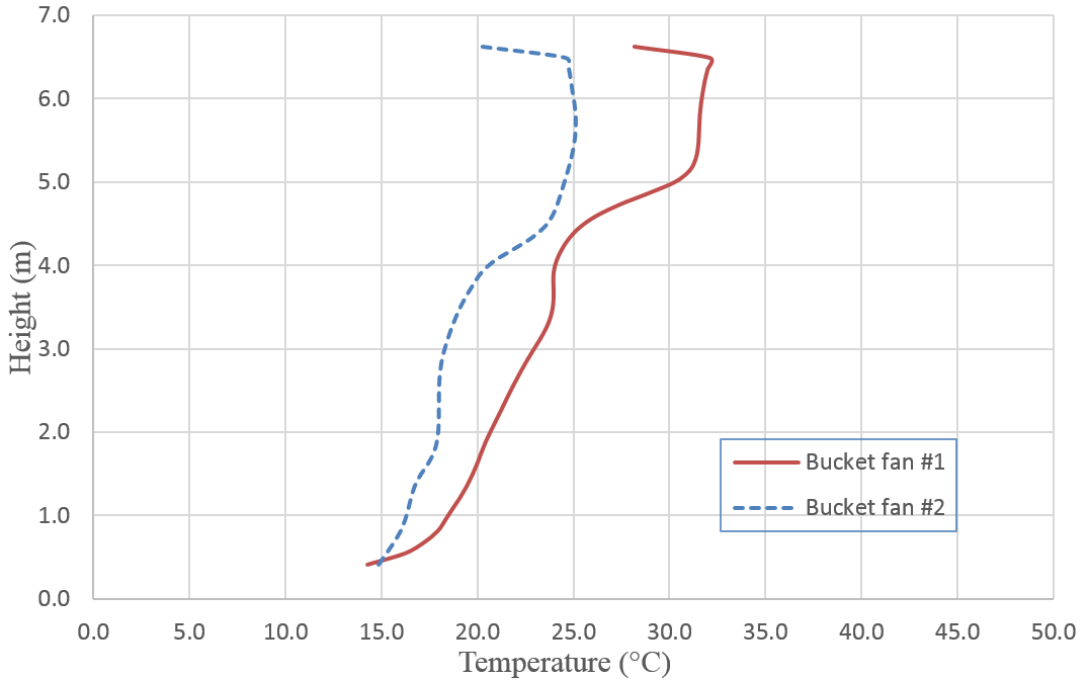

(c)

Figure 5-4. Temperature profile comparison of bucket fans running at different positions (position at bucket fan #1 vs. position at bucket fan #2). (a), (b) and (c) present results from location 1, 2 and 3 respectively.

Bucket fan #2 blows air downward and is angled towards the center of the empty space in the warehouse. As observed in Figure 4-13, the case of fan #2 has a non-uniformity coefficient ranging from 0.09 to 0.16. This is lower than in the case with bucket fan #1 running. In the case of bucket fan #1, the non-uniformity coefficient is around 0.19 at locations 1, 2 and 3.

In the case where bucket fan #1 is running, the overall temperature is higher along all three locations compared to those in the case where bucket fan #2 is running. Especially for the highest part in all three locations, the temperature is 5-7 ˚C higher than in the case where bucket fan #2 is running. Under the same heating conditions, the case with bucket fan #2 running lost more heat (750 W) through the ground surface as shown in Figure 4-11 but lost less heat (around 100 W) through the roof and exterior walls. The temperature distribution difference lead to the difference in the rate of heat flow through the ground, roof and walls.

However, one factor that should be taken into consideration is that locations 1 and 2 are at the projection area of fan #2. It is thus expected that fan #2 has an immediate mixing effect on the air around locations 1 and 2. Location 3 is far away from both bucket fan #1 and #2. The temperature at location 3 shows that the case where bucket fan #2 is running has more uniform temperature than the case where bucket fan #1 is running.

In conclusion for this part, installing a fan which blows air toward the center of the warehouse's empty space can improve the air-mixing effect.

5.1.4 The effects of increasing the number of Bucket fans

Increasing the number of bucket fans results in a higher volume flow rate. The larger the volume flow rate, the more air being blown down by the fan into the mixing process. The non-uniformity coefficient of temperature decreases from 0.194 to an average of 0.146 and then to 0.095 as the number of fans increases from 1 to 2 and to 3 respectively. The mixing effect can be observed in Figure 5-5 as the temperature profile tends to be more vertical as the number of fans is increased.

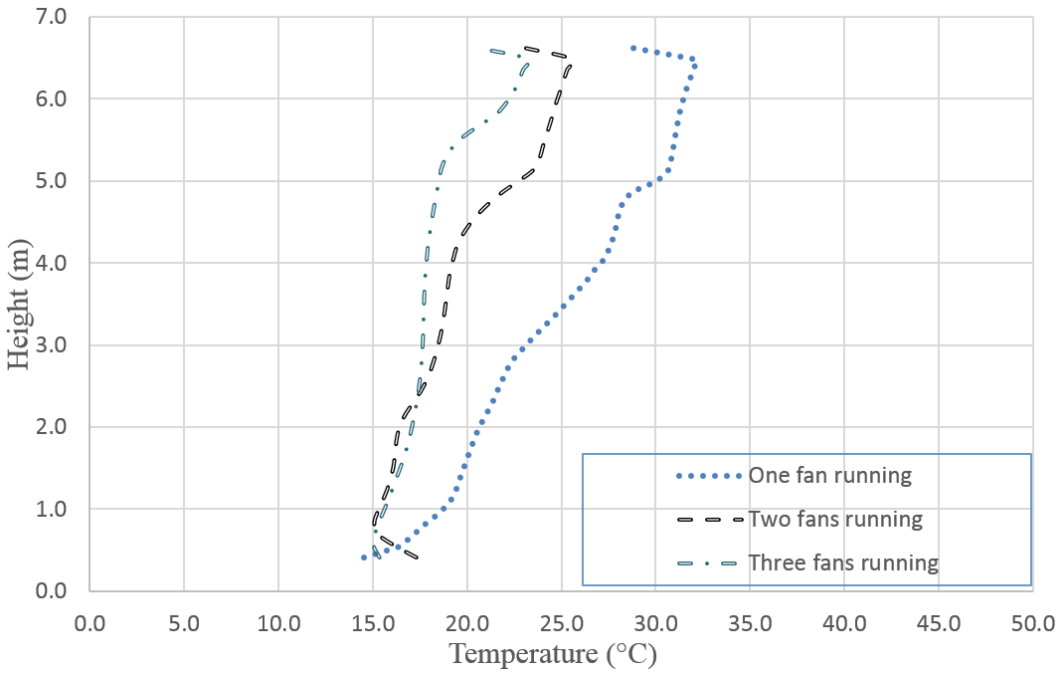
7.0
6.0
5.0
4.0
3.0
2.0
1.0
0.0
Height (m)
0.0
5.0
10.0
15.0
20.0
25.0
30.0
35.0
40.0
45.0
50.0
Temperature (°C)
One fan running
Two fans running
Three fans running

(a)

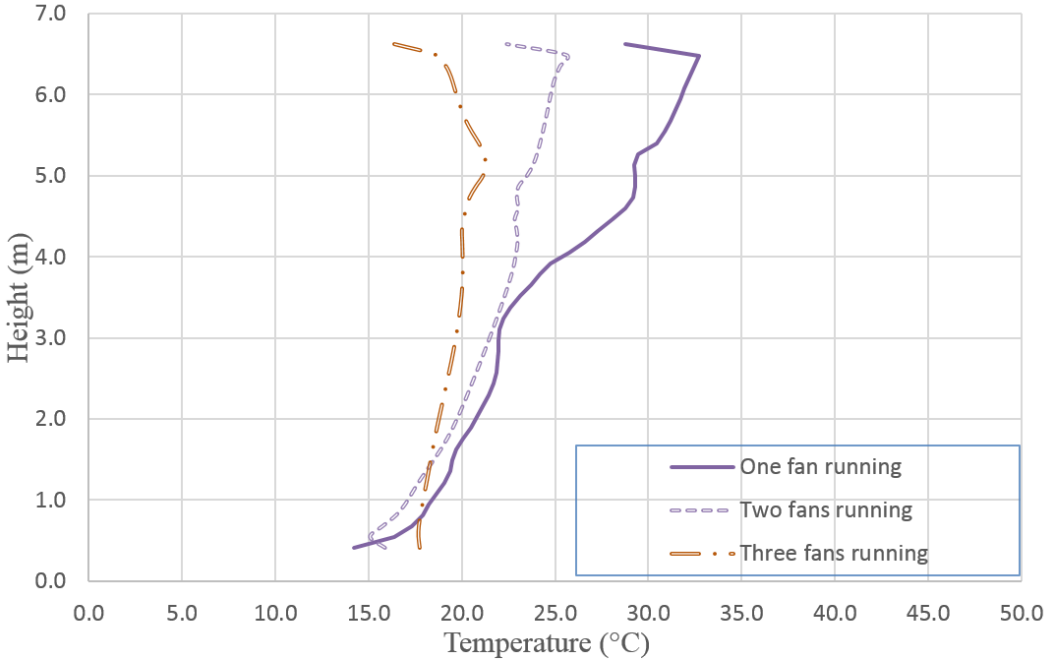
7.0
6.0
5.0
4.0
3.0
2.0
1.0
0.0
Height (m)
0.0
5.0
10.0
15.0
20.0
25.0
30.0
35.0
40.0
45.0
50.0
Temperature (°C)
One fan running
Two fans running
Three fans running

(b)

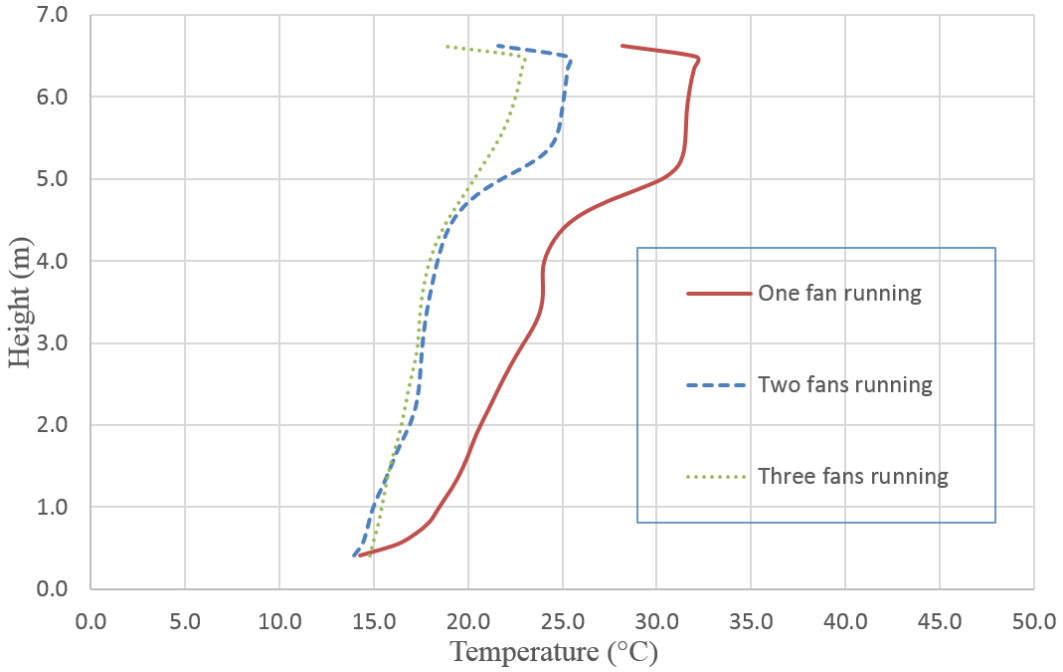

(c)

Figure 5-5. The temperature profile when increasing the number of running fans. A, b, and c present the results of locations 1, 2 and 3.

When the total air change rate (ACH: the volume of air flow through the fan per hour divided by the total indoor air volume) of all the fans reaches 3, any further increase in the number of fans does not significantly improve the reduction of thermal stratification. Each fan has a volume flow rate of 670 cfm, which is equivalent to 0.316 m^3/s. The air volume in the warehouse is 739.4 m^3, so each fan works for 1.54 ACH. The cases of fans 1, 2 and 3 thus have an air change rate of 1.54, 3.08 and 4.62 respectively. As can be observed in Figure 5-5, the improvement of the reduction of thermal stratification by increasing the number of fans from 2 to 3 is not as large as when increasing that number from 1 to 2.

On the other hand, one characteristic that should be pointed out is that the average temperature decreases as the number of fan increases. This can be explained by the fact that more fans generate more air movement along the bottom. As can be observed in Figure 4-11, two major differences in the rate of heat flow distribution were seen in these three cases. One difference is in the rate of heat flow through the roof. Another difference is in the rate of heat flow through the ground. At the other boundaries, the rates of heat flow are similar to each other.

A large share of heat is lost through the ground boundary in the cases with 2 or 3 fans running. The rate of heat flow lost through the ground increases as the number of fans increases. This indicates that the rate of heat flow is strongly influenced by the air velocity near the ground. The roof and the ground have different boundary condition settings. The roof has a constant outdoor temperature, a constant heat transfer coefficient at the outside air surface and a constant heat U-value for the wall material. Thus, a greater air velocity at the inner boundary of the roof only improves the heat transfer coefficient of the inside air boundary. However, the ground boundary is set to have a constant temperature at the ground surface, so the increase in air velocity will drastically increase the heat transfer coefficient between the indoor air and the ground boundary.

The excess energy lost through the ground boundary is caused by the model's deficiency. The question of how to improve the model so that it can also perform well when the air speed at the ground surface is high remains for further investigation. In Figure 5-5, the overall temperature decreases as the number of fans increases. If there is not extra heat lost through the ground, the temperature profiles of the cases with two and three fans will be shifted to the right. On the other hand, this extra heat lost through the ground boundary indicates the potential energy saved by increasing the number of mixing fans.

The air movement increases the heat transfer coefficient, so heat is easily transferred to the surface with a constant temperature. The case with only one fan running has a higher rate of heat flow through the roof. As there is less mixing in the warehouse and hence greater thermal stratification, the temperature at the upper part of the space is higher than in the other two cases. The average temperature surplus is around 10 ˚C. The larger temperature difference between the air beneath the ceiling and the outdoor air leads to more intense heat loss through the roof.

In conclusion, the more fans deployed to mix the air, the less stratification there will be in the warehouse. Increasing the number of mixing fans shows potential in saving heating energy.

5.1.5 Comparison of cases with the ceiling fan running and bucket fan running

Considering all the simulated scenarios, the case where the ceiling fan is running has the lowest non-uniformity coefficient of temperature. It ranges from 0.057 to 0.077, which is less than the value of 0.194 seen in the case where bucket fan #1 is running. The temperature difference is less

than 5 ˚C in the case where the air is mixed by a ceiling fan. In contrary, the temperature difference is around 17 ˚C in the case with one bucket fan running. The ceiling fan shows a significantly greater performance in mixing the air temperature compared with the bucket fan. This is attributable to the large volume flow rate of the ceiling fan.

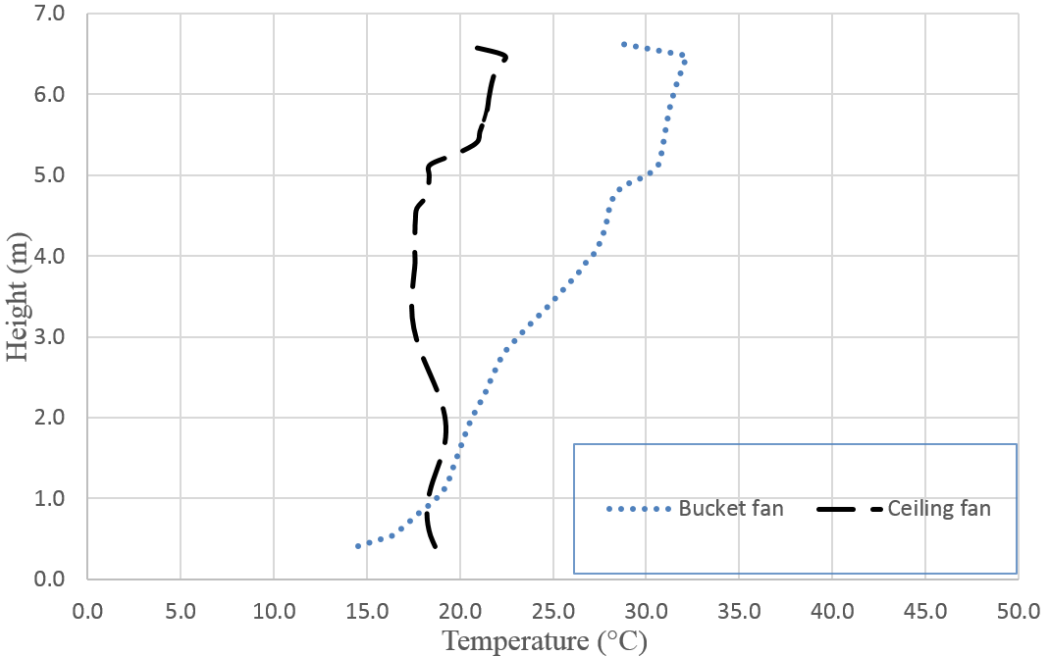

(a)

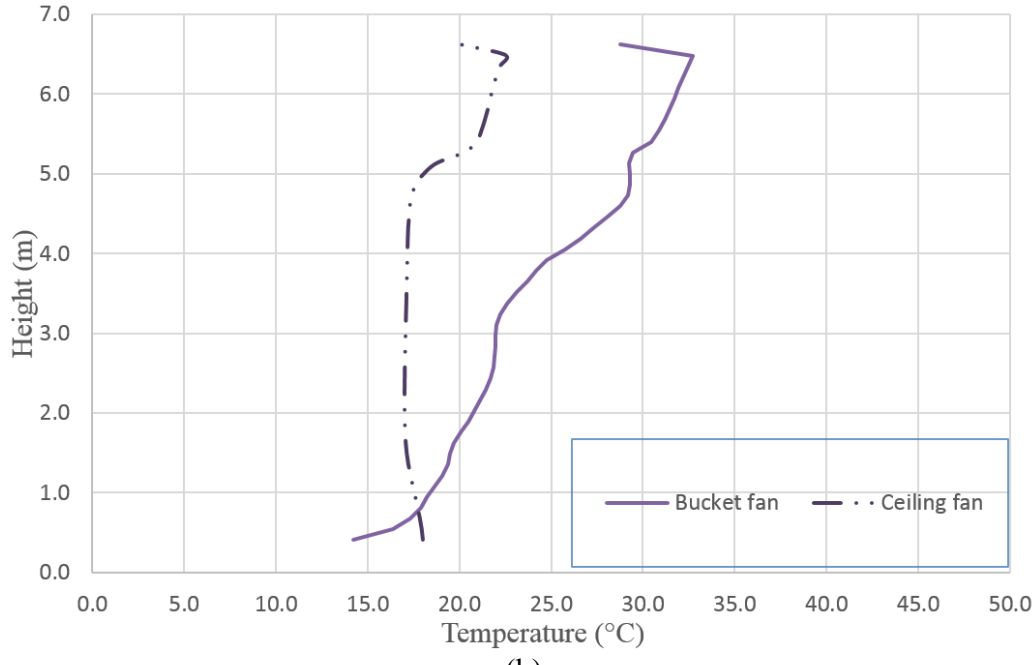

(b)

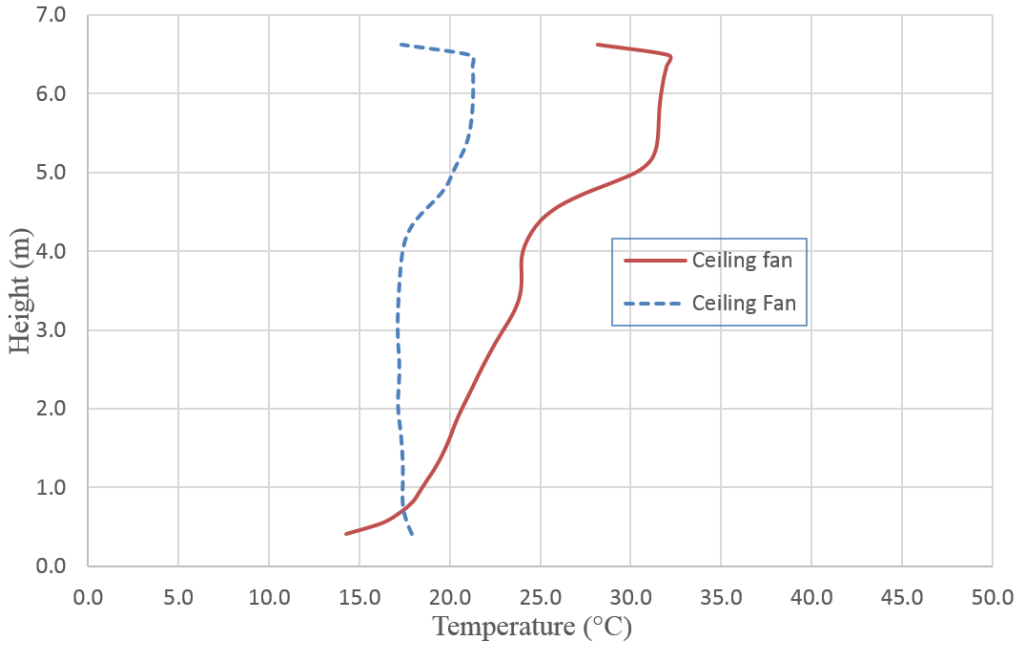

(c)

Figure 5-6. Temperature profile comparison between the case with the bucket fan running and the case with the ceiling fan running. A, b, and c present the results from locations 1,2 and 3 respectively.

Furthermore, a lower average temperature was observed in Figure 5-6. The ceiling fan pushes the air more powerfully as it has a larger blade and electric motor. This leads to greater air velocity at the boundary layer of the building's inner envelope. This velocity at the boundary layer increases the thermal conductance on the ground. This phenomenon is also indicated by Figure 4-11. For the case where the ceiling fan is running, the rate of heat flow lost through the ground surface is 1500 W. In comparison, the case where the bucket fan is running has a very low rate of heat flow through the ground. So the temperature change via the boundary layer is higher in comparison with the slower air speed conditions in the case where the bucket fan is running. Due to the above reason, the case where the ceiling fan is running has a lower average temperature. If the deficiency of the ground boundary in the model was improved, the average temperature in the case where the ceiling fan is running would be shifted rightward.

In this comparison, it was revealed that a ceiling fan neutralizes temperature difference more effectively than a bucket fan.

5.2 KS warehouse

5.2.1 Effect of different fan speeds (0, 30%, 100%)

Increasing fan speed has obvious effects on mixing air and removing stratification. Based on the comparison of the three cases, the non-uniformity coefficient of temperature decreases as fan speed increases. In the case where no fan is running, the average non-uniformity coefficient of temperature of all five locations is 0.79. In the cases where the fans are running at 30% and 100% volume flow rate, the average non-uniformity coefficients of temperature are 0.068 and 0.035 respectively. As fan speed increases, the temperature of the lower part of the air volume also increases. Meanwhile, the temperature of the higher part decreases with the increase of fan speed.

The temperature in the warehouse has been divided into two layers. The transition height is from 2 m to 2.5 m. This range is where the temperature profiles of the three different fan speed cases overlap each other. This kind of thermal stratification has been described by Andersen (1998) as type D vertical temperature distribution in heated space. This type of temperature profile occurs when the heat source is near the ceiling and the mixing effect is not strong enough to bring the warm air down to ground level. The mixing effect of bucket fans can be observed in the fact that as the fan speed increases, the vertical temperature profile tends to be closer to a straight vertical shape.

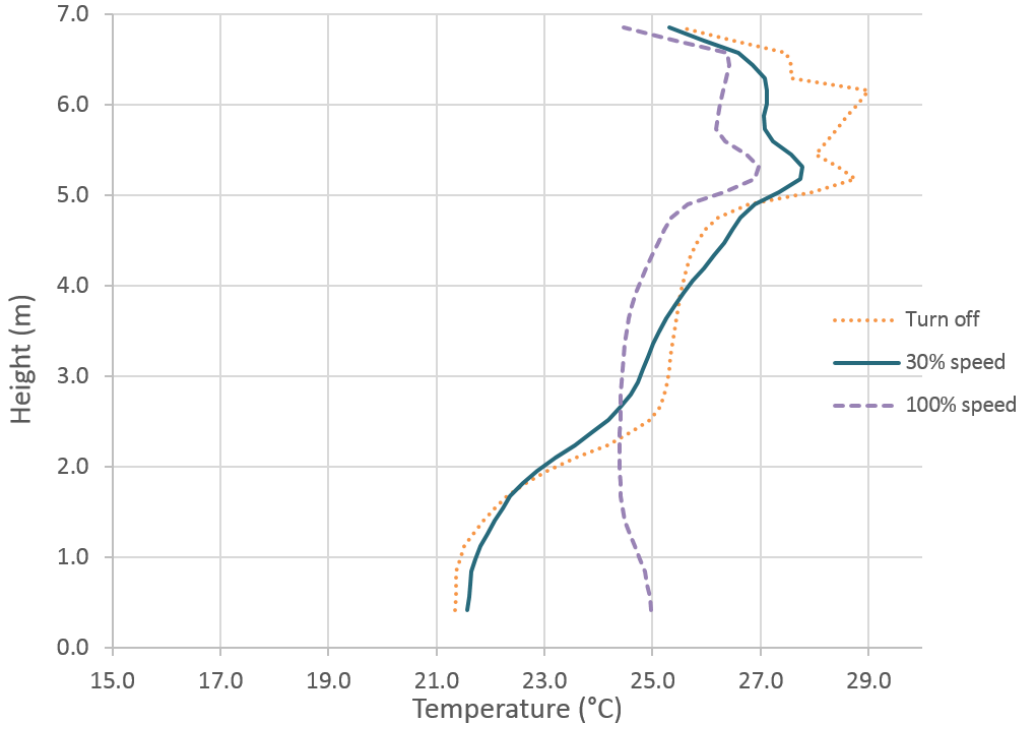
7.0
6.0
5.0
4.0
3.0
2.0
1.0
0.0
Height (m)
15.0
17.0
19.0
21.0
23.0
25.0
27.0
29.0
Temperature (°C)
Turn off
30% speed
100% speed

(a)

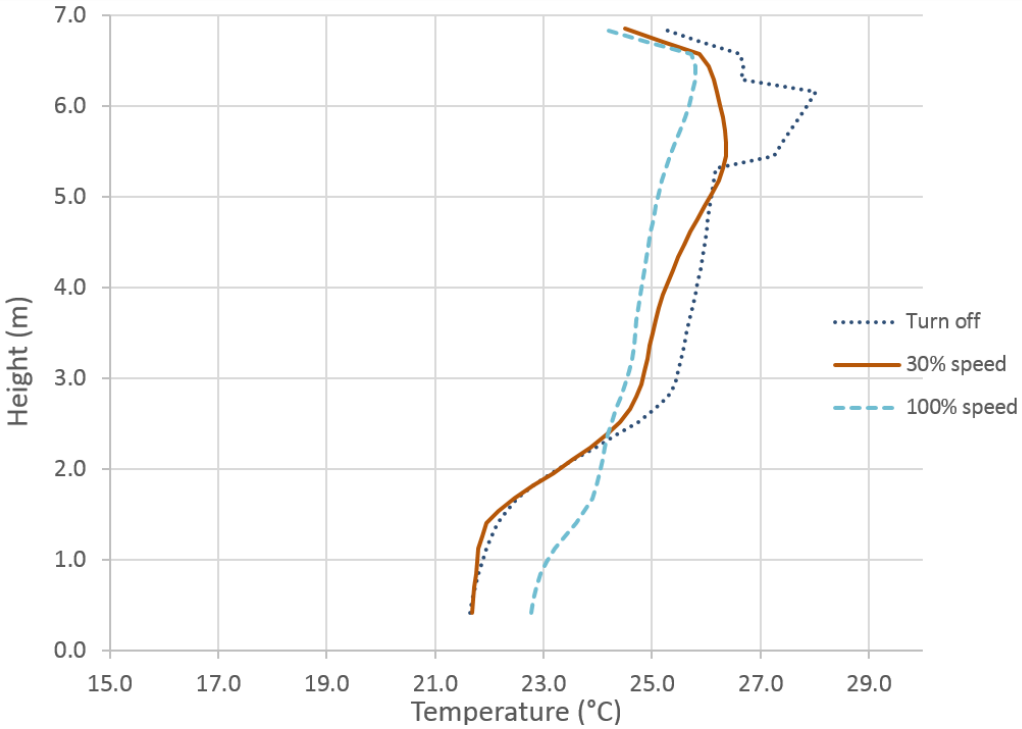
7.0
6.0
5.0
4.0
3.0
2.0
1.0
0.0
Height (m)
15.0
17.0
19.0
21.0
23.0
25.0
27.0
29.0
Temperature (°C)
Turn off
30% speed
100% speed

(b)

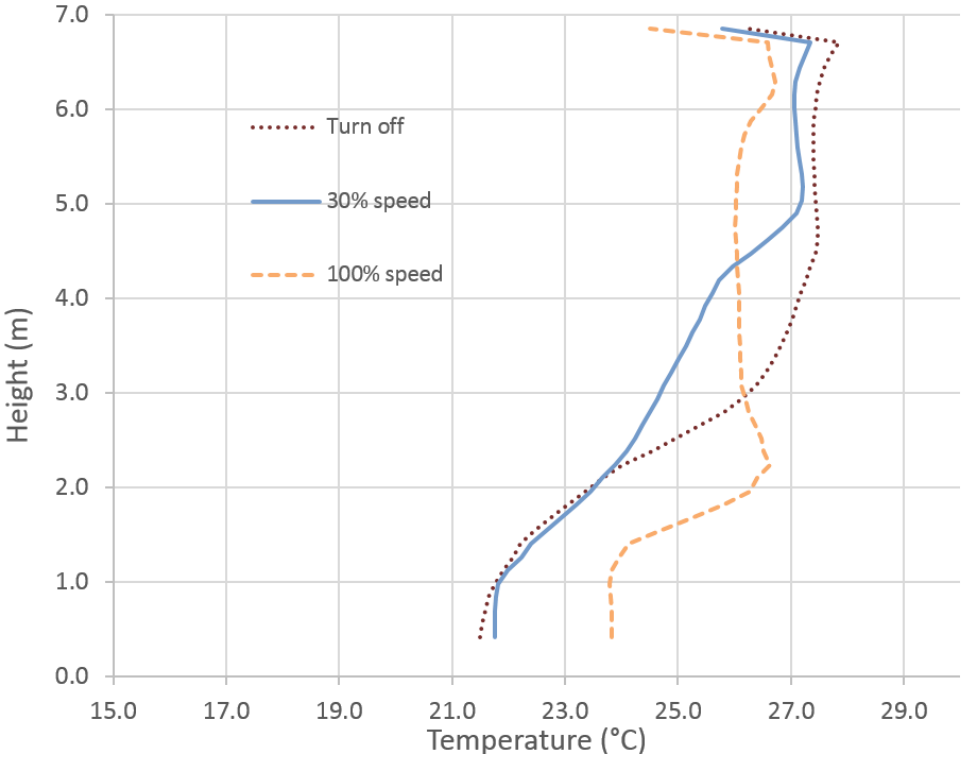
Turn off
30% speed
100% speed
Height (m)
Temperature (°C)
0.0
1.0
2.0
3.0
4.0
5.0
6.0
7.0
15.0
17.0
19.0
21.0
23.0
25.0
27.0
29.0

(c)

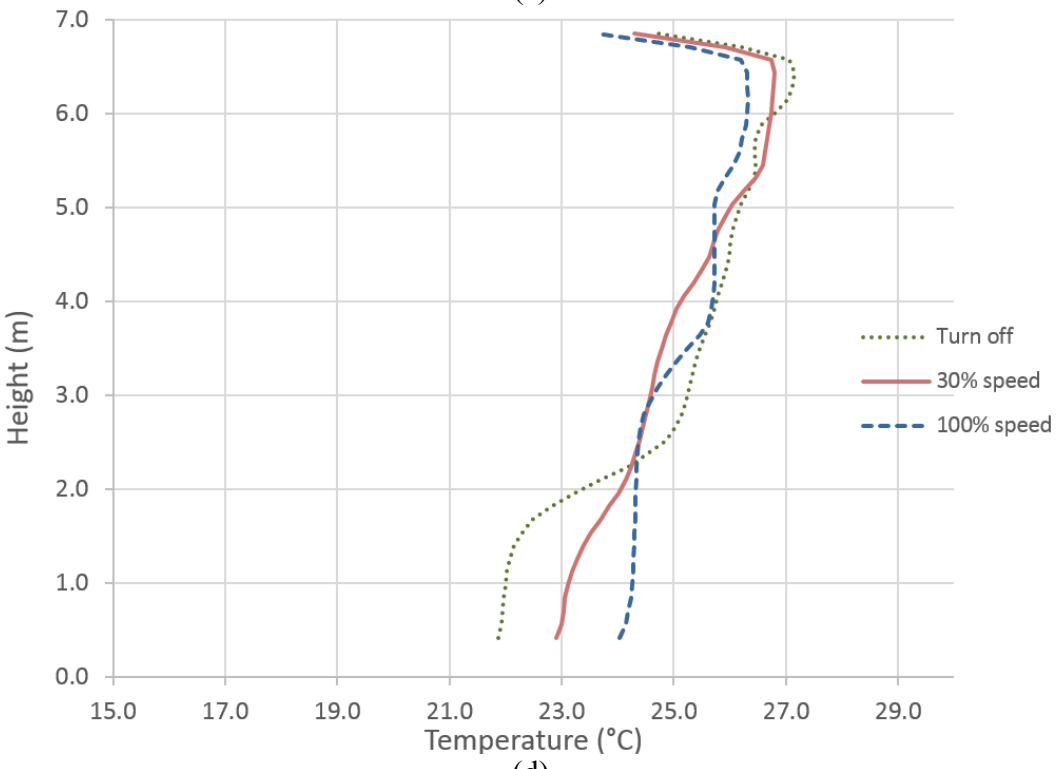
Turn off
30% speed
100% speed
Height (m)
Temperature (°C)
0.0
1.0
2.0
3.0
4.0
5.0
6.0
7.0
15.0
17.0
19.0
21.0
23.0
25.0
27.0
29.0

(d)

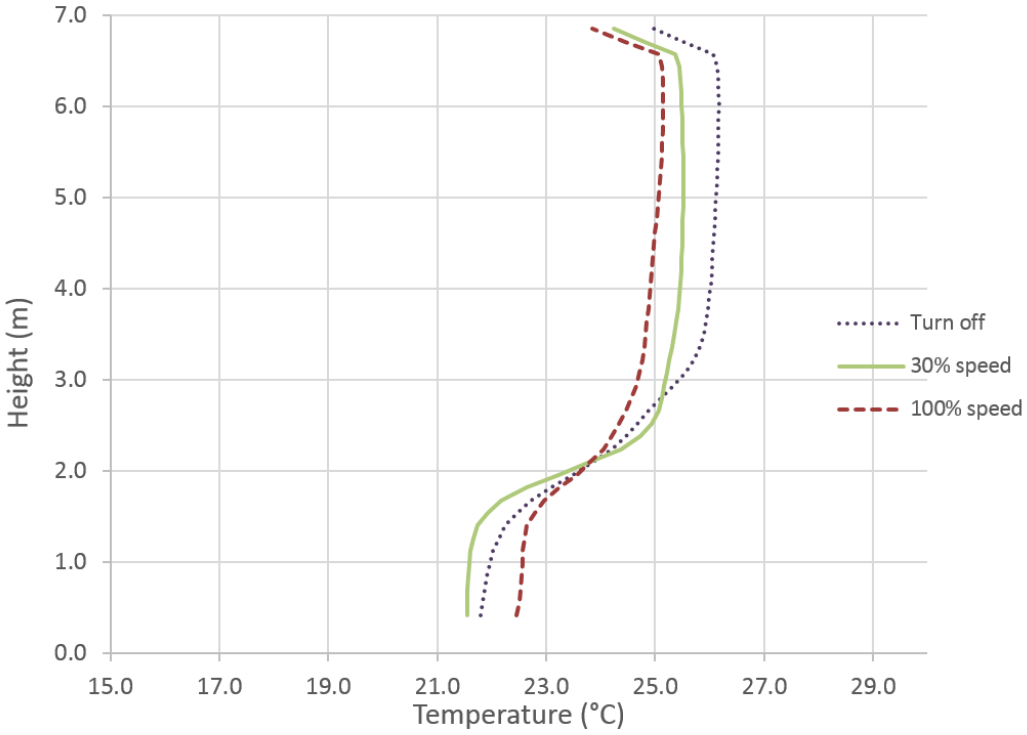

(e)

Figure 5-7. Temperature profile comparison among cases where the fan is turned off, running at 30% speed and running at 100% speed. A, b, c, d, and e present results from locations 1,2,3,4, and 5 respectively.

In the case where the fan is running at 100%, the temperature at the occupant zone is higher than in the other cases. Under the same heating conditions, the mixing fan can improve the temperature at the occupant zone. On the other hand, if the warehouse doesn't have any mixing fans working, it requires more heating energy to achieve a comfortable temperature at the occupant zone. The mixing fan is thus an effective way of improving the heating energy efficiency in the warehouse during the heating season.

At different locations, different temperature changes were observed. In the lower part of the air volume, which spans from ground level to 2.2 m in height, the temperature profile is almost the same in the cases where the fan is not running and where the fan is running at 30 % speed, as 30 % of the fan's maximum volume flow rate is not strong enough to push warm air down to ground level and affect the lower part of the air volume. However, a fan running at 30% speed does mix the air at the higher level. Since location 5 is far away from the fan, it is not strongly affected by

the mixing fan. The temperature change at location 5 is not as obvious as it is at the other 4 locations. However, the temperature stratification is still reduced as the fan speed increases.

5.2.2 Fresh air projection angle (Horizontal, 45 degrees, and downward)

Changing the projection direction of fresh warm air from the fabric diffuser has a profound effect on temperature stratification removal. In the original case, where the fresh warm air is injected into space horizontally, the average non-uniformity coefficient of temperature is 0.068. In the cases where fresh warm air is injected into space 45 degrees downward and vertically downward from the fabric diffuser cylinder, the average non-uniformity coefficients of temperature are 0.030 and 0.014 respectively.

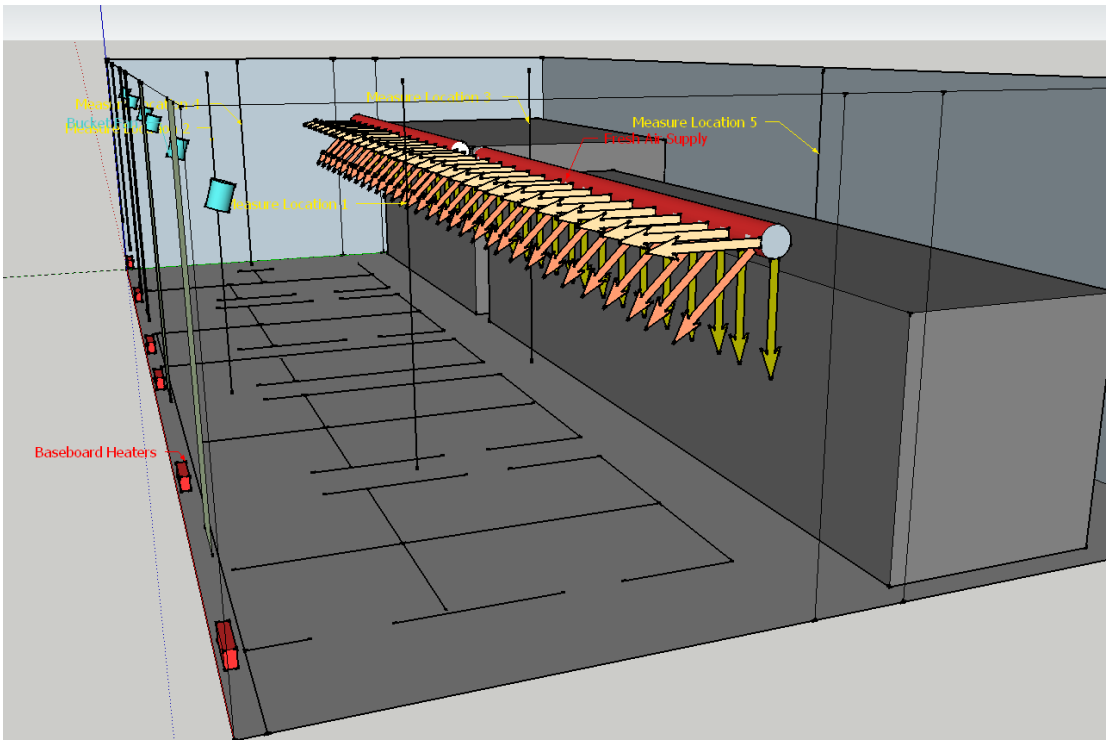

Figure 5-8. Schematic diagram of horizontal, 45 degree and vertically downward fresh air projection directions.

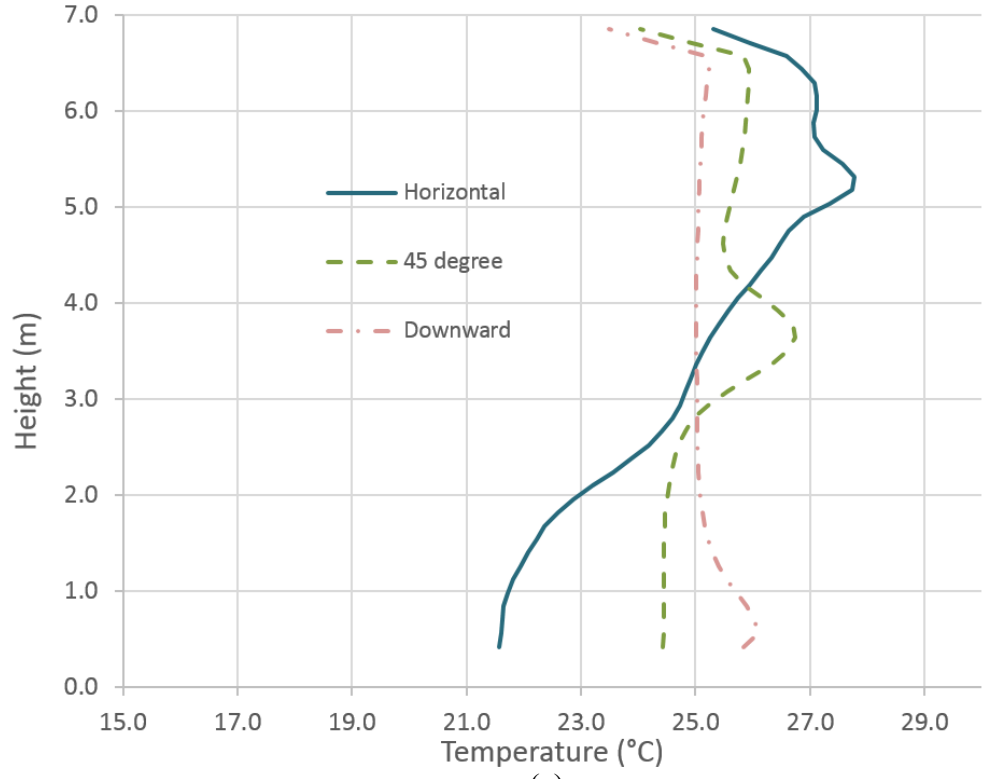
7.0
6.0
5.0
4.0
3.0
2.0
1.0
0.0
Height (m)
Horizontal
45 degree
Downward
15.0
17.0
19.0
21.0
23.0
25.0
27.0
29.0
Temperature (°C)

(a)

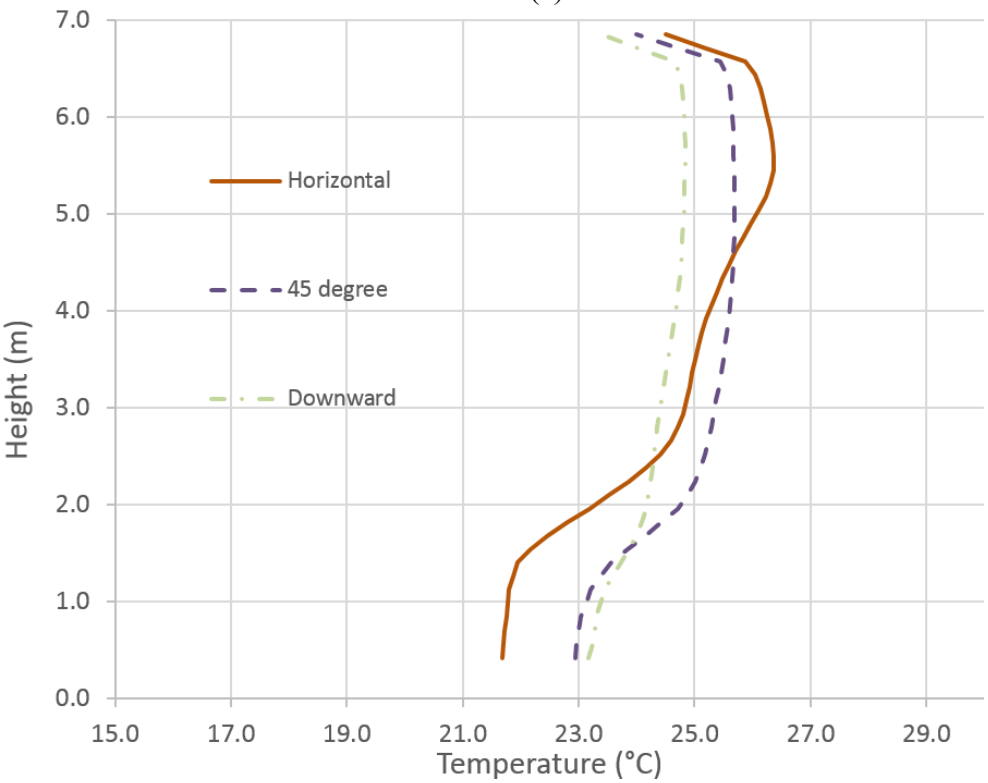
7.0
6.0
5.0
4.0
3.0
2.0
1.0
0.0
Height (m)
Horizontal
45 degree
Downward
15.0
17.0
19.0
21.0
23.0
25.0
27.0
29.0
Temperature (°C)

(b)

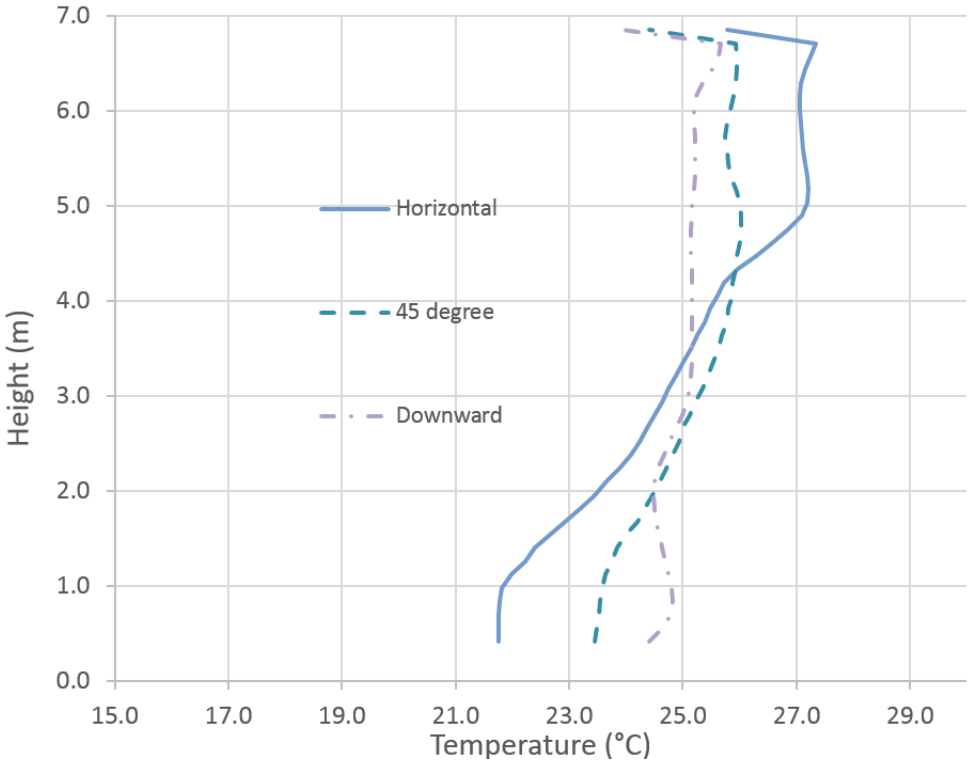
7.0
6.0
5.0
4.0
3.0
2.0
1.0
0.0
Height (m)
Horizontal
45 degree
Downward
15.0
17.0
19.0
21.0
23.0
25.0
27.0
29.0
Temperature (°C)

(c)

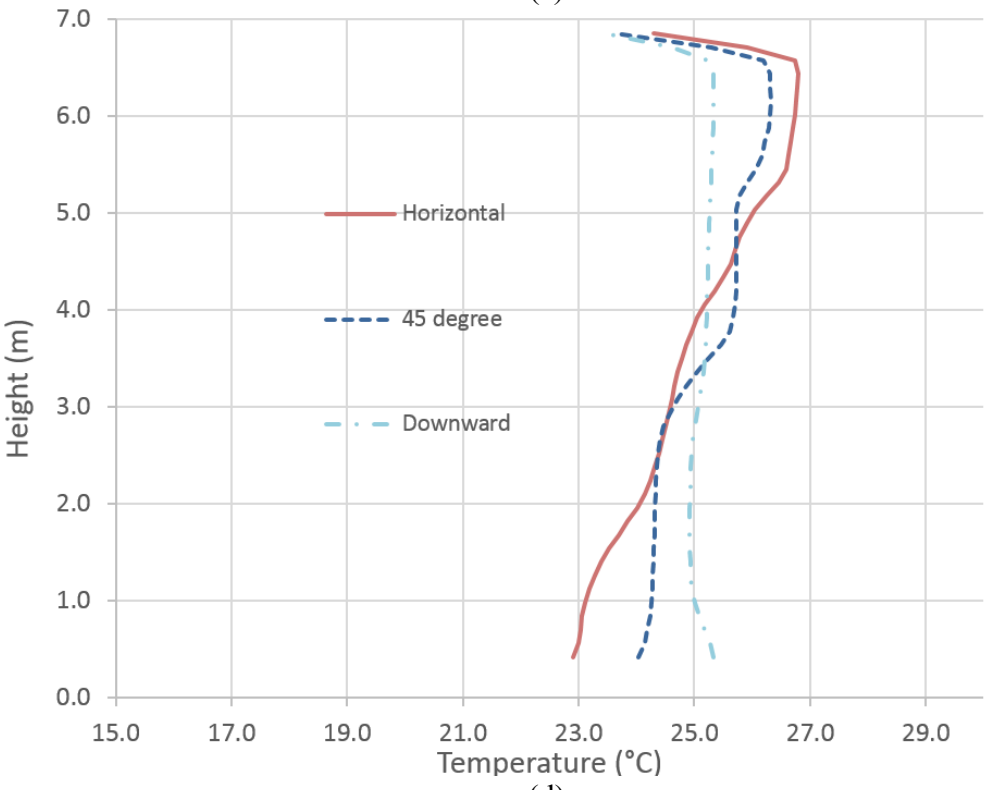
7.0
6.0
5.0
4.0
3.0
2.0
1.0
0.0
Height (m)
Horizontal
45 degree
Downward
15.0
17.0
19.0
21.0
23.0
25.0
27.0
29.0
Temperature (°C)

(d)

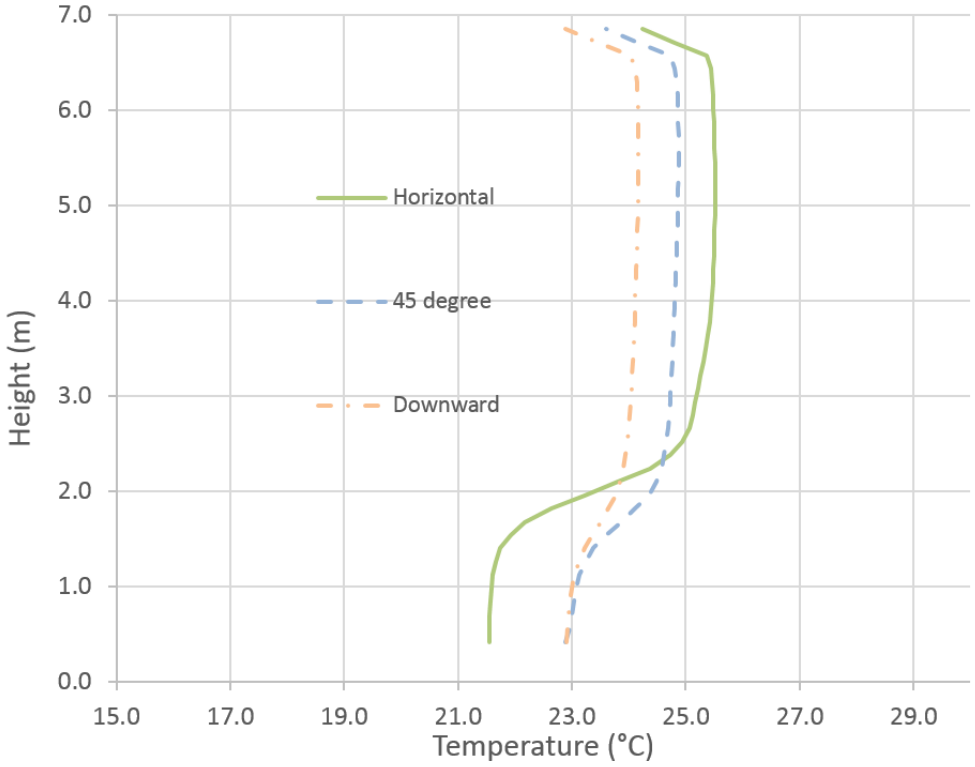

(e)

Figure 5-9. Temperature profile results for cases with different fresh air supply directions. (a), (b), (c), (d), and (e) present results from locations 1,2,3,4, and 5 respectively.

The temperature at the occupant zone also increases as the projection angle of warm air is turned downwards. The temperature improvement ranges from 2 ˚C to 4.5 ˚C depending on the locations.

However, when the fresh warm air is injected vertically downwards, it generates an air draft which affects occupant comfort. This is a concern that limits the use of downward fresh air projection angles. If the building is tall enough, such as the MG building (Figure 7-4), a downward fresh air projection angle is recommended.

CHAPTER 6. CONCLUSIONS AND FUTURE WORK

This thesis is composed of field measurements and CFD simulations. Based on the field measurements, the conditions of thermal stratification in five buildings were studied. Furthermore, CFD simulations of cases representing different mixing fan settings were analyzed. The major conclusions are listed as follows.

6.1.1 Conclusions based on field measurement

1. Four of the five buildings showed temperature stratification, as observed in the field measurements. The temperature difference ranged from 2.7 ˚C to 20.6 ˚C. The non-uniformity coefficient of temperature ranged from 0.020 to 0.148. The most severe thermal stratification had a temperature difference of 20.6 ˚C, as observed in the QT warehouse.
2. The degree of thermal stratification varied significantly depending on the heating method used by the warehouse. The type of heaters and the number and distribution of heating sources all play a role in affecting the formation of thermal stratification. In the QT warehouse, which had a single force air heater, the non-uniformity coefficient of temperature reached 0.148. If the heat sources are dispersed across a wide area rather than concentrated in one single heater, such as in the DT warehouse, which had 6 infrared heaters distributed in different positions, the average non-uniformity coefficient of temperature can be brought down to 0.034. Furthermore, widely distributed heating sources used in tandem with the air-mixing momentum provided by diffusers, such as in the MG building, can bring thermal stratification down to less than 1 ˚C.
3. Building geometry affects the formation of thermal stratification. The cooling effect from the roof prevents the formation of thermal stratification. Warehouses whose roofs make up a larger area percentage of their total surface area, such as DT (39.6% of the total area) and XL (41.6%), have less thermal stratification. However, while the thermal stratification is lower in this condition, it does not lead to less heating energy loss.

6.1.2 Conclusions based on numerical simulation

The simulation of the ceiling fans was validated with the velocity component measurement data. Also, the temperature results from the simulation of the whole warehouse were validated with the field measurement data. Based on the comparison of results from the simulation cases, the conclusions are listed as follows:

1. A mixing fan has direct effects in neutralizing thermal stratification. Mixing fans can reduce temperature at high levels and increase temperature at low levels. Mixing fans also reduce the average non-uniformity coefficient of temperature from 0.488 to 0.194.
2. Mixing fans can reduce the heating energy requirement. Lower temperature at high levels leads to a lower rate of heat flow through the roof. For instance, in the QT warehouse, a mixing fan can reduce the rate of heat flow from the roof by 21.2% compared to cases with no fan running. Furthermore, the utilization of mixing fans increases the temperature at the occupant zone. In occupant zone of QT warehouse, the temperature of the fan running case is 10 ˚C higher than no fan running case. This indicates that a warehouse with mixing fans running requires less heating energy to reach the same heating conditions in compared with a warehouse without a mixing fan running.
3. Mixing fans with a downward air projection direction are more efficient in reducing thermal stratification than those with an upward projection direction. A downward projection direction can mix the air at all heights. In contrast, an upward projection direction can only achieve uniformity in the section of air which is higher than the fan. In the case comparison for the QT warehouse, the average non-uniformity coefficient of temperature for the upward projection direction case and the downward projection direction case are 0.356 and 0.194 respectively.
4. A fan blowing the air toward the center of empty space in the warehouse has a greater mixing effect than one blowing air toward the edges. In the case comparison for the QT warehouse, the fan #1 case and fan #2 case have average non-uniformity coefficients of temperature of 0.194 and 0.137 respectively. There is a 15.0 % increase in the rate of heat flow from the roof when changing the downward projection direction to an upward projection direction.
5. Increasing the volume flow rate of the fans has the effect of decreasing thermal stratification. Both the QT warehouse cases in which the number of mixing fans was increased and the KS

warehouse case in which the fan speed was increased show that thermal stratification decreases as the total volume flow rate increases. An air change rate of 3 is recommended for design based on the comparison of results from the QT warehouse cases. Further increasing the volume flow rate does not produce obvious improvements in reducing thermal stratification as the air temperature has reached uniformity.

6. Setting HVAC diffusers to project air downwards in a warehouse has the effect of reducing thermal stratification. In a comparison of cases wherein the diffusers in the KS warehouse were set to project air horizontally, 45˚ downward, and vertically downward, the average non-uniformity coefficients of temperature were 0.068, 0.030 and 0.014 respectively. The low thermal stratification observed in the MG building is also attributable to the downward projection angle of the diffusers beneath the ceiling.

6.2 Summary

In this study, five rounds of field measurements were conducted to record thermal stratification in large warehouses in the Montreal region. Different degrees of thermal stratification were revealed from the measurement data. The measurement results indicated that thermal stratification was common among the warehouses.

Mixing fans proved to be an effective method of solving the temperature stratification problem with low financial investment. Furthermore, different mixing fan settings was tested and compared via CFD simulation. The most recommended method of mixing air is the installation of a series of bucket fans beneath the ceiling of the warehouse. This case has the best performance in terms of the mixing results as well as the factors of fan noise and air drafts.

6.3 Future work

This study sheds light on future work which could be done to further explore the function of mixing fans in large buildings. This study is focused on the simulation of single instances of time based on the instances when the measurements were taken. More accurate settings for the boundary conditions on the ground would improve the simulation. Further research, such as simulations which can cover the whole diurnal cycle or even the entire heating season of the warehouse, would

provide more detailed information on the reduction of energy use via air mixing fans. A feedback simulation process which allows the temperature to stay within a certain range is proposed. While the heating sources can be adjusted according to the temperature feedback, it is recommended to create additional energy simulation models so that an entire year of mixing fan energy saving performance can be simulated. Furthermore, issues such as the noise level of the fans and air drafts at the occupant zone are also a consideration.

References

Allen, J. A. (1877). *The Influence of Physical Conditions in the Genesis of Species.*

Andersen, K. T. (1998). Design of natural ventilation by thermal buoyancy with temperature stratification. *In International conference on air distribution in rooms.*

Anodisers, M. (2015). *Environmental Technology Centre*. (Mansfield Anodisers) Retrieved from https://nottingham.ac.uk/etc/cs-mansfieldanodisers.php

ANSYS, I. (2009, 01 29). *Setting Up a Single Rotating Reference Frame Problem*. Retrieved from ANSYS FLUENT 12.0 User's Guide: http://www.afs.enea.it/project/neptunius/docs/fluent/html/ug/node375.htm#sec-move-setup

Armstong, M., Chihata, B., & MacDonald, R. (2009). Cold weather destratification energy savings of a warehousing facility. *ASHRAE Transactions*, 115(2).

ASHRAE. (2013). ASHRAE 41.1:2013, Standard Method For Temperature Measurement. *ASHRAE*.

Aynsley, R. (2005). Saving energy with in door air movement. *The International Journal of Ventilation, 4(2)*, 167-175.

Aynsley, R. (2005). Saving energy with indoor air movement. *4(2)*, 167-175.

Aynsley, R. (2005). Saving heating costs in warehouses. *ASHRAE journal 47.12*, 46-51.

Aynsley, R. (2007). Circulating fans for summer and winter comfort and indoor energy efficiency. *Environment Design Guide*.

Aynsley, R., & M, A. (2005). Temperature profiles and winter destratification energy savings. *EcoLibrium*, 18-23.

Behidj, N., Brugger, M., Kwan, R., Leblanc, S., Liu, Y., Warbanski, M., & Yamada, F. (2011). *Energy Efficiency Trends in Canada, 1990 to 2009.* Retrieved from Natural Resources Canada: http://oee.nrcan.gc.ca/corporate/statistics/neud/dpa/data_e/publications.cfm

Blackburn, T., M., K., J. Gaston, & Natasha, L. (1999). Geographic gradients in body size: a clarification of Bergmann's rule. *Diversity and distributions 5*, 165-174.

Boon, C., & Battams, V. (1988). Air mixing fans in a broiler building—their use and efficiency. *Journal of Agricultural Engineering Research 39, no. 2*, 137-147.

Bottcher, R. W., Baughman, G. R., Driggers., & B., L. (1988). Temperature stratification in broiler houses and the effects of ceiling fans. *Transaction of the ASAE 4, no. 1*, 66-70.

Chen, K., Qing-Ping, L., Geng-Hua, L., Ying, Y., Lu-Quan, R., & Zhi-Wu, H. (2012). Aerodynamic noise reduction of small axial fan using hush characteristics of eagle owl feather. *Journal of Jilin University(Engineering and Technology Edition)*, 79-84.

CLEAR. (2016). *Level Eleven: Surface Area to Volume Ratio*. Retrieved from Clear Comfortable Low Energy ARchitecture: http://www.new-learn.info/packages/clear/interactive/matrix/level_11_surface_area_to_volume_ratio.html

Cøengel, Y. A. (2007). *Heat and mass transfer: a practical approach.* New York: McGraw-Hill.

Hutcheon, N. B., & Handegord, G. O. (1983). *Building science for a cold climate.* Wiley.

James, F., & Ieuan, O. (2010). *MegaFan Warehouse Case Study: Final Report.* University of Liverpool.

Li, Q., Hiroshi, Y., Akashi, M., Bo, L., Qinglin, M., Lihua, Z., & Yufat, L. (2009). CFD study of the thermal environment in an air-conditioned train station building. *Building and Environment, 44(7)*, 1452-1465.

Lian, Z. W., & Qi, D. H. (2009). Modification for evaluation indexes of air distribution. *Journal of Chongqing University*, 32 (8), 937-942.

Lian, Z. W., Qi, D. H., Liu, W. W., & Song, J. L. (2010). Influence of indoor partition on air distribution of ceiling-mounted cassette type indoor unit. *Journal of Central South University (Science and Technology)*, 364-369.

MarcoAir. (2015, 03). *What is HVLS?* Retrieved from Marco Air, Engineer of Air: http://macroairfans.com/#whatishvls

Mathews, E. H. (1989). Numerical solutions of fluid problems related to buildings, structures and the environment. *Building and Environment, 24(1)*, 1.

McQuiston, F. C., & Parker, J. D. (1982). *Heating, ventilating, and air conditioning: analysis and design.* New York: John Wiley and Sons., Inc.

Momoi, Y., Sagara, K., Yamanaka, T., & Kotani., H. (2004, September 5-8). Modeling of ceiling fan based on velocity measurement for CFD simulation of airflow in large room. *Proceedings of 9th international conference on air distribution in rooms, Coimbra, Portugal*, 14.

Nielsen, P. V. (1998). *The selection of turbulence models for prediction of room airflow.* Dept. of Building Technology and Structural Engineering.

NOAA. (2016, 04). *What are temperature inversions?* Retrieved from National Oceanic and Atmospheric Administration: http://www.wrh.noaa.gov/slc/climate/TemperatureInversions.php

Porras-Amores, C., Mazarrón, F. R., & Cañas, I. (2014). Study of the vertical distribution of air temperature in warehouses. *Energies, 7(3)*, 1193-1206.

Puravent. (2016). *Destratification Fan Guide*. Retrieved from www.puravent.co.uk: http://www.puravent.co.uk/blog/space-heating/destratification-fan-guide/

Qi, D. D., Wang, L. L., & & Zmeureanu, R. (2013, May). Large Eddy Simulation of Thermal Comfort and Energy Utilization Indices for Indoor Airflows. *In ASHRAE 2013 Annual Conference*, 22-26.

Ramki. (2012, 10 12). *Destratification Fans*. Retrieved from www.ramki.co.uk: http://www.ramki.co.uk/plumbing-services/destratification-fans/

Said, M. N., MacDonald, R. A., & Durrant., G. C. (1996). Measurement of thermal stratification in large single-cell buildings. *Energy and buildings 24, no. 2*, 105-115.

Stoakes, P. J. (2009). *"Numerical simulations of airflow and heat transfer in buildings."*. Virginia Polytechnic Institute and State University.

Su, X., Zhang, X., & Gao., J. (2009). Evaluation method of natural ventilation system based on thermal comfort in China. *Energy and Buildings, 41(1)*, 67-70.

Wang, Y., Jens, K., Fu-Yun, Z., & Hartmut, S. (2013). Indoor environment of a classroom in a passive school building with displacement ventilation. *In Proceedings of Building Simulation*, pp. 1902-1909.

Wei, L., Zhaoxia, P., & Shigong, W. (2013). Numerical simulation of the life cycle of a persistent wintertime inversion over Salt Lake City. *Boundary-layer meteorology*, 399-418.

Zhu, S., Srebric, J., Rudnick, S. N., Vincent, R. L., & Nardell, E. A. (2014). Numerical modeling of indoor environment with a ceiling fan and an upper-room ultraviolet germicidal irradiation system. *Building and environment, 72*, 116-124.

ZooFans. (2015). *Zoo fans, Lowering the Cost of High Ceilings*. Retrieved from Destratification Fans: Energy Efficiency | ZooFans.com: http://www.zoofans.com/architects-engineers/

APPENDICES

Appendix A: Thermocouple calibration

The following is the calibration information for the two thermocouple trees.

Table 10. Table of thermocouple calibration result.

	1	2	3	4	5	6	7	8	9	10	11	12
Thermocouple series A in Ice & water	0.21	0.26	0.34	0.35	0.37	0.35	0.39	0.45	0.48	0.50	0.51	0.55
Thermocouple series A in Boiling water	99.70	99.64	99.82	100.01	99.81	99.79	99.94	99.88	100.07	100.15	99.93	100.01
Thermocouple series B in Ice & water	0.50	0.52	0.54	0.53	0.68	0.62	0.55	0.56	0.59	0.73	0.60	0.63
Thermocouple series B in Boiling water	99.79	99.83	99.89	99.83	99.83	99.91	100.02	99.98	100.03	100.04	100.00	99.91

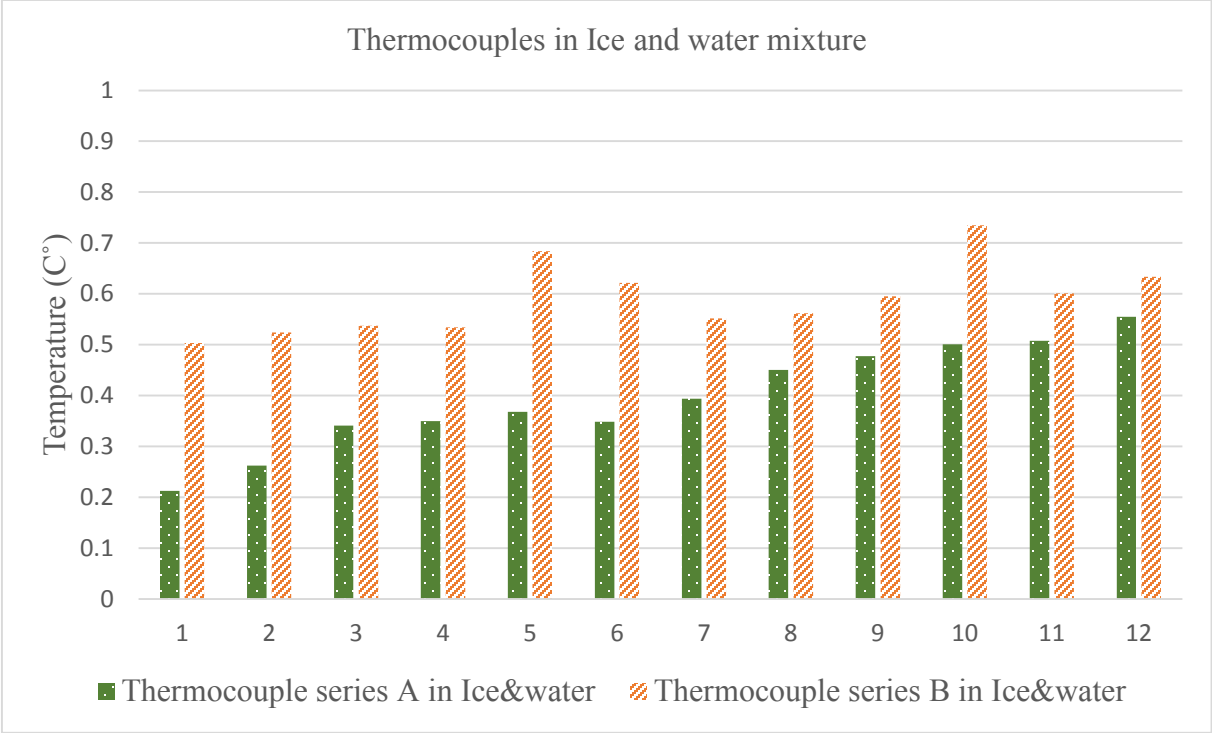

Figure 7-1. The measurement results of thermocouples in ice and water mixture.

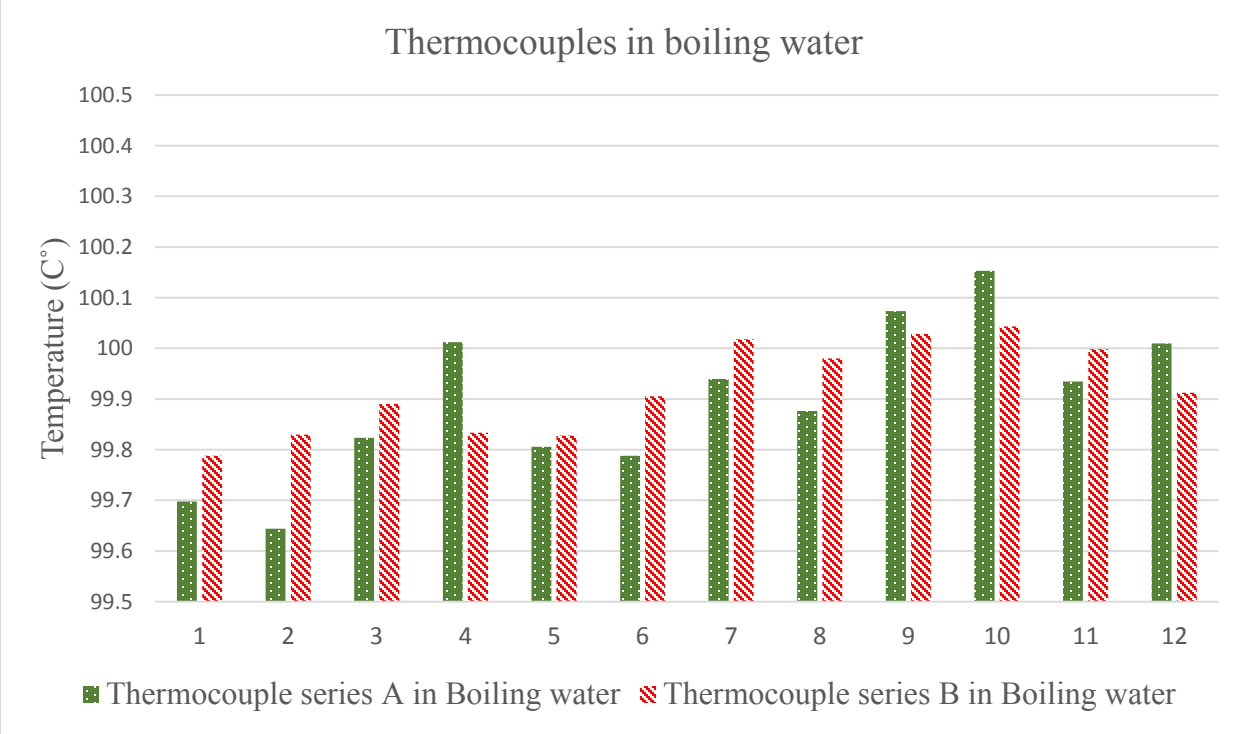

Figure 7-2. The measurement results of the thermocouples in boiling water.

Appendix B: The supply air velocity measurement result of MG building.

The velocity and temperature of supply air were measured from the diffusers on the walls of the MG building.

Table 11. Velocity and temperature measurements of supply air in MG buildings.

South wall, diffuser No.2		
Reading	Velocity (m/s)	Temperature (˚C)
1	6.0	22.2
2	5.4	22.4
3	5.8	22.4
4	4.2	22.4
Average	5.4	22.4
South wall, diffuser No.4		
Reading	Velocity (m/s)	Temperature (˚C)
1	6.4	22.5
2	3.5	22.6
3	3.5	22.5
4	4.2	22.5
Average	4.4	22.5
North wall, diffuser No.1		
Reading	Velocity (m/s)	Temperature (˚C)
1	3.5	22.1
2	2.5	22.1
Average	3.0	22.1

Figure 7-3. The air diffuser on the south wall of the MG building.

Figure 7-4. The fabric diffusers beneath the roof of MG building.

Appendix C: Measurement data

Temperature measurement data of the QT warehouse

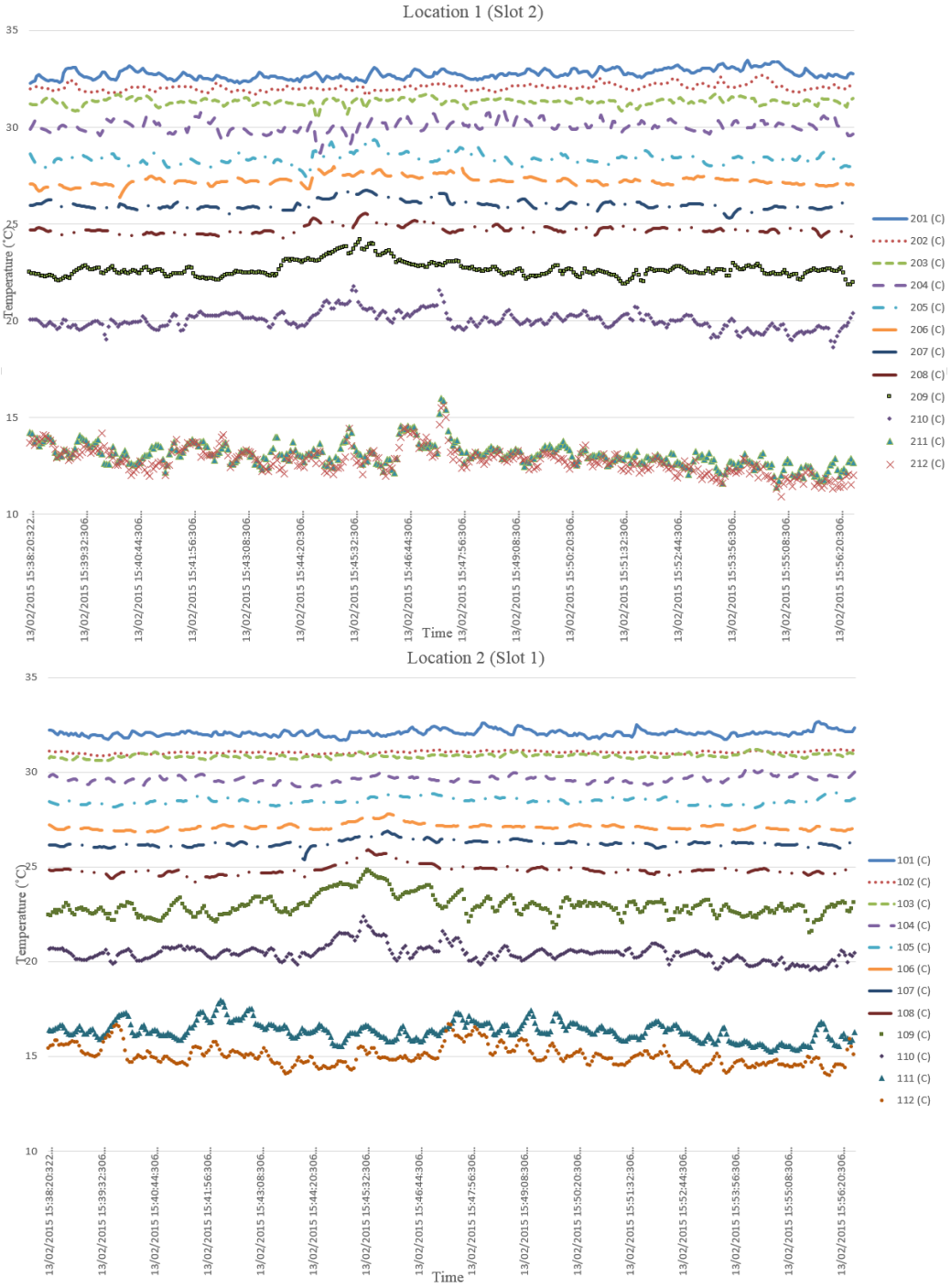

Figure 7-5. Temperature measurement data while the bucket fan was running at QT warehouse.

Figure 7-6 is the temperature data taken while the bucket fan in the warehouse was turned off. During the measurement, the loading machine broke the rope on which hung the thermocouple tree for location 1. The location 1 thermocouple tree fell onto the ground. As can be seen in the figure 7-6, there are two sudden drops in temperature which were caused by the opening of the deck door.

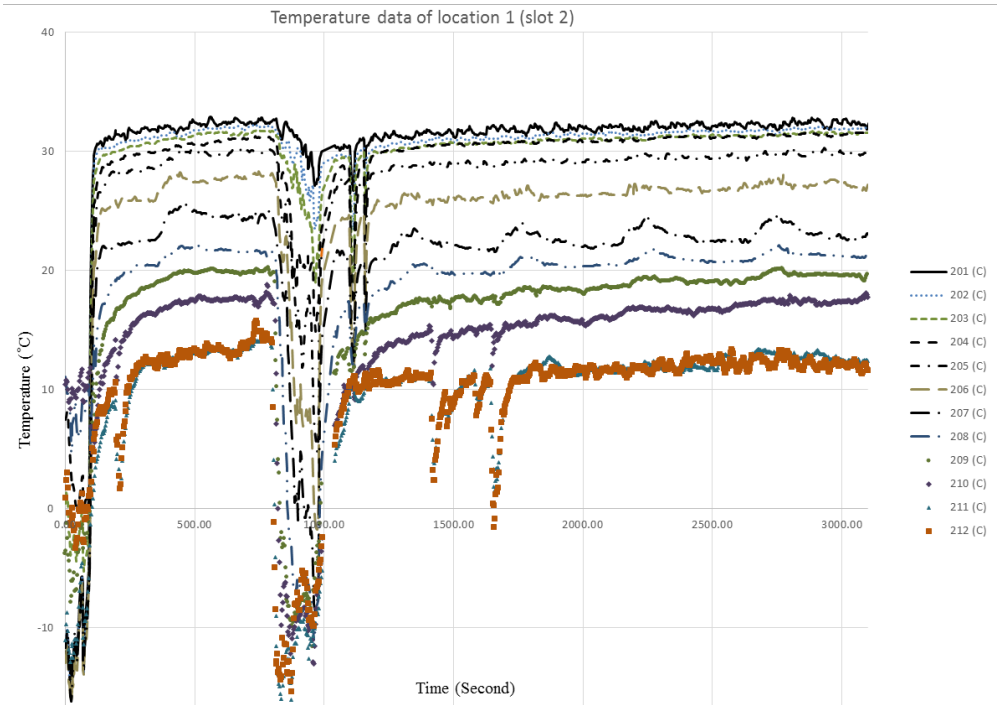

(a)

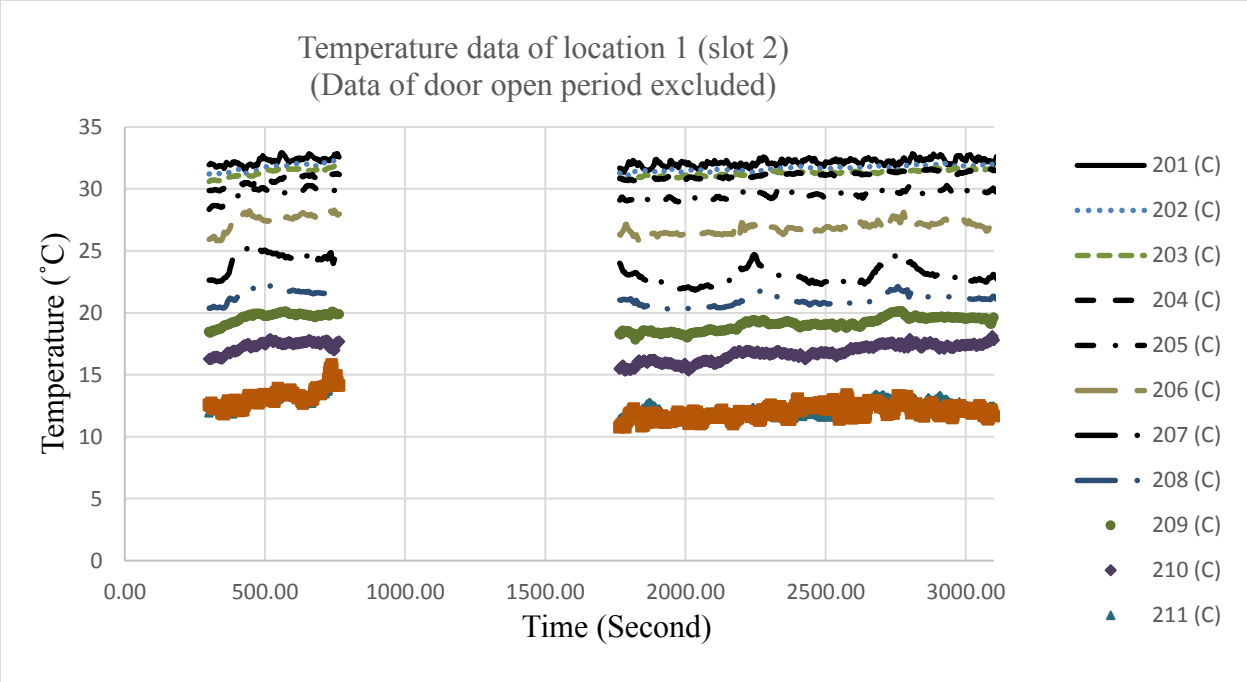
Temperature data of location 1 (slot 2)
(Data of door open period excluded)
Temperature (°C)
35
30
25
20
15
10
5
0
0.00
500.00
1000.00
1500.00
2000.00
2500.00
3000.00
Time (Second)
201 (C)
202 (C)
203 (C)
204 (C)
205 (C)
206 (C)
207 (C)
208 (C)
209 (C)
210 (C)
211 (C)

(b)

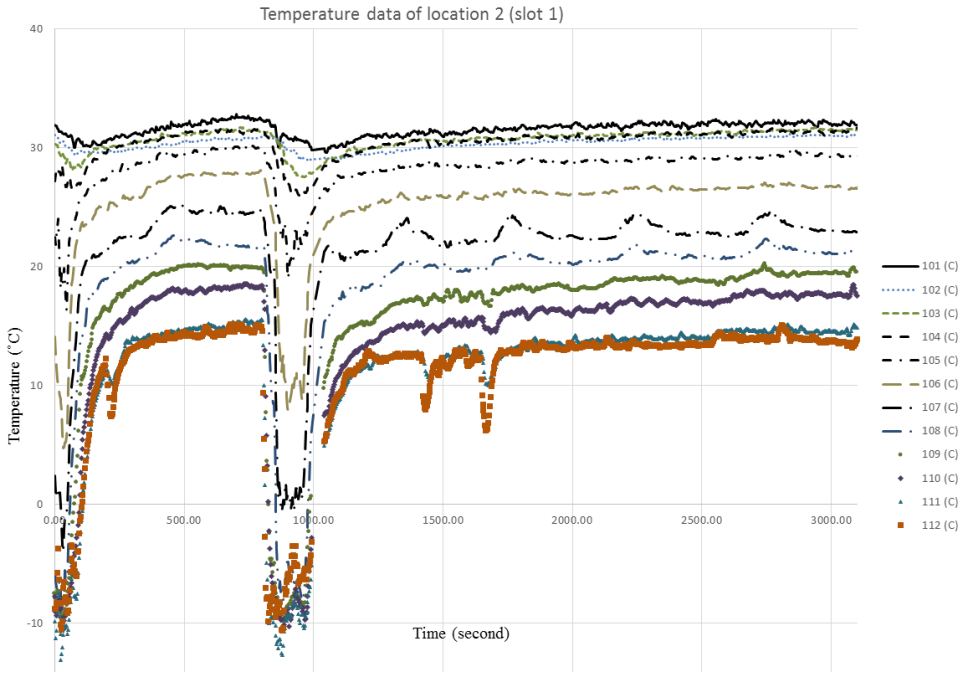
Temperature data of location 2 (slot 1)
Temperature (°C)
40
30
20
10
0
-10
0.00
500.00
1000.00
1500.00
2000.00
2500.00
3000.00
Time (second)
101 (C)
102 (C)
103 (C)
104 (C)
105 (C)
106 (C)
107 (C)
108 (C)
109 (C)
110 (C)
111 (C)
112 (C)

(c)

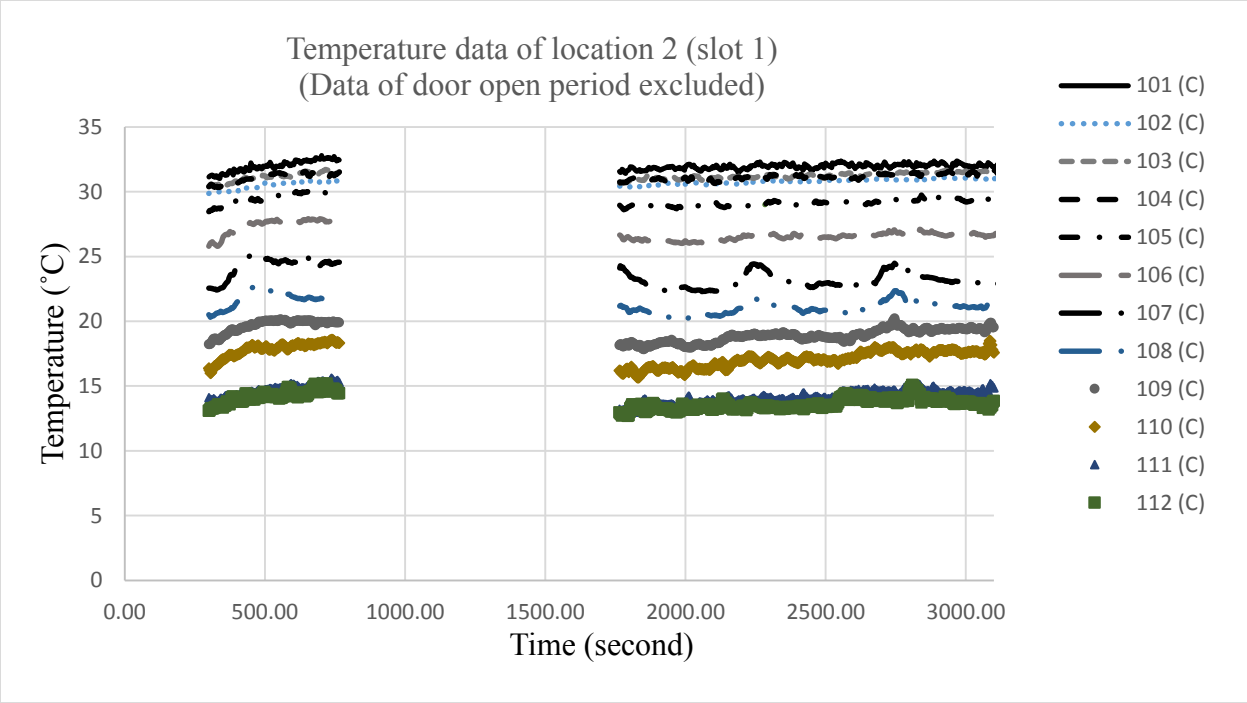

(d)

Figure 7-6. Temperature measurement data while the bucket fan was off at the QT warehouse.

The measurements in the case when the fan was turned off do not fully represent the warehouse's thermal conditions in a state of equilibrium. During the measurement, the deck door was opened for two long periods to allow for goods to be loaded. The infiltration of outdoor air (Figure 7-6 (a) and (c) in appendix C) also disturbed the temperature conditions.

Temperature measurement data of the MG stadium

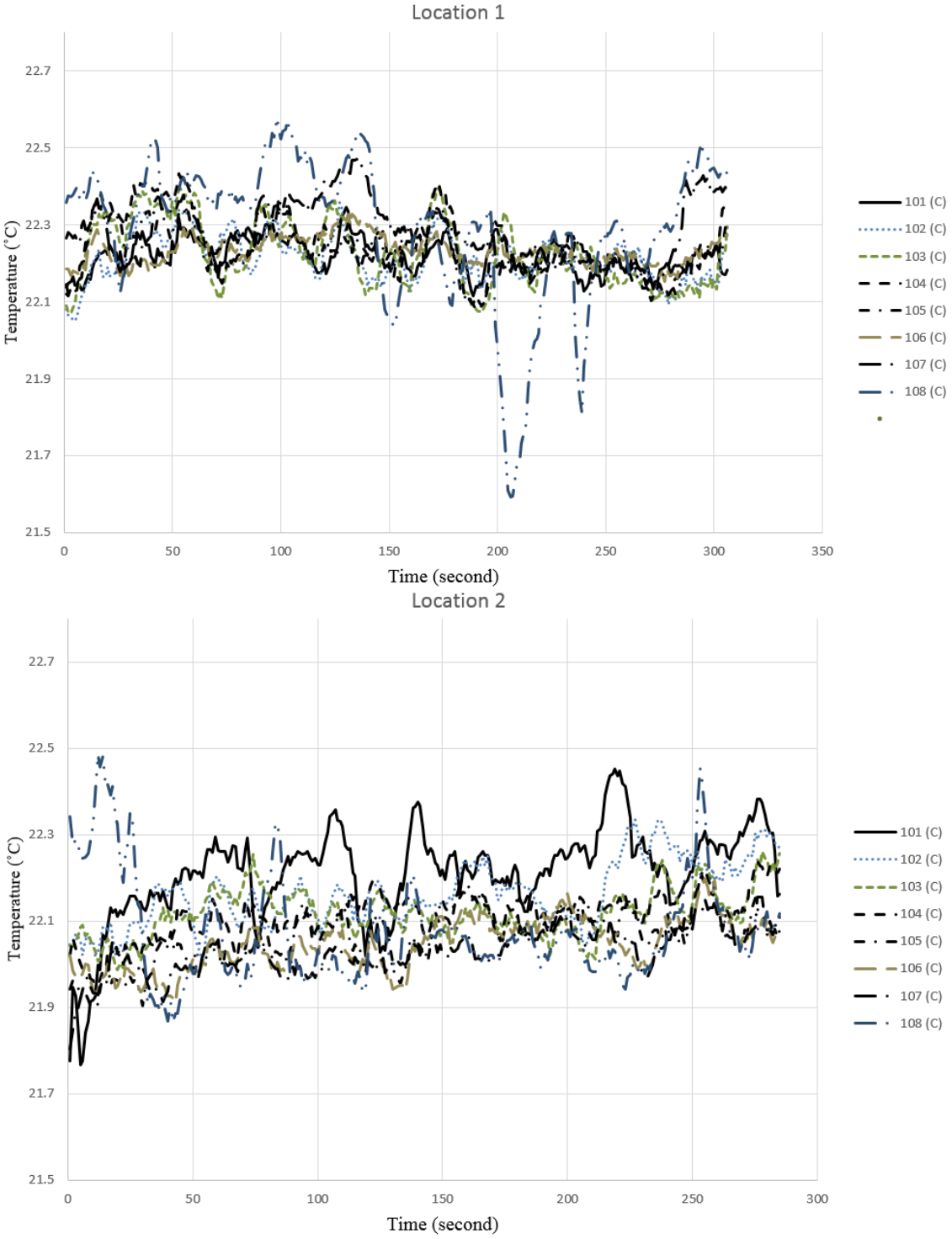

Figure 7-7. Temperature measurement data of the MG stadium.

Temperature measurement data of the KS warehouse

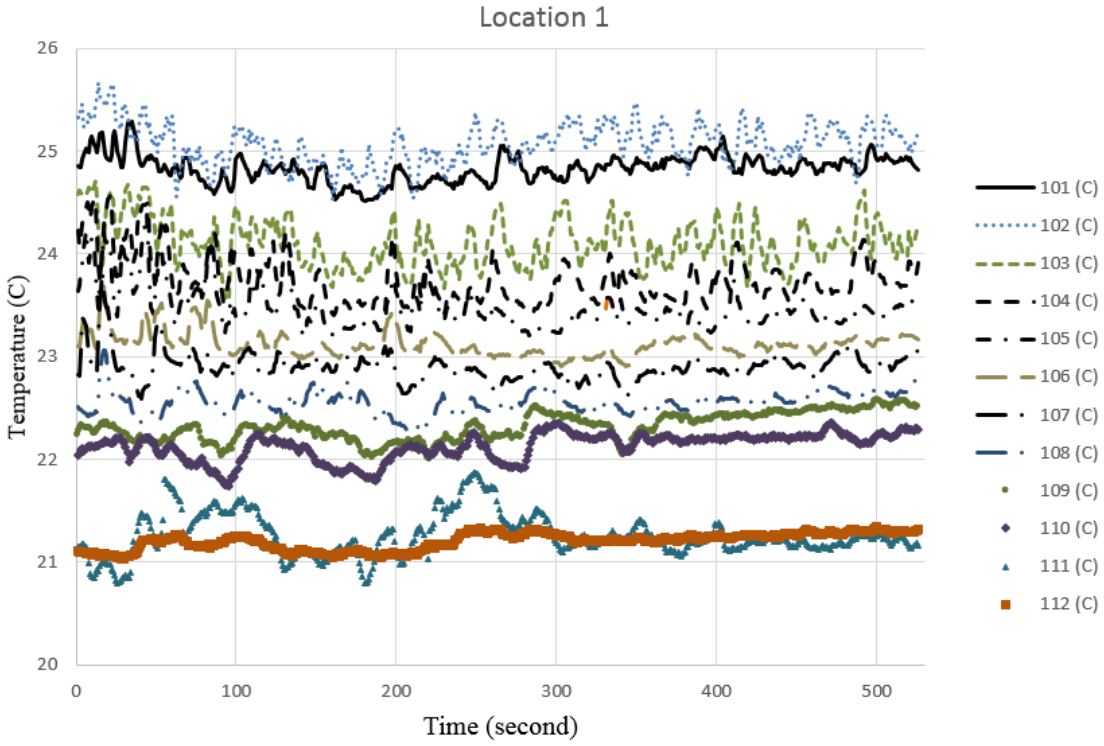

(a)

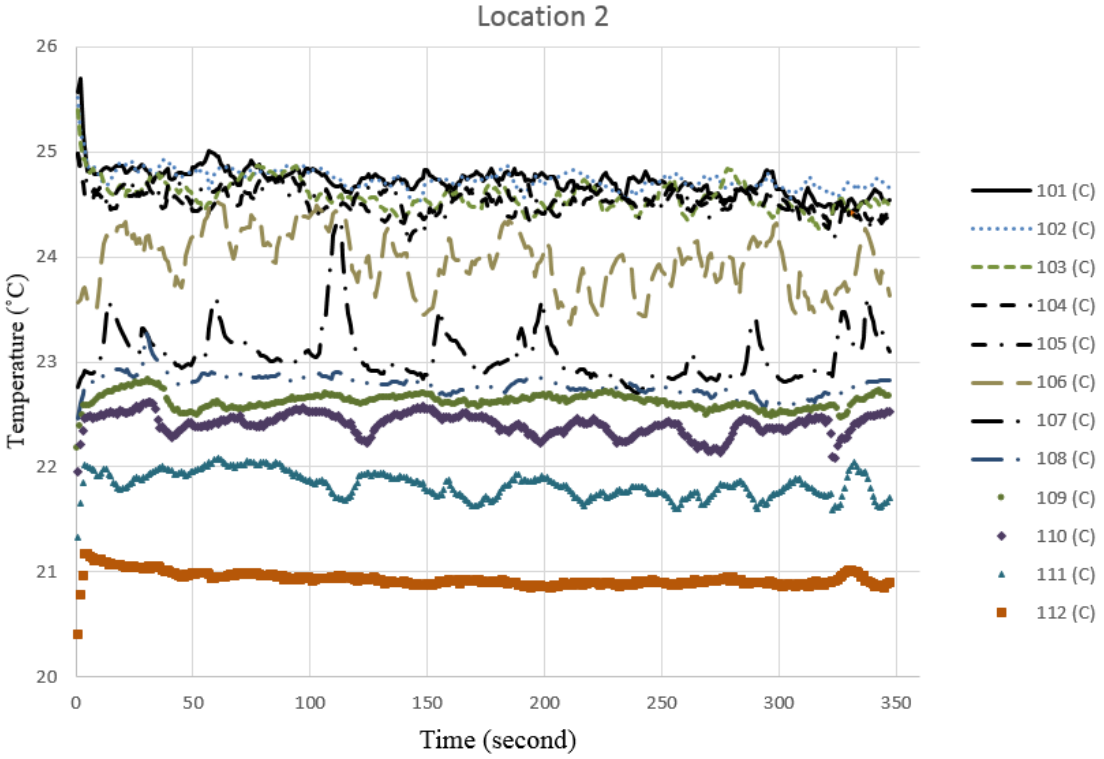

(b)

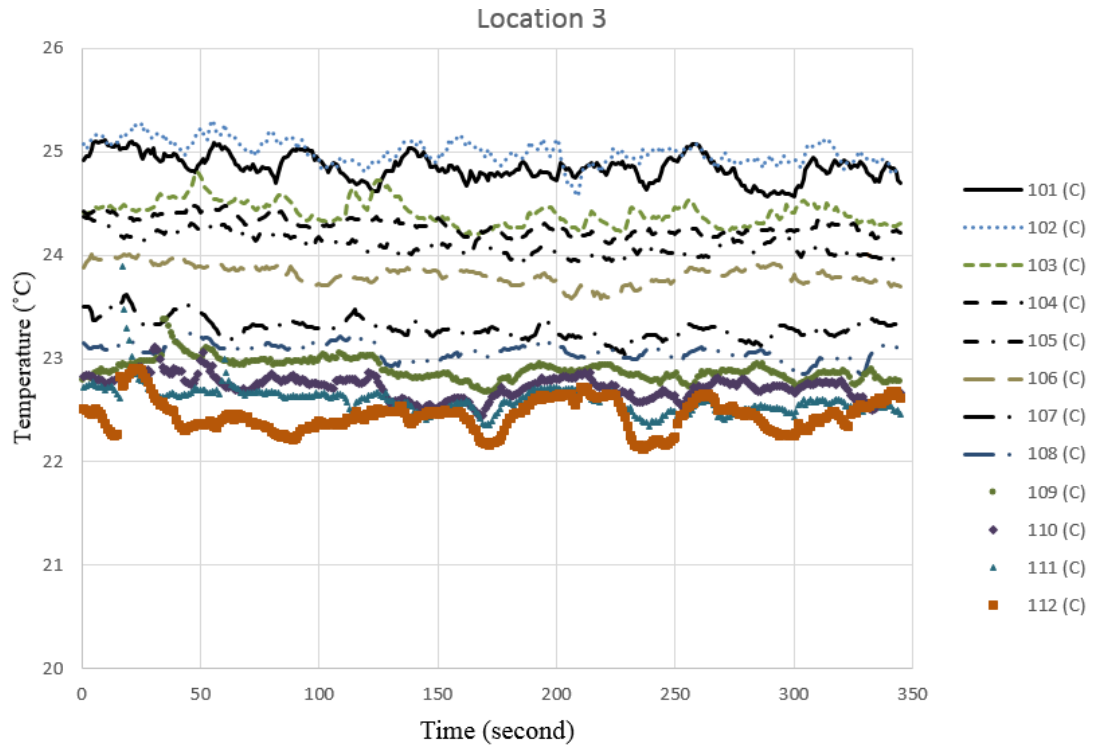
Location 3
Temperature (°C)
Time (second)
101 (C)
102 (C)
103 (C)
104 (C)
105 (C)
106 (C)
107 (C)
108 (C)
109 (C)
110 (C)
111 (C)
112 (C)

(c)

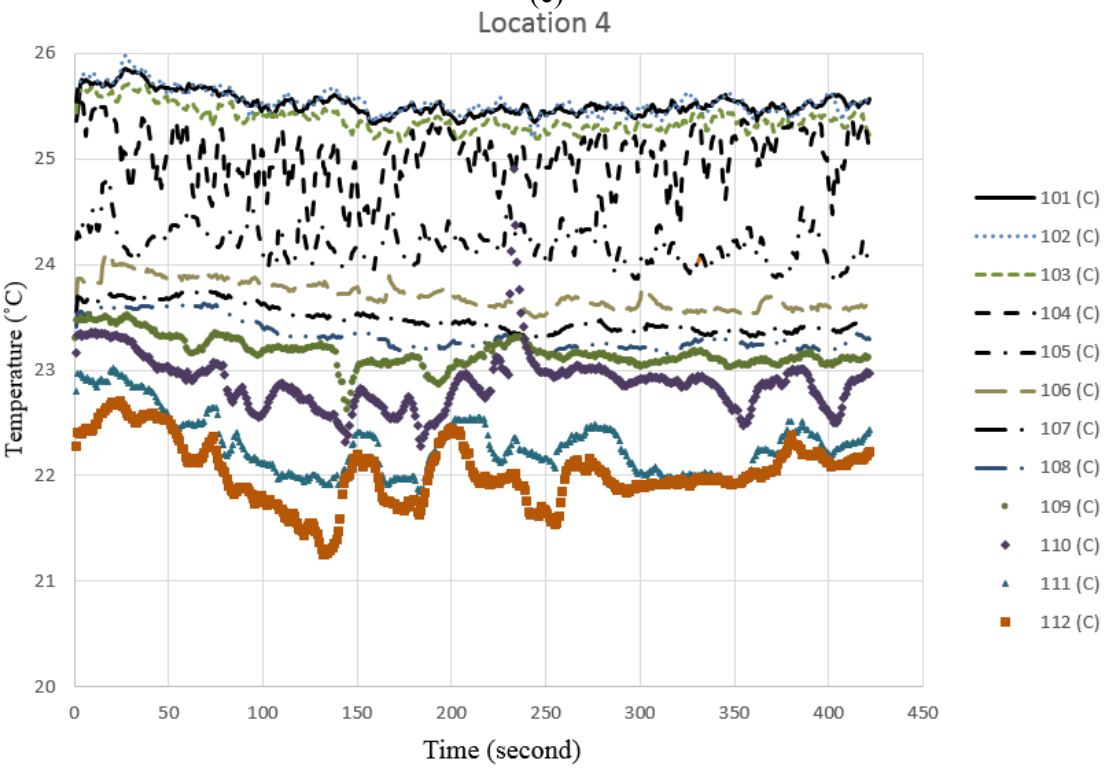
Location 4
Temperature (°C)
Time (second)
101 (C)
102 (C)
103 (C)
104 (C)
105 (C)
106 (C)
107 (C)
108 (C)
109 (C)
110 (C)
111 (C)
112 (C)

(d)

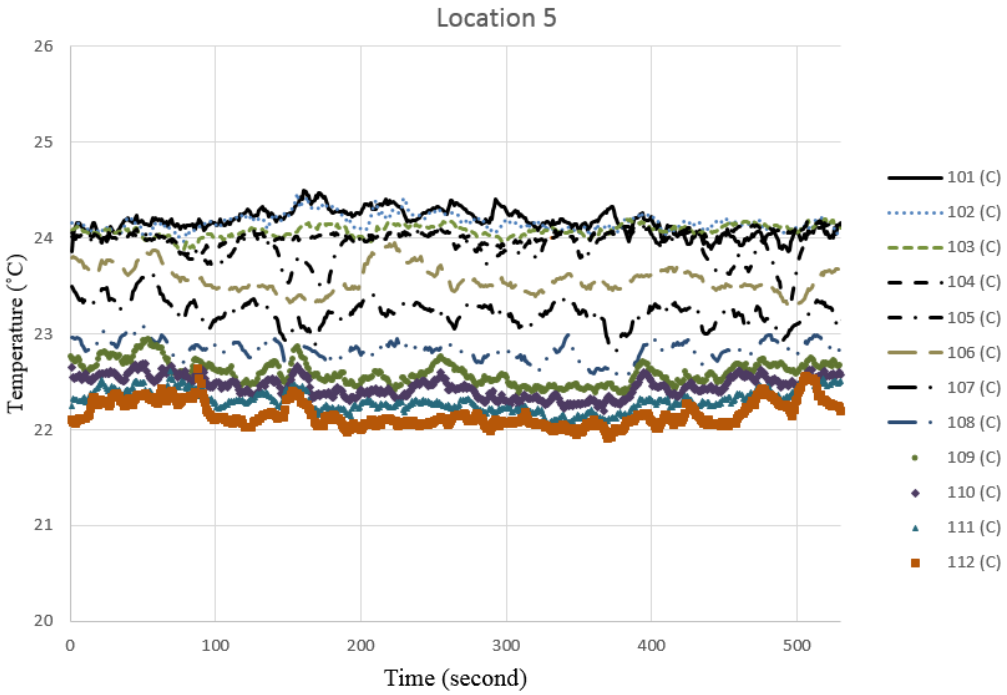

(e)

Figure 7-8. Temperature measurement data of the KS warehouse.

Temperature measurement data of the XL warehouse

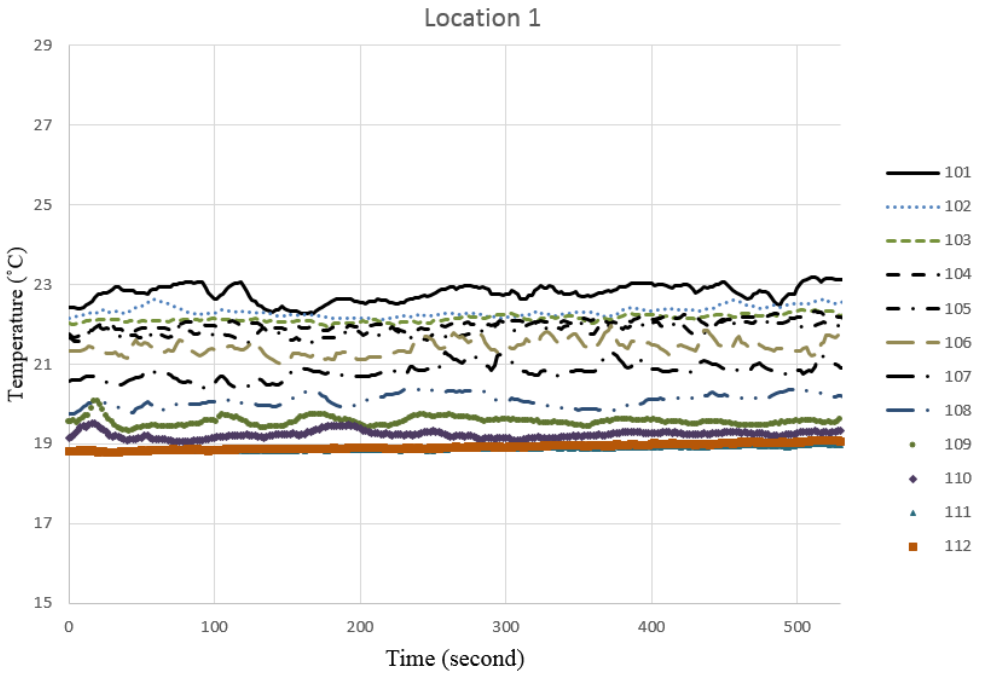

(a)

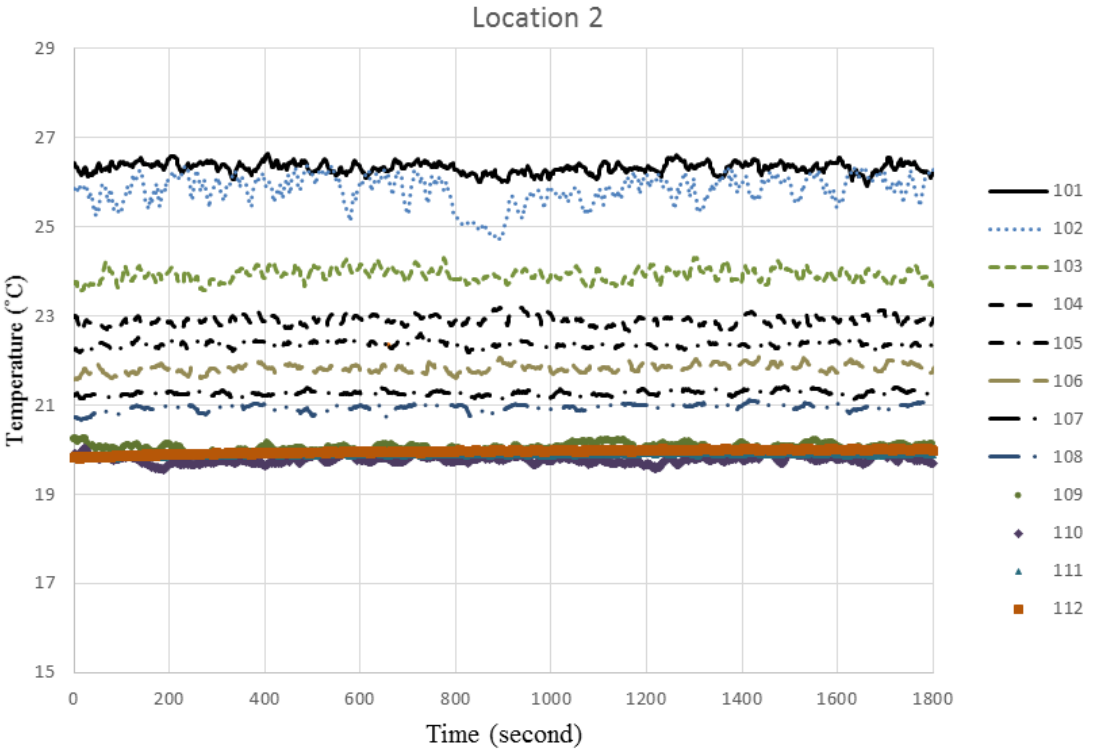
Location 2
Temperature (°C)
29
27
25
23
21
19
17
15
0
200
400
600
800
1000
1200
1400
1600
1800
Time (second)
101
102
103
104
105
106
107
108
109
110
111
112

(b)

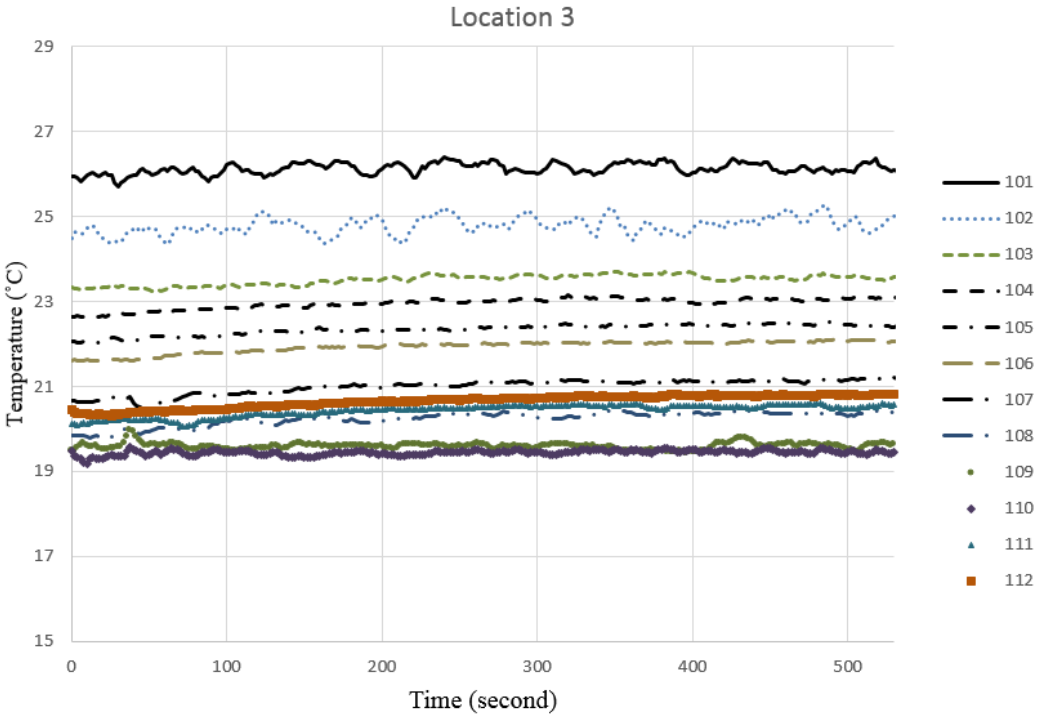
Location 3
Temperature (°C)
29
27
25
23
21
19
17
15
0
100
200
300
400
500
Time (second)
101
102
103
104
105
106
107
108
109
110
111
112

(c)

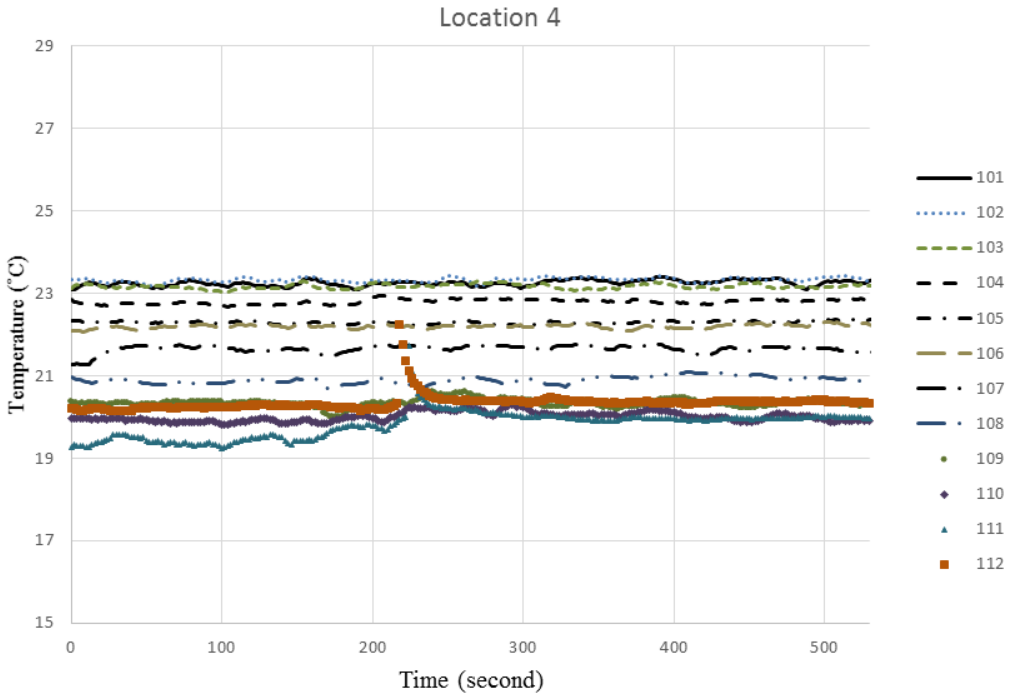

(d)

Figure 7-9. Temperature measurement data of the XL warehouse.

Temperature measurement data of the DT warehouse

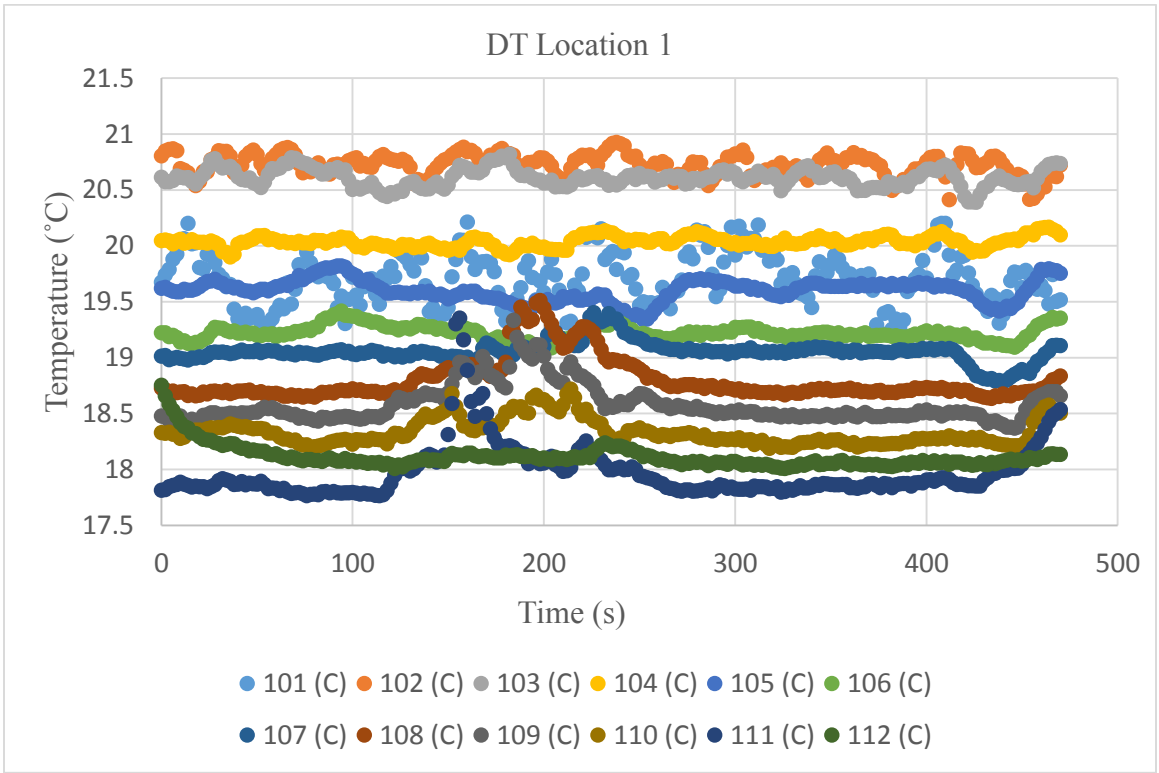

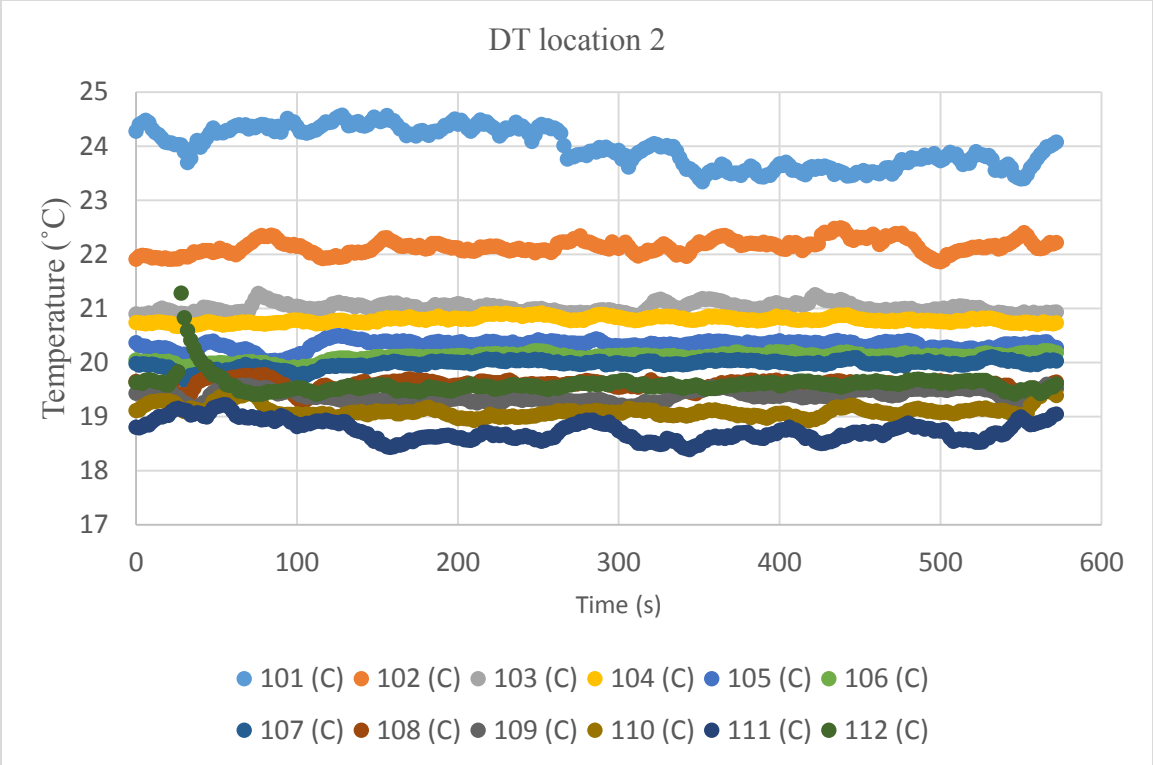
DT location 2
Temperature (˚C)
25
24
23
22
21
20
19
18
17
0
100
200
300
400
500
600
Time (s)
101 (C)
102 (C)
103 (C)
104 (C)
105 (C)
106 (C)
107 (C)
108 (C)
109 (C)
110 (C)
111 (C)
112 (C)

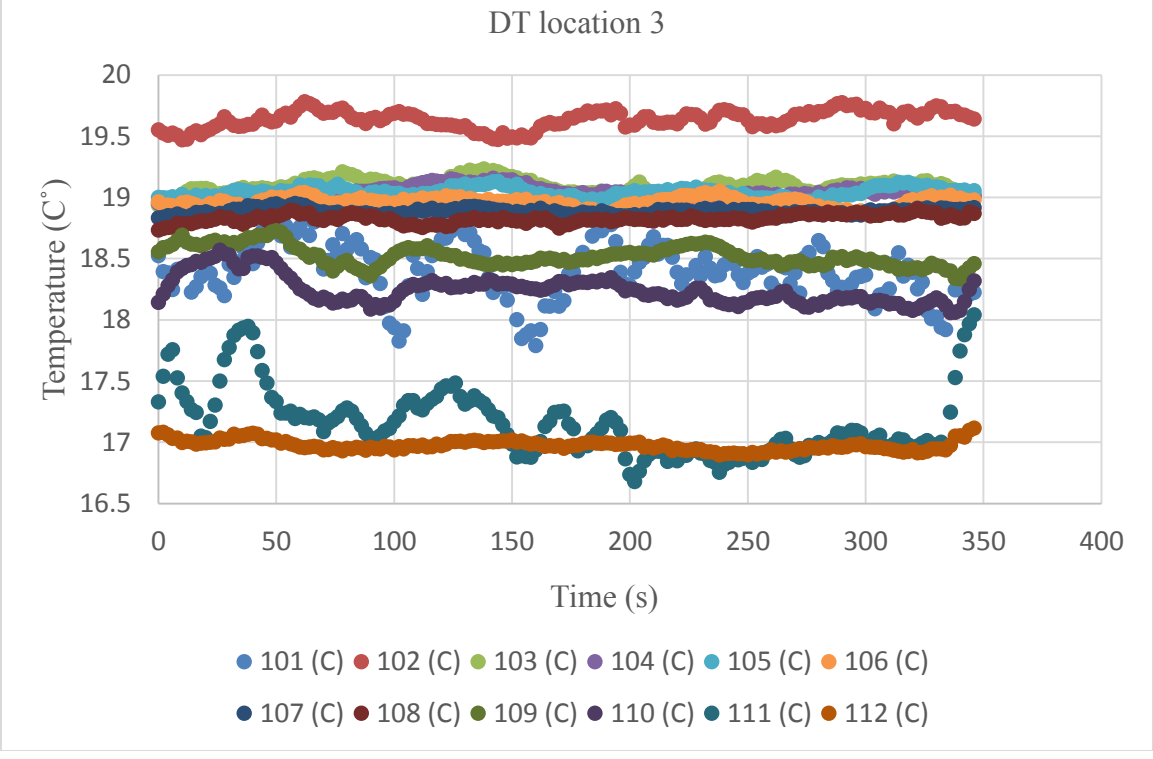
DT location 3
Temperature (C˚)
20
19.5
19
18.5
18
17.5
17
16.5
0
50
100
150
200
250
300
350
400
Time (s)
101 (C)
102 (C)
103 (C)
104 (C)
105 (C)
106 (C)
107 (C)
108 (C)
109 (C)
110 (C)
111 (C)
112 (C)

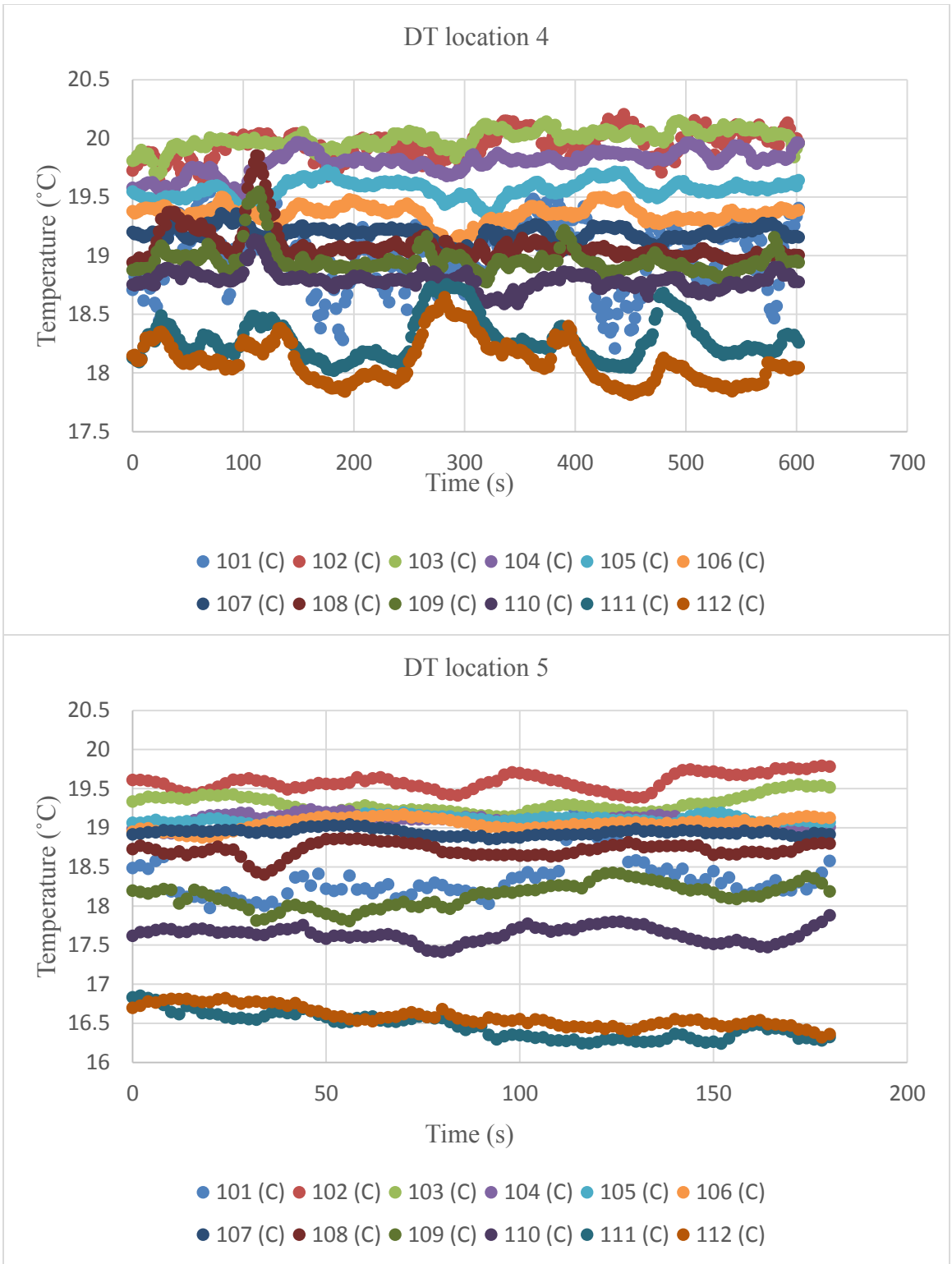

Figure 7-10. Temperature measurement data of the DT warehouse.

Appendix D. Hand calculation

QT warehouse:

Outdoor wind speed (according to weather data)	24	km/h
Airport wind speed	6.666666667	m/s
Measurement height	10	m
Gradient height	250	m
Open mean speed exponent	0.11	
Gradient wind speed	9.49909305	m/s
Laval gradient height	400	m
Mean speed exponent	0.25	
Roof height	7	m
Roof wind speed	3.454949104	
Wall height	3.5	m
Wall wind speed	2.905254317	
Door height	2	m
Wind speed at door	2.52594938	

	v=	3.454949104	m/s		
Position	x=L	10.47887324	m	take the center of the roof	
Kinematic viscosity	ν=	0.00001132	m^2/s	air at 250 K	
Reynolds number	Re=	3198230.893		Re=(V*x)/v	formula 7-10 <Heat and Mass Transfer - A practical approach> (Cøengel, 2007)
Prantl number	Pr			Pr = μ cp / k	
Dynamic viscosity	μ	0.00001599	kg/m s		
Specific heat capacity	Cp	1003.8	j/kg.K		
	k	0.02428	W/m.K		

	Pr=	0.661069275			
Nusselt number	Nu=hL/k=0.037*$Re^{0.8}$*$Pr^{1/3}$			formula 7-22 in <Heat and Mass Transfer - A practical approach> (Cøengel, 2007)	
	h=k*Nu/L				
Force heat transfer coefficient	h=	11.9438955	w/m^2.K	for Roof	
For wall					
Wall wind speed	2.905254317	m/s	16.95049184	W/m^2.K	formula from ASHREA 2001 page 3.14
Radiative heat exchange part	hr	hr=ε*σ*(Ts^4-Ta^4)/(Ts-Ta)		Formula from <Building Science> page 178 formula 8-10 (Hutcheon & Handegord, 1983)	
	surface emissivity	ε=	0.9		
	Stefan-Boltzmann constant	σ=	5.67E-08	5.6704*10^{-8} $W.M^{-2}$ K^{-4}	
	surrounding temperature	Ts=	273.15		
	Area temperature	Ta=	252.15	Take the middle temperature of outside and the inside temperature	
		hr=	3.704343903		
Outdoor					
Heat transfer coefficient	For Roof	h_Roof =	**15.64823941**		
	For out wall	h_wall=	**20.65483574**		
Indoor wall	heat transfer coefficent	h_ interior wall=	**2.087084533**	formula from table 8.7 p177 <Building science> (Hutcheon & Handegord, 1983) hc=1.42*(dt/L)0.25	
	of interior wall boundary	L _ inside wall	**0.857142857**		

Calculate the pressure difference					
Stack pressure	Ti=	298.15	K	take 25 degree	
	To=	252.15	K		
	ROo =	1.412	kg/m^3		
	g=	9.8	m/m^2		
	H	6.62	m		
	Hnpl	3.31	m	take as h which is the vertical distance from neutral pressure level	
	Po outside pressure	101325	pa		
	gas constant for air	287.058	J/kg/K		
Stack pressure	Delta P_st	7.005918368		< Heating, ventilating, and air conditioning: analysis and design. > (McQuiston & Parker, 1982)	
Wind pressure	Air density	1.412			
	Cp wind pressure coefficient	-0.5		The theta degree take as 100 degree for figure 6-2 in < Heating, ventilating, and air	

				conditioning: analysis and design. > (McQuiston & Parker, 1982)	
	Wind speed	2.905254317			
Wind pressure		-2.979497434	Leeward side	Formula P163 - 6-7b < Heating, ventilating, and air conditioning: analysis and design. > (McQuiston & Parker, 1982)	
Delta P total pressure		4.026420935			
Air Change rate					
	Total volume	739.4	m^3		
		9.5	L/(s.m)	take 1/4 inch crack (K=80)	
	Crack length	19.6		p167 < Heating, ventilating, and air conditioning: analysis and design. > (McQuiston & Parker, 1982)	
	ACH=	**0.906572897**			

KS warehouse:

Outdoor wind speed		according to weather data		
take as	12.2	km/h	take average of the above weather wind speed from 10 am to 2 pm	
Airport wind speed	3.388888889	m/s		
Measurement height	10	m		
Gradient height	250	m		
Open mean speed exponent	0.11			
Gradient wind speed	4.828705634	m/s		
Laval gradient height	400	m		
Mean speed exponent	0.25			
Roof height	7	m		
Roof wind speed	1.756265795			
Wall height	3.5	m		
Wall wind speed	1.476837611			
Roof convection calculation		p177<Building Science for a cold climate> (Hutcheon & Handegord, 1983)		
Building length	Based on google map		62.49	m
			36.63	m
L= characteristic dimension	46.18661622			
Calculate the heat transfer coefficient for roof				
	V=	1.756265795	m/s	
Position	x=L	46.18661622	m	take the center of the roof
Kinematic viscosity	ν =	0.00001132	m^2/s	air at 250 K
Reynolds number	Re=	7165722.107	Re=(V*x)/v	Formula 7-10 < Heating, ventilating, and air conditioning: analysis and design. > (McQuiston & Parker, 1982)

Prantl number	Pr			Pr = μ cp / k
Dynamic viscosity	μ	0.00001599	kg/m s	
Specific heat capacity	Cp	1003.8	j/kg.K	
	k	0.02428	W/m.K	
	Pr=	0.661069275		
Nusselt number	Nu=hL/k=0.037Re0.8Pr1/3	formula 7-22 in <Heat and Mass Transfer - A practical approach>		
Heat transfer coefficient	h=	**5.166834544**	$w/m^2.K$	**for Roof**
For wall				
Wall wind speed	1.476837611	m/s		
Heat transfer coefficient		**11.37966668**	$W/m^2.K$,formula from ASHREA 2001 page 3.14	**for wall**